MODEL REALIZATION USING SENSITIVITY FUNCTIONS

by

Ernest Edward Saunders, Jr.

Thesis submitted to the Graduate Faculty of the
Virginia Polytechnic Institute and State University
in partial fulfillment of the requirements for the degree of
DOCTOR OF PHILOSOPHY
in
Electrical Engineering

APPROVED:

Dr. W. F. VanLandingham

Dr. C. F. Smith

Prof. G. C. Barnes

Dr. T. P. Kabaservice

Dr. C. B. Ling

May, 1972

Blacksburg, Virginia

ACKNOWLEDGMENT

The author wishes to thank his committee, and in particular Dr. H. F. VanLandingham, for the guidance he received during the course of this research. Also, thanks should be extended to Bell Telephone Laboratories and Dr. D. L. Hester for the initialization of this research work.

The support received through Dr. W. A. Blackwell and the Virginia Polytechnic Institute and State University in the form of a three-year Title IV National Defense Education Association (NDEA) Fellowship is also gratefully acknowledged. And last, sincere appreciation is extended to for doing an excellent job in typing this manuscript.

TABLE OF CONTENTS

LIST OF FIGURES

LIST OF SYMBOLS

v, $v(t)$	- time domain voltage
V, $V(jw)$	- frequency domain voltage
i, $i(t)$	- time domain current
I, $I(jw)$	- frequency domain current
ψ, $\psi(t)$	- adjoint model time domain voltage
Ψ, $\Psi(jw)$	- adjoint model frequency domain voltage
ϕ, $\phi(t)$	- adjoint model time domain current
Φ, $\Phi(jw)$	- adjoint model frequency domain current
R_i	- ith circuit resistance
L_i	- ith circuit inductor
S_i	- ith circuit elastance
Γ_i	- ith circuit inverse inductance
C_i	- ith circuit capacitance
G_i	- ith circuit conductance
ω	- frequency in radians/sec ($2\pi f$)
VDV	- voltage dependent voltage
VCV	- voltage controlled voltage
μ	- dependent source voltage amplification factor
β	- dependent source current amplification factor
r_m	- dependent source current to voltage amplification factor
g_m	- dependent source voltage to current amplification factor
$\bar{G}$	- a vector of sensitivity G-components (Table 2.1)
$\overline{\Delta p}$	- a vector of circuit elements (Table 2.1)

VCI - voltage controlled current

ICI - current controlled current

ICV - current controlled voltage

IDV - current dependent voltage

IDI - current dependent current

VDI - voltage dependent current

α - gyrator transformation term

$\bar{p}$ - a vector of R, L, S, Γ, C, G

$\ell_{\bar{p}}$ - lower bound on parameters in $\bar{p}$

$u_{\bar{p}}$ - upper bound on parameters in $\bar{p}$

t_o - initial time point

t_f - final time point

$W_v(t)$ - time domain weighting function

$W_i(t)$ - time domain weighting function

$\dot{f}(t)$ - time derivative of function f(t)

t - time

ξ - reversed time

τ - Lagrange multiplier

$\hat{E}$ - time domain index of performance or error function

E_{AC} - frequency domain index of performance or error function

$\hat{E}'$ - time domain maximum allowable block error function

$\hat{E}''$ - time domain maximum allowable configuration error

E^j_{ik} - jth iterate error function for blocks i through k

$\delta\hat{E}$ - first variation of time domain error function E

$\delta\bar{p}$ - variation of p-vector

$\overline{\nabla E}$ - gradient vector of the error function

Ω - a specified frequency range

α_K - Kth iterate scalar multiplier

N - a given network

N_A - adjoint network to the network N

$\frac{\partial E_{AC}}{\partial \mu \beta}$ - summation of the voltage gain and current gain gradients

$\hat{f}_1(t), \hat{f}_2(jw)$ - "hat" denotes optimal or desired response function for V, v, I, i

I. INTRODUCTION

Device modeling in both the frequency and time domains has been a rather undefined process in terms of the many different techniques incorporated by design engineers to emulate device responses. Sensitivity function development, initially by Leeds and Ugron [4], and later by Director and Rohrer [5], has opened a new frontier to approaching the device modeling problem. Sensitivity functions are the first partial derivatives of network functions with respect to parameters contained in the network. Taken incrementally, they yield a percentage change in the network function created by a percentage change in a parameters value. Hence, they lend themselves rather handily to device modeling problems where the device circuit structure is known and an optimization technique is required to incrementally adjust the structures element values to yield a desired network response [10]. Kokotovic and Heller [8] have done extensive work in this area.

However, Director and Rohrer [5] have introduced a revolutionary method for calculating sensitivity functions in a manner other than direct partial differentiation of a network function expression with respect to an element value contained in the expression. Their technique relates sensitivity functions to voltages and currents obtained from a network structure and the networks adjoint structure. Hence, two circuit analysis using a general digital computer electronic circuit analysis program such as ECAP [1] will yield these sensitivity functions. The sensitivity functions can then be incorporated into a basic

optimization technique such as the negative gradient technique to adjust the device models' element values to yield a desired network function. Although this technique offers a clearly defined general approach to device modeling, it also suffers from many disadvantages. Among them are that

1) a long computer-computation time is required,
2) the chance of getting stuck in a local valley or flat portion of the index of performance (IP) surface is possible,
3) and there is no direct method for choosing the correct index of performance to achieve a desired network response function.

Chapter V of this dissertation indicates how the design engineer might circumvent these problems by omitting the optimization process from the design procedure in the specific case of small-signal transistor modeling.

Director and Rohrer's technique has another significant advantage, however, in that their sensitivity function calculation technique applies equally well to a zero-valued circuit structure; i.e. one containing only short circuits for current determination and open circuits for voltage determination. Hence, initial "growth"-indicator gradients can be calculated for the zero-valued structure and the appropriate gradient indicated elements can then be placed into the structure. This yields a variable structure technique by which the structure topology can be determined element by element and then developed by an optimization process. However, other than having the obvious pitfall of requiring

an optimization process, it also requires a circuit analysis program capable of analysing circuit structures under continual topological change. This places exceptional requirements on an already complex circuit analysis program such as ECAP, and is not easily implemented. Chapter VI approaches this device modeling concept from a fixed structure viewpoint with the advantages that

1) the circuit topology remains the same throughout and each block can be analysed with the same circuit analysis program,
2) the final circuit realization can be reduced to a minimal number of elements by omitting those elements used only to preserve circuit topology, hence yielding a variable structure technique, and
3) the demands made upon the index of performance for the device model are kept realizable and minimal by using the proposed cascaded-model configuration and having each cascaded block meet only a minimal realizagle index of performance between the desired network function and the achievable response function.

II. SENSITIVITY COMPUTATION USING TELLEGEN'S (WEYL'S) THEOREM

Tellegen's (Weyl's) Theorem and elementary calculus methods show that only two network analyses suffice to determine all element sensitivities. Proof of Tellegen's Theorem [6] and its application to the linear resistive case [3] and frequency domain case [10] are reviewed in this chapter in order to promote a better appreciation of the main results presented in Chapters V and VI.

2.1 Tellegen's Theorem

Consider a network graph having n_b branches and n nodes. Let (v_K, i_K) be the complete set of branch voltages and currents ($K = 1,2, \ldots,n_b$) with the reference directions of Figure 2.1, but otherwise arbitrary. Then Tellegen's Theorem requires that

$$\sum_{K=1}^{n_b} v_K i_K = 0 \qquad (2.1)$$

The proof begins by representing branch connections between all nodes (including self-incident branches at all nodes), where appropriate currents are in fact zero in Equation (2.1) (Figure 2.1c). Let the total number of branches be $n_{b'}$, so that

$$\sum_{K=1}^{n_b} v_K i_K = \sum_{K=1}^{n_{b'}} v_K i_K$$

Since one and only one branch exists between every pair of nodes, this summation over all branches can be replaced by a summation over all nodes. For this purpose, the branch currents and voltages are resubscripted as shown in Figure 2.1e, where the node voltages are

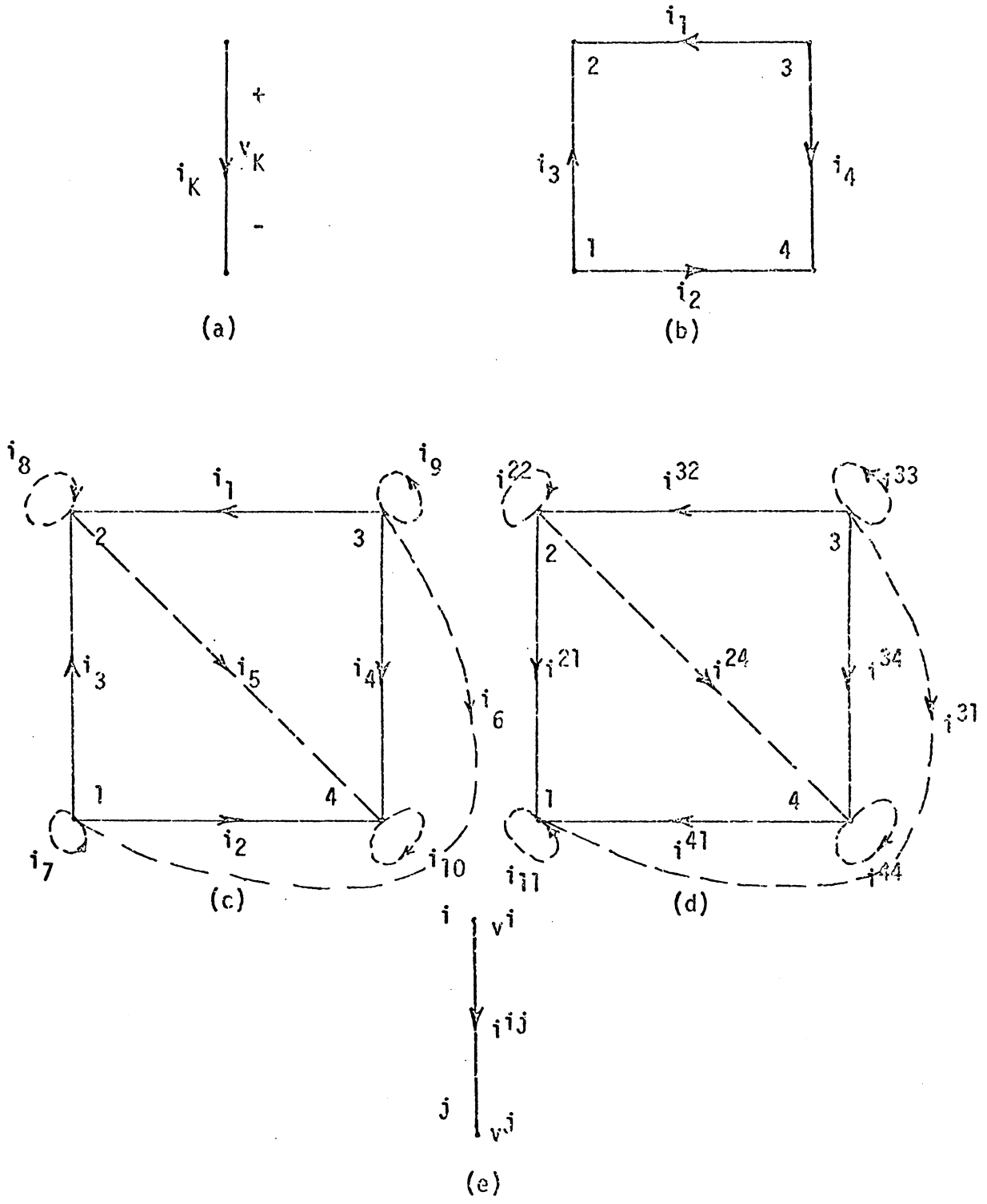

Figure 2.1. Definition in proof of Tellegen's theorem

measured with respect to an arbitrary reference. The $v_K i_K$ summation of branches incident at the j^{th} node is then

$$\sum_{i=1}^{n} (v^i - v^j) i^{ij}$$

For example, at node 1 in Figure 2.1d, this sum is

$$(v^1 - v^1) i^{11} + (v^2 - v^1) i^{21} + (v^3 - v^1) i^{31} + (v^4 - v^1) i^{41}$$

$$= (v_7)(i_7) + (-v_3)(-i_3) + (v_6)(i_6) + (-v_2)(-i_2)$$

$$= v_7 i_7 + v_3 i_3 + v_6 i_6 + v_2 i_2 \qquad (2.2)$$

Note that the signs of the $v_K i_K$ terms of Equation (2.2) are always positive. If we sum over all nodes (j = 1,2,...,n), then it is clear that each $v_K i_K$ product will be represented twice, so that

$$\sum_{K=1}^{n_b} v_K i_K = 1/2 \sum_{j=1}^{n} \sum_{i=1}^{n} (v^i - v^j) i^{ij}$$

$$\sum_{K=1}^{n_b} v_K i_K = 1/2 \sum_{i=1}^{n} v^i \left(\sum_{j=1}^{n} i^{ij} \right) + 1/2 \sum_{j=1}^{n} v^j \left(\sum_{i=1}^{n} i^{ji} \right) \qquad (2.3)$$

where identity $i^{ij} = -i^{ji}$ has been used in the second term. But the two current summations in (2.3) are both zero from KCL, since they represent the total currents flowing into nodes j and i respectively. Therefore,

$$\sum_{K=1}^{n_b} v_K i_K = 0 \qquad (2.4)$$

Equation (2.4) is not surprising on physical grounds, since it represents the conservation of instantaneous power in a circuit. However,

inspection of Equation (2.3) and its derivation reveals a rather remarkable fact: there is no requirement that the branch current i^{ij} and the node voltages v^i and v^j be in the same graph! The voltage can be defined in one graph and the current in another, so long as both have the same directed structure. In fact, if we permit representation of open- and short-circuited branches, then the two graphs need only have the same number of nodes (Figure 2.2)!

Therefore, Tellegen's Theorem applied to Figure 2.2 would yield:

$$\sum_{K=1}^{5} i_K \psi_K = 0$$

2.2 The Linear Resistive Case

Let $v_K(t)$, $i_K(t)$, $\psi_K(t)$ and $\phi_K(t)$ represent branch variables in two networks, N and N_A respectively, which have identical graphs in the Tellegen sense. Then

$$\sum_K v_K(t)\phi_K(t) = 0$$

$$\sum_K \psi_K(t) i_K(t) = 0$$

Now let the voltage and current in N change by amounts $\Delta v_K(t)$ and $\Delta i_K(t)$. Tellegen's Theorem must still be satisfied so that

$$\sum_K (v_K(t) + \Delta v_K(t))\phi_K(t) = 0$$

$$\sum_K \psi_K(t)(i_K(t) + \Delta i_K(t)) = 0$$

which requires both

$$\sum_K \Delta v_K(t)\phi_K(t) = 0 \tag{2.5}$$

$$\sum_K \psi_K(t)\Delta i_K(t) = 0 \tag{2.6}$$

and, subtracting (2.6) from (2.5),

$$\sum_K (\Delta v_K(t)\phi_K(t) - \Delta i_K(t)\psi_K(t)) = 0 \tag{2.7}$$

Equation (2.7) provides the key to sensitivity calculation methods. To see this, consider the problem of calculating the sensitivities $\partial v_o/\partial R_1$ and $\partial v_o/\partial R_2$ for the circuit of Figure 2.3a.

The output is formally replaced by an infinite resistance branch (Figure 2.3b), and a network of the same structure is composed with as yet unknown branch relationships (Figure 2.3c). Equation (2.7) can now be written

$$(\Delta v_S\phi_S - \Delta i_S\psi_S) + (\Delta v_{R_1}\phi_{R_1} - \Delta i_{R_1}\psi_{R_1})$$

$$+ (\Delta v_{R_2}\phi_{R_2} - \Delta i_{R_2}\psi_{R_2}) + (\Delta v_o\phi_o - \Delta i_o\psi_o) = 0 \tag{2.8}$$

Now assume that R_1 changes by ΔR_1; this will, in general, cause changes in all network branch currents and voltages, which can be calculated as follows:

$$\Delta v_{R_1} = \frac{\partial v_{R_1}}{\partial R_1}\Delta R_1 + \frac{\partial v_{R_1}}{\partial i_{R_1}}\Delta i_{R_1}$$

$$\Delta v_{R_1} = i_{R_1}\Delta R_1 + R_1\Delta i_{R_1}$$

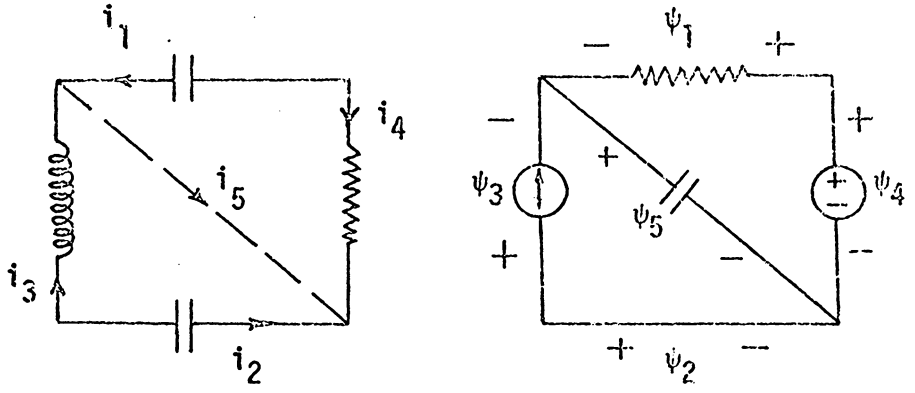

Figure 2.2. Example circuits

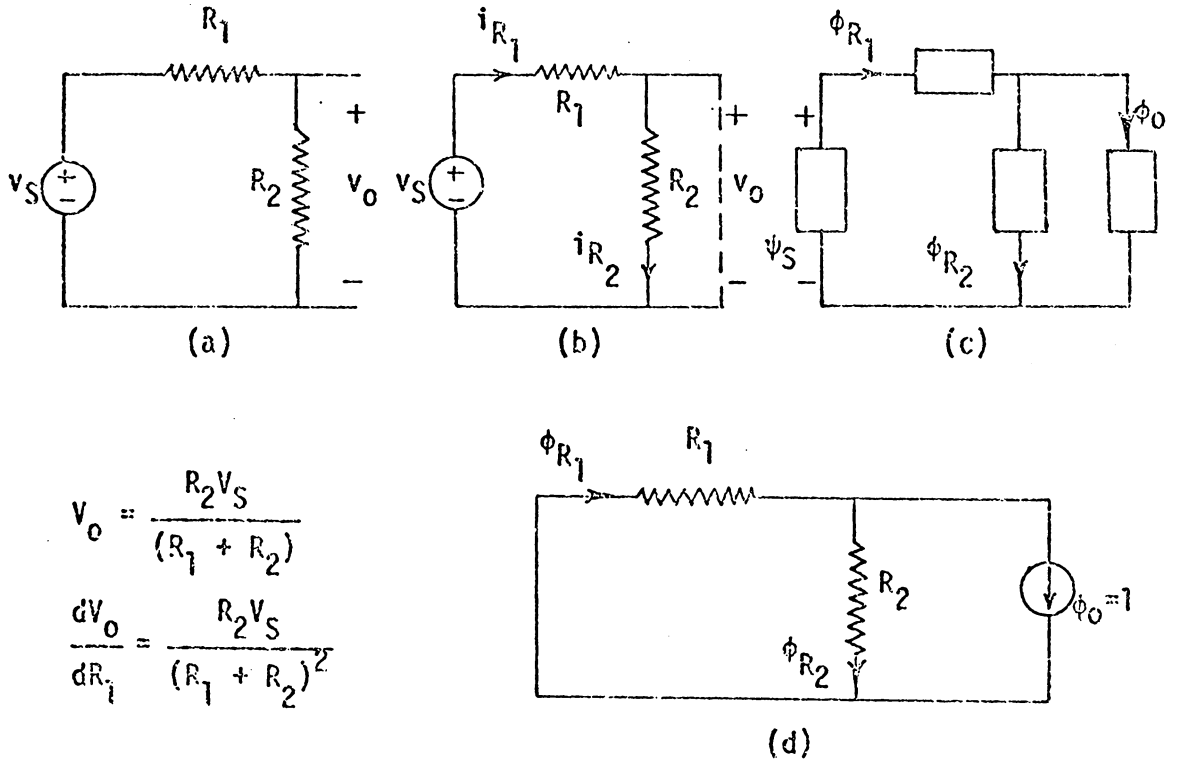

Figure 2.3. Simple network example

and

$$\Delta v_{R_2} = \frac{\partial v_{R_2}}{\partial i_{R_2}} \Delta i_{R_2} = R_2 \Delta i_{R_2}$$

Now attempt to set the terms of Equation (2.8) to zero. First, $\Delta v_S = 0$, since the voltage v_S does not change value. Setting $\psi_S = 0$ then forces the entire first term to zero. The third term is of the form

$$R_2 \Delta i_{R_2} \phi_{R_2} - \Delta i_{R_2} \psi_{R_2} = (R_2 \phi_{R_2} - \psi_{R_2}) \Delta i_{R_2}$$

which becomes zero if the adjoint network contains an identical resistance R_2, so that $\psi_{R_2} = R_2 \phi_{R_2}$. If R_1 is also duplicated in the adjoint network, the remaining two terms of Equation (2.8) become

$$(\Delta v_{R_1} \phi_{R_1} - \Delta i_{R_1} \psi_{R_1}) + (\Delta v_o \phi_o - \Delta i_o \psi_o) = (i_{R_1} \Delta R_1 \phi_{R_1})$$

$$+ (\Delta v_o \phi_o - \Delta i_o \psi_o) \equiv 0$$

$$= i_{R_1} \Delta R_1 \phi_{R_1} + \Delta v_o \phi_o \equiv 0 \qquad (2.9)$$

since $\Delta i_o = i_o = 0$. Finally, setting $\phi_o = 1$ yields

$$\frac{\Delta v_o}{\Delta R_1} = \frac{dv_o}{dR_1} = -i_{R_1} \phi_{R_1} = \frac{-v_S}{(R_1 + R_2)} \cdot \frac{R_2}{(R_1 + R_2)} \qquad (2.10)$$

which checks with the calculation in Figure 2.3. Calculation of dv_o/dR_2 proceeds in an identical fashion to yield

$$\frac{dv_o}{dR_2} = -i_{R_2} \phi_{R_2}$$

In both cases, the adjoint network is identical to the original, except for the shorted input and a unit source across the output. Therefore, only two network analyses need be performed to compute both sensitivities.

2.3 Frequency Domain Sensitivity Calculation

In the frequency domain equation (2.7) can be expressed in phasor terms as

$$\sum_K (\Delta V_K(j\omega)\Phi_K(j\omega) - \Delta I_K(j\omega)\Psi_K(j\omega)) = 0 \qquad (2.11)$$

Now consider the branch relations of the original network "N". At the same time define the branches of the adjoint network "N_A" in such a way as to render expression (2.11) independent of all ΔV and ΔI terms, which are associated with nonsource branches. The reasoning behind this approach is that an expression is desired that depends only on parameter and source variations. Next, the derivation of the adjoint elements for resistances, capacitances, and voltage controlled voltage sources is demonstrated. The adjoint models for the remaining element types are derived by means of similar techniques; the results are summarized in Table 2.1. Consider resistive branches first. Let

$$V_R = RI_R \qquad (2.12)$$

where the subscript R denotes resistance element. This subscripting scheme will be employed throughout. Since the resistance is varied,

$$V_R + \Delta V_R = (R + \Delta R)(I_R + \Delta I_R) \qquad (2.13)$$

Comparing equations (2.12) and (2.13), notice that

$$\Delta V_R = R\Delta I_R + I_R \Delta R$$

(neglecting second-order terms). Therefore, the terms of equation (2.11) associated with resistance branches of N can be written

$$\sum_R [(R\Phi_R - \Psi_R)\Delta I_R + I_R \Phi_R \Delta R] \tag{2.14}$$

where the subscripts on the summation indicate that it is to be taken over all such branches. To achieve the goal of eliminating the dependence of equation (2.14) on ΔI_R, choose

$$\Psi_R = R\Phi_R,$$

which is the branch relation for a resistance of value R in the adjoint network "N_A".

The capacitance branch relation is

$$I_C = j\omega C V_C$$

so that

$$\Delta I_C = j\omega C \Delta V_C + j\omega V_C \Delta C$$

(neglecting higher-order terms). Terms of equation (2.11) associated with capacitance branches of N can be written as

$$\sum_C [(\Phi_C - j\omega C \Psi_C)\Delta V_C - j\omega V_C \Psi_C \Delta C]$$

Thus, the expression describing the adjoint element associated with a capacitance is

$$\Phi_C = j\omega C \Psi_C ,$$

a capacitance branch relation itself. Thus, a capacitance in the original network of value C is associated with a capacitance in the adjoint network of value C.

Consider a two-branch model for the four basic types of dependent sources. The branch relations for voltage controlled voltage (VCV), (VDV implies voltage dependent voltage), sources are

$$V_{VDV} = \mu V_{VCV}$$

and

$$I_{VCV} = 0$$

so that

$$\Delta V_{VDV} = \mu \Delta V_{VCV} + V_{VCV} \Delta\mu$$

and

$$\Delta I_{VCV} = 0$$

(neglecting second-order terms). Terms of equation (2.11) corresponding to voltage controlled voltage sources may now be written as

$$\sum_{VCV} [(\Phi_{VCV} + \mu \Phi_{VDV}) \Delta V_{VCV} - \Psi_{VDV} \Delta I_{VDV} + V_{VCV} \Phi_{VDV} \Delta\mu]$$

so that the adjoint branch relations become

$$\Phi_{VCV} = -\mu \Phi_{VDV}$$

and

$$\Psi_{VDV} = 0$$

Table 2.1

Element Type	Branch Relation	Corresponding Term of Expression (2.11)	Branch Relation in Adjoint	Sensitivity G-comp.	Comp. of Δp
Resistance	$V_R=RI_R$	$(R\Phi_R-\Psi_R)\Delta I_R+I_R\Phi_R\Delta R$	$\Psi_R=R\Phi_R$	$-I_R\Phi_R$	ΔR
Conductance	$I_G=GV_G$	$(\Phi_G-G\Psi_G)\Delta V_G-V_G\Psi_G\Delta G$	$\Phi_G=G\Psi_G$	$V_G\Psi_G$	ΔG
Capacitance	$I_C=j\omega CV_C$	$(\Phi_C-j\omega\Psi_C)\Delta V_C-j\omega V_C\Psi_C\Delta C$	$\Phi_C=j\omega C\Psi_C$	$j\omega V_C\Psi_C$	ΔC
Elastance	$SI_S=j\omega V_S$	$(\frac{1}{j\omega}S\Phi_S-\Psi_S)\Delta I_S+\frac{1}{j\omega}I_S\Phi_S\Delta S$	$S\Phi_S=j\omega\Psi_S$	$-\frac{1}{j\omega}I_S\Phi_S$	ΔS
Inductance	$V_L=j\omega LI_L$	$(j\omega L\Phi_L-\Psi_L)\Delta I_L+j\omega I_L\Phi_L\Delta L$	$\Psi_L=j\omega L\Phi_L$	$-j\omega I_L\Phi_L$	ΔL
Reciprocal Inductance	$T\Psi_T=j\omega\Phi_T$	$(\Phi_T-\frac{1}{j\omega}T\Psi_T)\Delta V_T-\frac{1}{j\omega}V_T\Psi_T\Delta T$	$T\Psi_T=j\omega\Phi_T$	$\frac{1}{j\omega}V_T\Psi_T$	ΔT
Transformer	$V_{T2}=nV_{T1}$ $I_{T1}=-nI_{T2}$	$-(n\Phi_{T2}+\Phi_{T1})\Delta V_{T1}+(\Psi_{T2}-n\Psi_{T1})\cdot$ $\Delta I_{T2}-(V_{T1}\Phi_{T2}+I_{T2}\Psi_{T1})\Delta n$	$n\Psi_{T1}=\Psi_{T2}$ $-n\Phi_{T2}=\Phi_{T1}$	$-(V_{T1}\Phi_{T2}+$ $I_{T2}\Psi_{T1})$	Δn

Table 2.1 (continued)

Element Type	Branch Relation	Corresponding Term of Expression (2.11)	Branch Relation in Adjoint	Sensitivity G-comp.	Comp. of Δp
Gyrator	$V_{GY1}=\alpha I_{GY2}$ $V_{GY2}=-\alpha I_{GY1}$	$(\alpha\Phi_{GY2}+\Psi_{GY1})\Delta I_{GY1}-(\alpha I_{GY1}-\Psi_{GY2})$ $\cdot\Delta I_{GY2}-(I_{GY2}\Phi_{GY1}-I_{GY1}\Phi_{GY2})\Delta\alpha$	$\Psi_{GY1}=-\alpha\Phi_{GY2}$ $\Psi_{GY2}=\alpha\Phi_{GY1}$	$-(I_{GY2}\Phi_{GY1}-$ $I_{GY1}\Phi_{GY2}$	$\Delta\alpha$
Voltage Controlled Voltage Source	$V_{VDV}=\mu V_{VCV}$ $I_{VCV}=0$	$(\Phi_{VCV}+\mu\Phi_{VDV})\Delta V_{VCV}-\Psi_{VDV}\Delta I_{VDV}$ $+V_{VCV}\Phi_{VDV}\ \Delta\mu$	$\Phi_{VDV}=-\mu\Phi_{VDV}$ $\Psi_{VDV}=0$	$-V_{VCV}\Phi_{VDV}$	$\Delta\mu$
Voltage Controlled Current Source	$I_{VDI}=g_m V_{VCI}$ $I_{VCI}=0$	$(\Phi_{VCI}-g_m\Psi_{VDI})\Delta V_{VCI}+\Phi_{VDI}\Delta V_{VDI}$ $-V_{VCI}\Psi_{VDI}\Delta g_m$	$\Phi_{VCI}=g_m\Psi_{VDI}$ $\Phi_{VDI}=0$	$V_{VCI}\Psi_{VDI}$	Δg_m
Current Controlled Voltage Source	$V_{IDV}=r_m I_{ICV}$ $V_{ICV}=0$	$(r_m\Phi_{IDV}-\Psi_{ICV})\Delta I_{ICV}+\Psi_{IDV}\Delta I_{IDV}$ $+I_{ICV}\Phi_{IDV}\Delta r_m$	$\Psi_{ICV}=r_m\Phi_{IDV}$ $\Psi_{IDV}=0$	$-\Phi_{ICV}\Phi_{IDV}$	Δr_m
Current Controlled Current Source	$I_{IDI}=\beta I_{ICI}$ $V_{ICI}=0$	$\Phi_{IDI}\Delta V_{IDI}-(\Psi_{ICI}+\beta\Psi_{IDI})\Delta I_{ICI}$ $-I_{ICI}\Psi_{IDI}\Delta\beta$	$\Psi_{ICI}=-\beta\Psi_{IDI}$ $\Phi_{IDI}=0$	$I_{ICI}\Psi_{IDI}$	$\Delta\beta$

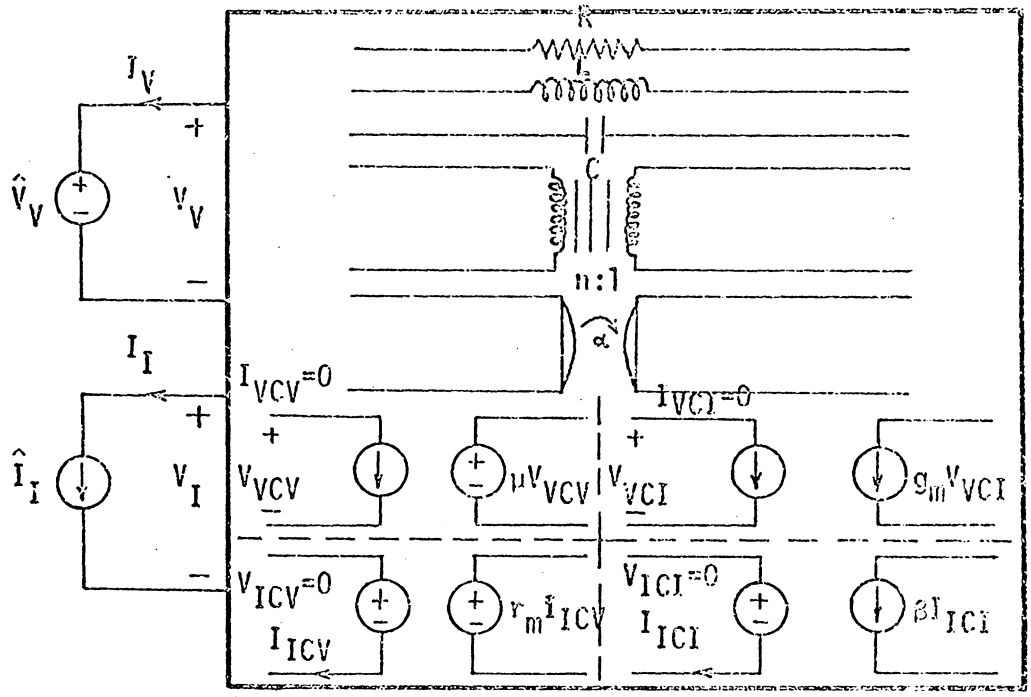

(a) Original network

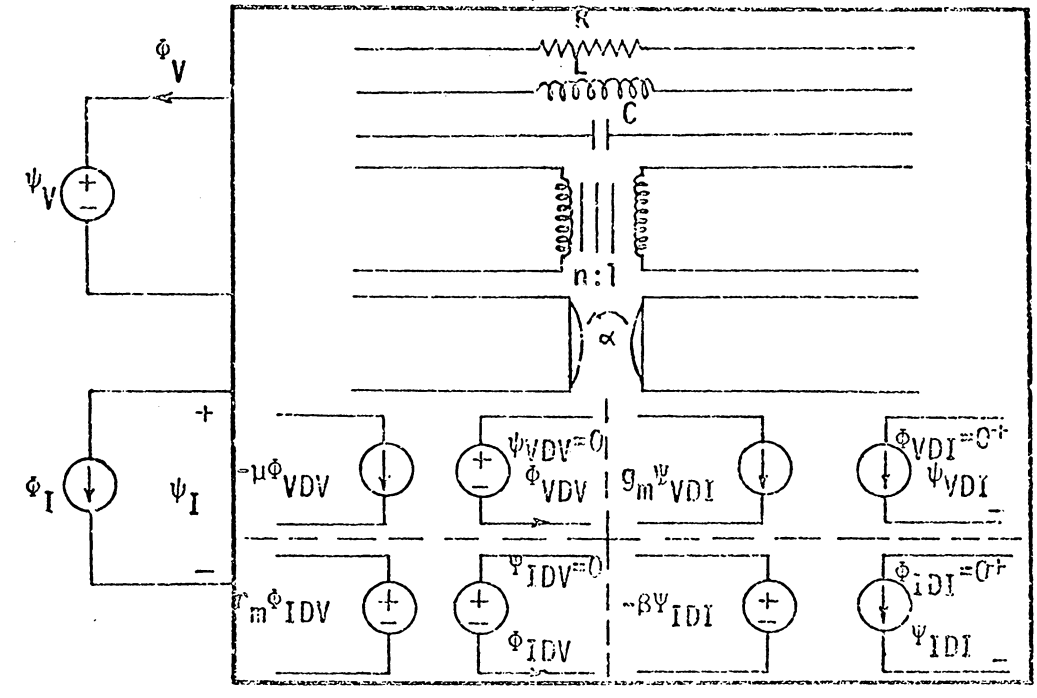

(b) Adjoint network

Figure 2.4. Lumped, linear, time-invariant multiport network

which describe a current controlled current source of current amplification factor - μ. Note the change of roles between controlling and dependent branches in the adjoint network.

The terms of equation (2.11) associated with the remaining element types of the network N can be manipulated in a similar manner. The results are presented in Table 2.1 along with the appropriate branch relations to be chosen for the related adjoint network N_A.

The network N and its adjoint N_A are shown symbolically in Figure 2.4. Expression (2.11) can now be written as

$$\sum_{V}[\Delta V_V \Phi_V - \Delta I_V \Psi_V] + \sum_{I}[\Delta V_I \Phi_I - \Delta I_I \Psi_I] = \bar{G}^T \bar{\Delta p} \qquad (2.15)$$

where the components of G and Δp are shown in Table 2.1.

Now, assume that the independent voltage source voltages and independent current source current of N are held constant so that

$$\Delta V_V = 0$$

and

$$\Delta I_I = 0$$

Thus, expression (2.15) becomes

$$\sum_{I}\Delta V_I \Phi_I - \sum_{V}\Delta I_V \Psi_V = \bar{G}^T \bar{\Delta p} \qquad (2.16)$$

From equation (2.16) the necessary sensitivities are easily calculated by applying the appropriate inputs to the adjoint network. Let

$$\Psi_V(j\omega) = -W_V(j\omega)[I_V^*(j\omega) - \hat{I}_V^*(j\omega)] \tag{2.17}$$

be the adjoint network independent port voltage source excitations and

$$\Phi_I(j\omega) = W_I(j\omega)[V_I^*(j\omega) - \hat{V}_I^*(j\omega)] \tag{2.18}$$

be the adjoint network independent port current source current excitations. In other words, the excitation of the K^{th} port of the adjoint network (Ψ_V, Φ_I) is the complex conjugate of the weighted (W_V, W_I) error between the actual (I_V, V_I) and desired ($\hat{I}_V$, $\hat{V}_I$) responses of the K^{th} port of the original network. If there is no desired response at a port of the original network, then the corresponding weighting function would have been set equal to zero, indicating a zero excitation at the K^{th} port of the adjoint network. Also, if there is a zero error at a given port of the original network, then the corresponding port of the adjoint network has zero excitation as well.

III. TIME DOMAIN PARAMETRIC SPACE GRADIENT CALCULATION

The preceding sensitivity computations were performed using Tellegen's Theorem. However, the initial sensitivity computations, i.e. postdating Leeds and Ugron's [4] work, were performed by Director and Rohrer [10] using variational calculus [31]. This method, although rigorous, proved to be much more tedious than the equally rigorous computation using Tellegen's Theorem. However, when considering the time domain case the variational calculus method will give, perhaps, a better insight into the complexities involved. Thus, the following time domain derivation has been performed with variational calculus [31] in lieu of Tellegen's Theorem. Also, the parametric space gradients calculated in this chapter will be used in Chapter VI which involves a new concept in the transient modeling of devices.

3.1 Variational Calculus Technique

Consider the simple fixed-structure, linear, time-invariant network in Figure 3.1 for which the element values are constrained by lower and upper bounds:

$$
\begin{aligned}
&\ell_R \le R \le \mu_R;\\
&\ell_L \le L \le \mu_L;\\
&\ell_S \le S \le \mu_S;\\
&\ell_T \le T \le \mu_T;\\
&\ell_C \le C \le \mu_C;\\
&\ell_G \le G \le \mu_G
\end{aligned}
\qquad (3.1)
$$

These bounds may be dictated a priori (by physical or economic considerations, perhaps), or they may be adjusted in the course of solution of the problem [31].

Now, let the excitation functions v_v, $t\varepsilon[t_o, t_f]$, and i_i, $t\varepsilon[t_o, t_f]$, be given for the time interval $T = [t_o, t_f]$ and accept the response functions for current i_v, $t\varepsilon[t_o, t_f]$, and the voltage v_i, $t\varepsilon[t_o, t_f]$, as those associated with the excitation sources. While the desired forms of the response functions $\hat{i}_v$, $t\varepsilon[t_o, t_f]$, and $\hat{v}_i$, $t\varepsilon[t_o, t_f]$ are assumed to be specified a priori over the time interval of interest, it is safely assumed that they can not be attained exactly for the given network structure in general. Hence, specify as an approximation criterion the minimization of

$$E(R,L,S,T,C,G) = \frac{1}{2}\int_{t_o}^{t_f}\{W_v(t)[i_v(t)-\hat{i}_v(t)]^2+W_i(t)[v_i(t)-\hat{v}_i(t)]^2\}dt \quad (3.2)$$

where R, L, S, T, C and G are the parameters to be optimized and W_v and W_i are the non-negative weighting functions. The following equations govern the time domain behavior of the network:

$$\begin{aligned} &v_v(t) + Ri_v(t) + L\dot{i}_v(t) + v_s(t) - v_i(t) = 0 \\ &Si_v(t) - \dot{v}_s(t) = 0 \\ &i_i(t) + Gv_i(t) + C\dot{v}_i(t) + i_T(t) + i_v(t) = 0 \\ &Tv_i(t) - \dot{i}_T(t) = 0 \end{aligned} \quad (3.3)$$

Expressions (3.1) and (3.3) constitute the set of mathematical constraints under which the approximation criterion of equation (3.2) is to be minimized. To proceed to the parameter optimization, first append the dynamic constraints of equations (3.3) to the approximation criterion of equation (3.2) by means of four Lagrange multiplier functions, τ_v, τ_S, τ_i and τ_Γ, in that order to obtain the augmented performance functional [31]

$$\begin{aligned} E = \int_{t_o}^{t_f} \{ & \tfrac{1}{2}W_v(t)[i_v(t) - \hat{i}_v(t)]^2 + \tfrac{1}{2}W_i(t)[v_i(t) - \hat{v}_i(t)]^2 \\ & + \tau_v(t)[v_v(t) + Ri_v(t) + L\dot{i}_v(t) + v_S(t) - v_i(t)] \\ & + \tau_S(t)[Si_v(t) - \dot{v}_S(t)] + \tau_i(t)[i_i(t) + Gv_i(t) + C\dot{v}_i(t) \\ & + i_\Gamma(t) + i_v(t)] + \tau_\Gamma(t)[\Gamma v_i(t) - \dot{i}_\Gamma(t)]\}dt \end{aligned} \tag{3.4}$$

Upon an integration-by-parts of equation (3.4), applying the necessary condition that the first variation $\delta\hat{E} \geq 0$ for a local minimum, and also applying the endpoint transversality conditions [31], there follow four adjoint Euler differential equations:

$$\begin{aligned} & W_v(t)[i_v(t) - \hat{i}_v(t)] + R\tau_v(t) - L\dot{\tau}_v(t) + S\tau_S(t) + \tau_i(t) = 0; \\ & \tau_v(t) + \dot{\tau}_S(t) = 0; \\ & W_i(t)[\hat{v}_i(t) - \hat{v}_i(t)] + G\tau_i(t) - C\dot{\tau}_i(t) + \Gamma\tau_\Gamma(t) - \tau_v(t) = 0; \\ & \tau_i(t) + \dot{\tau}_\Gamma(t) = 0. \end{aligned} \tag{3.5}$$

This set of coupled first-order differential equations is virtually identical to the original differential-state equations (3.3), and may be brought into closer correspondence with them upon making the following identifications:

$$\Psi_v(\xi) = W_v(t_o + t_f - \xi)[i_v(t_o + t_f - \xi) - \hat{i}_v(t_o + t_f - \xi)], \quad (3.6)$$

a voltage source voltage;

$$\phi_v(\xi) = \tau_v(t_o + t_f - \xi), \quad (3.7)$$

a voltage source current;

$$\Psi_s(\xi) = \tau_s(t_o + t_f - \xi), \quad (3.8)$$

an elastance voltage (note: τ_s must be an elastance charge);

$$\Psi_i(\xi) = -\tau_i(t_o + t_f - \xi), \quad (3.9)$$

a current source voltage;

$$\phi_i(\xi) = -W_i(t_o + t_f - \xi)[v_i(t_o + t_f - \xi) - \hat{v}_i(t_o + t_f - \xi)], \quad (3.10)$$

a current source current;

$$\phi_\Gamma(\xi) = -\Gamma\tau_\Gamma(t_o + t_f - \xi), \quad (3.11)$$

a reciprocal inductance current. The transfomed independent variable

$$\xi = t_o + t_f - t \quad (3.12)$$

provides the effect of running time backwards (i.e., $\xi = t_o \Leftrightarrow t = t_f$,

$\xi = t_f \Leftrightarrow t = t_o$ and $dt \Leftrightarrow -d\xi$) so that the adjoint-differential Euler equations (3.5) with the substitutions of equation (3.6) coincide in form almost exactly with the original differential equations (3.3):

$$\begin{aligned} &\Psi_v(\xi) + R\phi_v(\xi) + L\dot{\phi}_v(\xi) + \Psi_s(\xi) - \Psi_i(\xi) = 0 \\ &S\phi_v(\xi) - \dot{\Psi}_s(\xi) = 0 \\ &\phi_i(\xi) + G\Psi_i(\xi) + C\dot{\Psi}_i(\xi) + \phi_T(\xi) + \phi_v(\xi) = 0 \\ &T\Psi_i(\xi) - \dot{\phi}_T(\xi) = 0 \end{aligned} \tag{3.13}$$

Figure 3.2 gives the network representation of equations (3.13) and coincides exactly with that of Figure 3.1; the only differences between the two are the time reversal and the excitation by the weighted error functions.

Finally, from the coefficients of the parameter value variations, δR, δL, δS, δT, δC and δG, in the necessary condition for the first variation (omitted here, but found in reference [31], p. 1933), the element value parameter optimization criteria was obtained:

$$\int_{t_o}^{t_f} i_v(t)\tau_v(t)dt = \int_{t_o}^{t_f} i_v(t_o + t_f - \xi)\phi_v(\xi)d\xi \quad \begin{cases} < 0 = R = \mu_R \\ = 0 = \ell_R \le R \le \mu_R \\ > 0 = R = \ell_R \end{cases} \tag{3.14}$$

$$\int_{t_o}^{t_f} \dot{i}_v(t)\tau_v(t)dt = \int_{t_o}^{t_f} [-\dot{i}_v(t_o + t_f - \xi)\phi_v(\xi)]d\xi \quad \begin{cases} < 0 = L = \mu_L \\ = 0 = \ell_L \le L \le \mu_L \\ > 0 = L = \ell_L \end{cases} \tag{3.15}$$

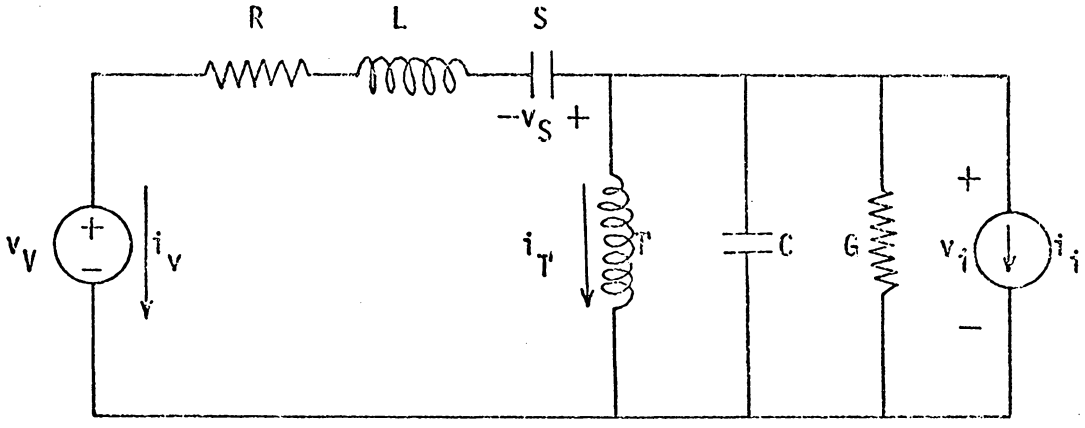

Figure 3.1. A simple fixed-structure, linear, time-invariant network

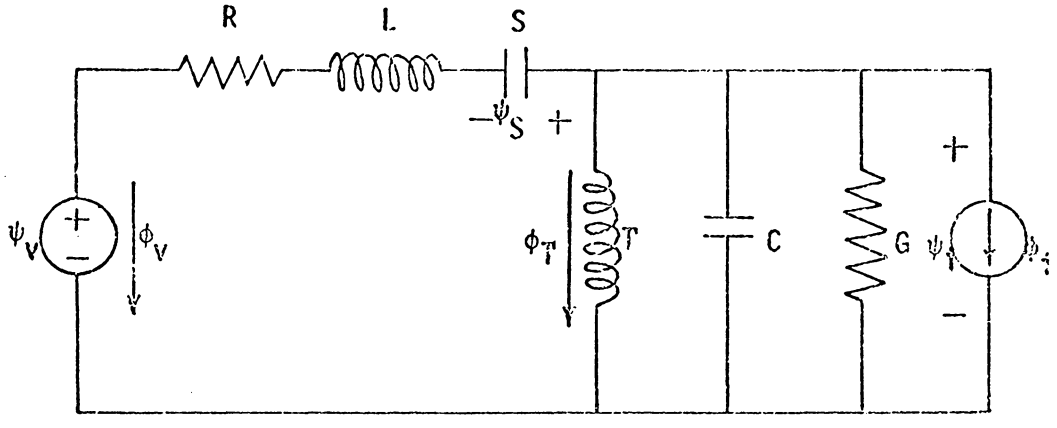

Figure 3.2. The network representation of the adjoint-differential Euler equations (3.13) in reversed time

$$\int_{t_o}^{t_f} i_v(t)\tau_S(t)dt = \int_{t_o}^{t_f} i_v(t_o + t_f - \xi)S^{-1}\Psi_S(\xi)d\xi \quad \begin{matrix} < 0 \Rightarrow S = \mu_S \\ = 0 \Rightarrow \ell_S \leq S \leq \mu_S \\ > 0 \Rightarrow S = \ell_S \end{matrix} \quad (3.16)$$

$$\int_{t_o}^{t_f} v_i(t)\tau_T(t)dt = \int_{t_o}^{t_f} [-v_i(t_o + t_f - \xi)T^{-1}\phi_T(\xi)]d\xi \quad \begin{matrix} < 0 \Rightarrow T = \mu_T \\ = 0 \Rightarrow \ell_T \leq T \leq \mu_T \\ > 0 \Rightarrow T = \ell_T \end{matrix} \quad (3.17)$$

$$\int_{t_o}^{t_f} \dot{v}_i(t)\tau_i(t)dt = \int_{t_o}^{t_f} \dot{v}_i(t_o + t_f - \xi)\Psi_i(\xi)d\xi \quad \begin{matrix} < 0 \Rightarrow C = \mu_C \\ = 0 \Rightarrow \ell_C \leq C \leq \mu_C \\ > 0 \Rightarrow C = \ell_C \end{matrix} \quad (3.18)$$

$$\int_{t_o}^{t_f} v_i(t)\tau_i(t)dt = \int_{t_o}^{t_f} [-v_i(t_o + t_f - \xi)\Psi_i(\xi)]d\xi \quad \begin{matrix} < 0 \Rightarrow G = \mu_G \\ = 0 \Rightarrow \ell_G \leq G \leq \mu_G \\ > 0 \Rightarrow G = \ell_G \end{matrix} \quad (3.19)$$

where each of the right-hand side expressions becomes convenient in subsequent computations. Now, employ the variational conditions derived above to obtain the gradient of the error functional in parameter space for the ultimate goal of processing an iterative network design technique. First, recognize that if the transversality conditions are satisfied along with expressions (3.3) and (3.13), the expression for the first variation of the augmented performance functional reduces to

$$\delta\hat{E} = \{\int_{t_o}^{t_f} i_v(t_o + t_f - \xi)\phi_v(\xi)d\xi\}\delta R + \{\int_{t_o}^{t_f} [-\dot{i}_v(t_o + t_f - \xi)\phi_v(\xi)d\xi]\}\delta L$$
$$+ \{\int_{t_o}^{t_f} i_v(t_o + t_f - \xi)S^{-1}\phi_S(\xi)d\xi\}\delta S + \{\int_{t_o}^{t_f} [-v_i(t_o + t_f - \xi)T^{-1}\phi_T(\xi)]d\xi\}\delta T \qquad (3.20)$$
$$+ \{\int_{t_o}^{t_f} v_i(t_o + t_f - \xi)\phi_i(\xi)d\xi\}\delta C + \{\int_{t_o}^{t_f} [-v_i(t_o + t_f - \xi)\phi_i(\xi)]d\xi\}\delta G$$

but the formula for the gradient of the augmented performance functional with respect to the parameters follows from

$$\delta\hat{E} = \nabla\hat{E}\delta\vec{p} = \frac{\partial\hat{E}}{\partial R}\delta R + \frac{\partial\hat{E}}{\partial L}\delta L + \frac{\partial\hat{E}}{\partial S}\delta S + \frac{\partial\hat{E}}{\partial T}\delta T + \frac{\partial\hat{E}}{\partial C}\delta C + \frac{\partial\hat{E}}{\partial G}\delta G; \quad (3.21)$$

so

$$\nabla\hat{E} \equiv \int_{t_o}^{t_f} \begin{bmatrix} -i_v(t_o + t_f - \xi)\phi_v(\xi) \\ \dot{i}_v(t_o + t_f - \xi)\phi_v(\xi) \\ -i_v(t_o + t_f - \xi)S^{-1}\phi_S(\xi) \\ -\dot{v}_i(t_o + t_f - \xi)\phi_i(\xi) \\ v_i(t_o + t_f - \xi)T^{-1}\phi_T(\xi) \\ v_i(t_o + t_f - \xi)\phi_i(\xi) \end{bmatrix} d\xi \qquad (3.22)$$

is the (unnormalized) gradient for

$$\delta\vec{p} = [\delta R, \delta L, \delta S, \delta T, \delta C, \delta G]^T \qquad (3.23)$$

IV. AUTOMATED NETWORK DESIGN

A fixed structure design algorithm [30] is reviewed in this chapter. Also, a basic variable structure design algorithm [31] along with iterative design based on the parameter space error gradients are presented in order to enhance an understanding of the present-day techniques.

4.1 Fixed Structure Design

The fixed structure case is one in which the node-branch-element network configuration has already been synthesized, leaving only the final element values to be determined by an iterative optimization scheme.

4.1.1 Frequency domain case

The fixed structure frequency domain design problem can be stated as follows. Find the element values of the lumped, linear, time-invariant fixed structure network N such that the complex-valued port excitation phasors

$$\hat{V}_1(j\omega),\ \hat{V}_2(j\omega),\ \ldots,\ \hat{V}_{n_V}(j\omega),$$

$$\hat{I}_{n_{V+1}}(j\omega),\ \hat{I}_{n_{V+2}}(j\omega),\ \ldots,\ \hat{I}_{n_V+n_I}(j\omega)$$

yield the desired complex-valued port response phasors

$$\hat{I}_1(j\omega),\ \hat{I}_2(j\omega),\ \ldots,\ \hat{I}_{n_V}(j\omega),$$

$$\hat{V}_{n_V+1}(j\omega),\ \hat{V}_{n_V+2}(j\omega),\ \ldots,\ \hat{V}_{n_V+n_I}(j\omega)$$

over a specified frequency range $\omega\varepsilon\Omega$, where n_V is the number of independent voltage sources and n_I is the number of independent current sources.

A weighted integral squared error criterion over the specified frequency range is employed as a performance measure:

$$E = \sum_V \int_\Omega \frac{1}{2} W_V(j\omega) |I_V(j\omega) - \hat{I}_V(j\omega)|^2 d\omega + \sum_I \int_\Omega \frac{1}{2} W_I(j\omega) |V_I(j\omega) - \hat{V}_I(j\omega)|^2 d\omega \tag{4.1}$$

where subscripts V and I of the summation sign denote summation over all voltage and current sources, respectively, and the $W_V(j\omega)$ and $W_I(j\omega)$ are real nonnegative weighting functions. The performance function is a function of the parameter values of the branch elements (resistances, capacitances, ...) via the response currents and voltages.

Now, ascertain the variation of the error function, expression (4.1), with respect to the element values:

$$\Delta E = \sum_p \frac{\partial E}{\partial p} \Delta p \tag{4.2}$$

where the summation is taken over all variable parameters. From equation (4.1)

$$\frac{\partial E}{\partial p} = \sum_V \int_\Omega \mathrm{Re}\{W_V(j\omega)[I_V^*(j\omega) - \hat{I}_V^*(j\omega)] \frac{\partial I_V(j\omega)}{\partial p}\} d\omega + \sum_I \int_\Omega \mathrm{Re}\{W_I(j\omega)[V_I^*(j\omega) - \hat{V}_I^*(j\omega)] \frac{\partial V_I(j\omega)}{\partial p}\} d\omega \tag{4.3}$$

Hence, the requirements are to obtain an expression for the unnormalized network sensitivities

$$\frac{\partial I_V(j\omega)}{\partial p}$$

and

$$\frac{\partial V_I(j\omega)}{\partial p} .$$

Thus, taking the real part of equation (2.16), after substitution of the adjoint excitations of equations (2.17) and (2.18), integrating over the specified frequency range Ω, and comparing the result with equations (4.2) and (4.3),

$$\Delta E = \left[\int_{\Omega} \mathrm{Re}\{G\}d\omega\right]^T \Delta p$$

where p is the network element vector and the "gradient vector" is

$$\overline{\nabla E} = \int_{\Omega} \mathrm{Re}\{\bar{G}\}d\omega . \qquad (4.4)$$

Hence, referring to Table 2.1 for the previously derived sensitivity $\bar{G}$-components, the gradient becomes

$$\frac{\partial E}{\partial R} = \int_{\Omega} \mathrm{Re}\{-I_R\Phi_R\}d\omega \qquad \text{for resistors,}$$

$$\frac{\partial E}{\partial G} = \int_{\Omega} \mathrm{Re}\{V_G\Psi_G\}d\omega \qquad \text{for conductances,}$$

$$\frac{\partial E}{\partial C} = \int_{\Omega} \mathrm{Re}\{j\omega V_C\Psi_C\}d\omega \qquad \text{for capacitors,}$$

$$\frac{\partial E}{\partial S} = \int_{\Omega} \mathrm{Re}\{-\frac{1}{j\omega} I_S \Phi_S\} d\omega \qquad \text{for elastances,}$$

$$\frac{\partial E}{\partial L} = \int_{\Omega} \mathrm{Re}\{-j\omega I_L \Phi_L\} d\omega \qquad \text{for inductances,}$$

and

$$\frac{\partial E}{\partial \Gamma} = \int_{\Omega} \mathrm{Re}\{\frac{1}{j\omega} V_\Gamma \Psi_\Gamma\} d\omega \qquad \text{for reciprocal inductances.}$$

Consequently, a fixed structure design algorithm can now be enunciated.

1) Make an initial guess as to the network structure and associated element values.

2) Calculate the gradient and output error.

3) Adjust the element values using a gradient method such as steepest descent, conjugate gradient, etc.

4) Repeat from 2) until a suitable termination criterion is met.

The fixed structure frequency-domain design procedure flow diagram is shown in Figure 4.1.

4.1.2 Time domain case

The fixed structure time domain case involves finding the structures (Figure 3.1) element values in an optimal fashion so as to best depict a desired (optimal) transient response. For any initial choice of parameters it is desired to reduce the error of equation (3.20) (i.e. to make $\delta\hat{E} \leq 0$); for example choose to alter the parameters in the direction of steepest descent:

$$\bar{p}_{K+1} = \bar{p}_K - \alpha_K (\overline{\nabla E})',$$

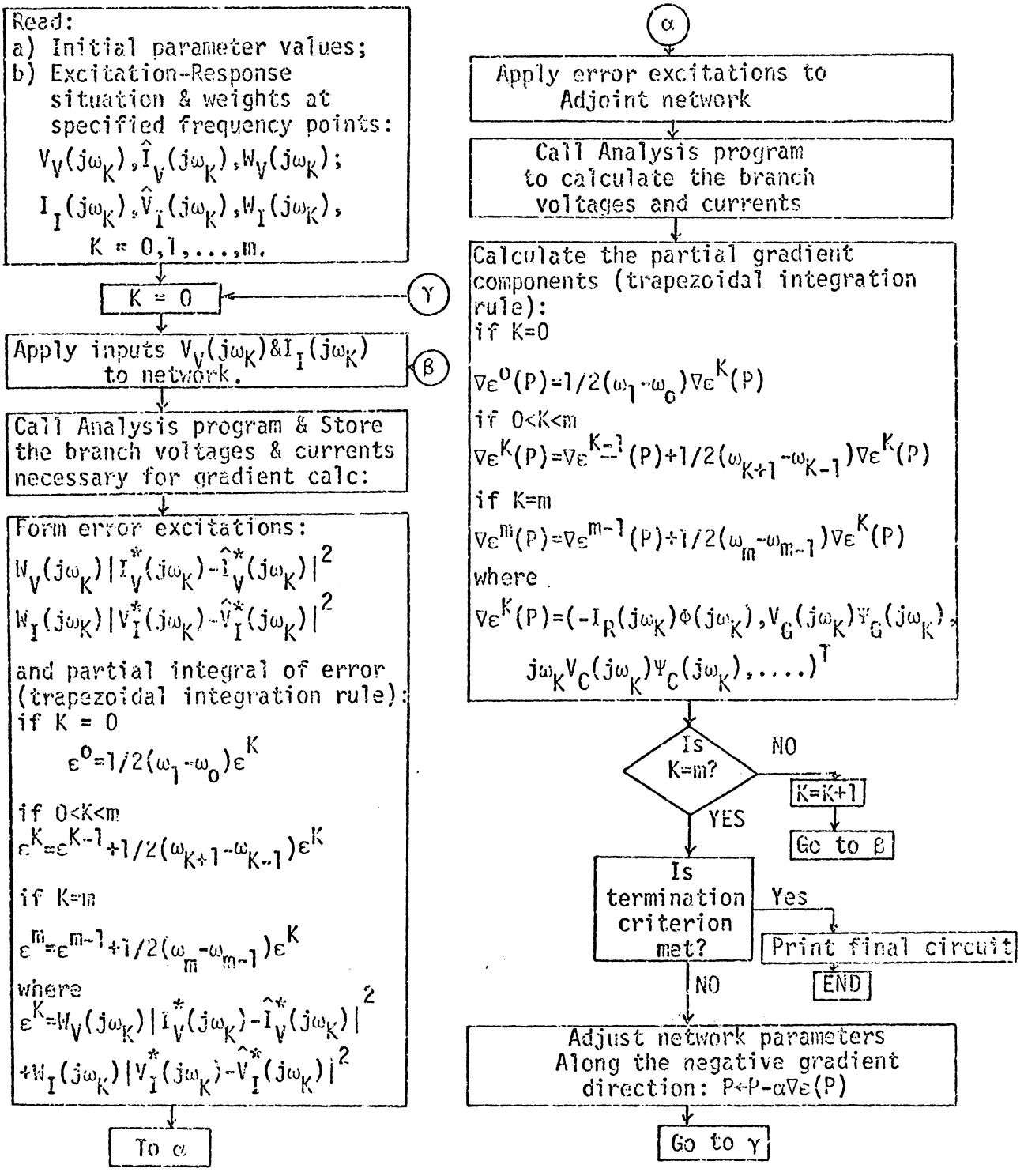

Figure 4.1. Flow diagram of frequency-domain design procedure

where α_K is a non-negative parameter. A problem which originally entails a multidimensional search in parameter space is reduced to a one-dimensional search in the non-negative parameter α_K (Appendix A).

The following iterative design scheme emerges [31]:

1) Choose a nominal set of element values, R_o, L_o, S_o, T_o, C_o and S_o.

2) For this set of element values compute and store the responses i_v, $\dot{i}_v$, v_i and $\dot{v}_i$, $t\varepsilon[t_o, t_f]$.

3) Form the adjoint error excitations ψ_v [equation (3.6)] and ϕ_i [equation (3.10)], $\xi\theta[t_o, t_f]$, in backward time.

4) For the same set of element values compute the responses ϕ_v, ψ_S, ϕ_T and ψ_i, $\xi\varepsilon[t_o, t_f]$, in backward time, while simultaneously computing the gradient components of equation (3.22).

5) Alter the element values according to some gradient technique (Negative-gradient technique [ ] with a Fibonacci search (Appendix A) on the scalar α_K is a useful one), and iterate along the parameter boundary, if attained.

6) Return to step 2) with this set of element values, and continue the process until an acceptably small error is obtained [i.e. E^{K+1} of equation (3.2), where $E^{K+1} \leq \hat{E}$ (acceptable error)].

4.2 Variable Structure Design

It is relatively easy to envision a design procedure that allows for network structural changes. Recall that the gradient components are dependent only on current and/or voltages, not on any element

value. Since voltages across any node pair (open circuit) and currents in any branch (short circuit) can always be determined, gradients can be calculated with respect to non-existent elements. If such a gradient indicates an increase in an element value (i.e. a negative valued gradient), an element is "grown" in that location. Every time an element is "grown" from an open circuit a new branch is added, and every time an element is "grown" in a short circuit a new branch and a new node are added to the network.

It now becomes clear why not only resistances, capacitances and inductances were considered, but also reciprocal resistances, capacitances and inductances. That is, because the "growth" gradients can be calculated for the open circuit case (voltage-voltage product) for G, C and T while the "growth" gradients can also be calculated in the short circuit case (current-current product) for R, S and L.

For example, an ac-amplifier design could first be approached from dc considerations only. Then the dc realization could be broad-banded by the examination of it for initial "growth" gradients of "zero valued" C's and S's, chosen to be placed at strategic open circuit and short circuit locations, respectively. Locating the initial "growth" gradient-indicated C's and S's into the dc circuit and following the procedure of Figure 4.1, the amplifier could then be broad-banded at a desired voltage gain over a frequency range.

4.2.1 Frequency domain case

The variable structure frequency domain design problem is one in which G's, C's and T's can be placed in open circuit locations and

R's, S's and L's can be placed in short circuit locations so as to change the network topology as well as enhance some network response to emulate a desired network response. Determining whether an R, S or L can be placed in the short circuit location "A" in Figure 4.2 and whether a G, C or T can be placed in the open circuit location "B" in Figure 4.2 is accomplished by calculating the "zero valued"-element "growth" indicator gradients.

These "growth" indicator gradients were derived in section 4.1.1 and for the typical network of Figure 4.2 are

$$\frac{\partial E}{\partial R} = \int_{\Omega} \mathrm{Re}\{-I_N \Phi_N\} d\omega \qquad \text{for resistors;}$$

$$\frac{\partial E}{\partial G} = \int_{\Omega} \mathrm{Re}\{V_N \Psi_N\} d\omega \qquad \text{for conductances;}$$

$$\frac{\partial E}{\partial C} = \int_{\Omega} \mathrm{Re}\{j\omega V_N \Psi_N\} d\omega \qquad \text{for capacitors;}$$

$$\frac{\partial E}{\partial S} = \int_{\Omega} \mathrm{Re}\{-\frac{1}{j\omega} I_N \Phi_N\} d\omega \qquad \text{for elastances;}$$

$$\frac{\partial E}{\partial L} = \int_{\Omega} \mathrm{Re}\{-j\omega I_N \Phi_N\} d\omega \qquad \text{for inductances;}$$

$$\frac{\partial E}{\partial T} = \int_{\Omega} \mathrm{Re}\{\frac{1}{j\omega} V_N \Psi_N\} d\omega \qquad \text{for reciprocal inductances.}$$

Hence, once these initial "growth" gradients have been calculated as outlined in section 2.3 (i.e. $\bar{G}$) the fixed network structure can be obtained by placing elements in the locations indicated by their respective negative-valued "growth" indicator gradients. Positive-valued "growth" indicator gradients simply mean that the element is omitted from the particular circuit location for which it was being considered, since its "growth" at that location can in no way enhance the network response toward a desired response. Once the fixed network structure has been realized in the preceding manner, the digital design algorithm shown in Figure 4.1 can then be implemented.

4.2.2 Time domain case

The variable structure time domain design problem is similar in nature to the frequency domain problem with two important exceptions:

1) The basic network building-block is that which is depicted in Figure 3.1. This block, or any portion of this block (as negative gradient indicated), can be cascaded until a minimal error function "E" is achieved for a desired response.

2) The "growth" indicator gradients for the "zero valued" case are those of expression (3.22). In the "zero valued" case for S = 0 we may assume $\psi_S(t_o) = 0$ and make the substitution

$$\int_{t_o}^{\xi} \phi_V(\eta)d\eta = S^{-1}\psi_S(\xi) \qquad (4.5)$$

and for T = 0 we may assume $\phi_I(t_o) = 0$ and make the substitution

$$\int_{t_o}^{\xi} \psi_i(\eta)d\eta = T^{-1}\phi_T(\xi) \ . \qquad (4.6)$$

Hence, the basic "growth" indicator gradients become

$$\frac{\partial \hat{E}}{\partial R} = \int_{t_o}^{t_f} -i_v(t_o + t_f - \xi)\phi_v(\xi)d\xi$$

for resistance branches;

$$\frac{\partial \hat{E}}{\partial L} = \int_{t_o}^{t_f} \dot{i}_v(t_o + t_f - \xi)\phi_v(\xi)d\xi$$

for inductive branches;

$$\frac{\partial \hat{E}}{\partial S} = \int_{t_o}^{t_f} -i_v(t_o + t_f - \xi) \int_{t_o}^{\xi} \phi_v(\eta)d\eta d\xi$$

for elastance branches [using equation (4.6)];

$$\frac{\partial \hat{E}}{\partial \Gamma} = \int_{t_o}^{t_f} v_i(t_o + t_f - \xi) \int_{t_o}^{\xi} \psi_i(\eta)d\eta d\xi$$

for reciprocal inductance [using equation (4.5)];

$$\frac{\partial \hat{E}}{\partial C} = \int_{t_o}^{t_f} -\dot{v}_i(t_o + t_f - \xi)\psi_i(\xi)d\xi$$

for capacitive branches;

$$\frac{\partial \hat{E}}{\partial G} = \int_{t_o}^{t_f} v_i(t_o + t_f - \xi)\psi_i(\xi)d\xi$$

for conductive branches. Figure 4.3 depicts the initial network building-block as well as the cascading of blocks to attain some desired transient response. Hence, the design procedure is one of determination of the initial network structure, optimizing it by the design algorithm listed in section 4.1.2, cascading another network structure and optimizing the total configuration, etc., etc., etc., until a final structure realizes the desired transient within the required error margin.

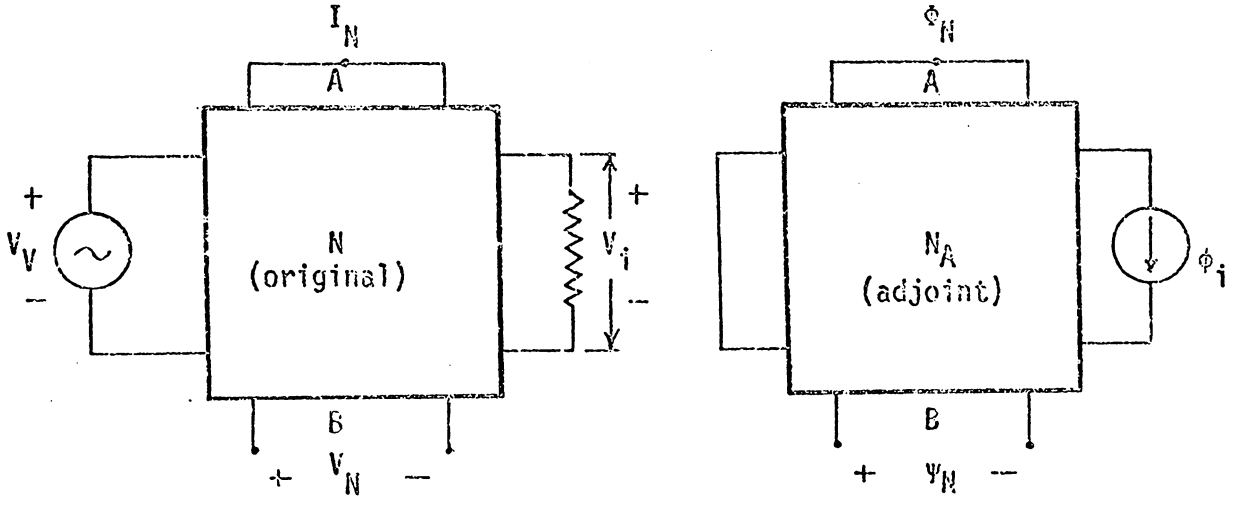

Figure 4.2. A typical network

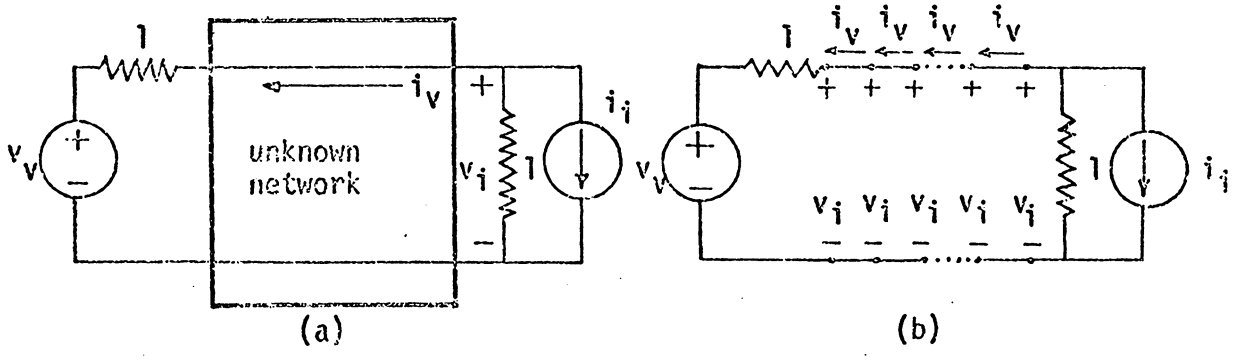

Figure 4.3. (a) The basic network for the calculation of the initial growth gradients
(b) Basic network cascading configuration

V. CHARACTERIZATION OF THE AC ERROR GRADIENT FOR SMALL SIGNAL TRANSISTOR MODELS

The main contribution of this research is contained in this chapter and the next chapter. This chapter reviews a basic automated design algorithm and develops a graphical technique by which small signal transistor models can be "grown" in a network, without the automated design algorithm requirement of a digital computer optimization process.

5.1 The Negative Gradient Technique

Director and Rohrer [35] have shown that fixed structure transistor models can be parametrically adjusted so as to yield desired network performances using gradient-adjustment techniques. Gradient components are obtained after two analyses, one on the original network and one on the topologically equivalent adjoint network. They can also be determined in the case of "zero valued" or non-existing transistors, thus indicating to the designer the possibility of "growing" transistor models in a network to obtain a desired response.

The design algorithm is based on the minimization of a desired performance function which adequately reflects the desired network response. A useful one is the integral of the squared error between the actual and desired responses over the frequency range of interest, i.e.

$$E_{AC} = \frac{1}{2} \int_{\Omega} [W(\omega)|V(\omega) - \hat{V}(\omega)|]^2 d\omega \qquad (5.1)$$

where $W(\omega)$ is a real non-negative weighting function, $\hat{V}(\omega)$ is the desired voltage-gain phasor, $V(\omega)$ is the actual voltage-gain phasor under unit excitation, and Ω is the frequency range of interest. Using this performance function Director and Rohrer [10] have shown by application of Tellegen's theorem in the weak form that the error gradient terms for resistance, conductance, capacitance, elastance, inductance, and reciprocal inductance in the frequency domain are those of section 4.2.1. They have also shown that for a transistor in the common-base configuration

$$\frac{\partial E_{AC}}{\partial \mu} = \int_{\Omega} \mathrm{Re}\{-V_1 \Psi_2\} d\omega \tag{5.2}$$

for the voltage gain. And for the common-collector configuration

$$\frac{\partial E_{AC}}{\partial \beta} = \int_{\Omega} \mathrm{Re}\{-I_1 \Psi_2\} d\omega \tag{5.3}$$

for the current gain. And for the common-emitter configuration

$$\frac{\partial E_{AC}}{\partial \mu\beta} = \frac{\partial E_{AC}}{\partial \mu} + \frac{\partial E_{AC}}{\partial \beta} = \int_{\Omega} [\mathrm{Re}\{-V_1 \Phi_2\} + \mathrm{Re}\{-I_1 \Psi_2\}] d\omega \tag{5.4}$$

for both voltage and current gain.

After two circuit analyses, one on the original network and the other on the adjoint network, it is possible to determine if a transistor should be "grown", and the appropriate configuration as indicated in Table 5.1.

Once it has been determined whether a certain transistor configuration need be "grown", the design algorithm takes the following form:

TABLE 5.1

$\partial E_{AC}/\partial \mu$	$\partial E_{AC}/\partial \beta$	Transistor Configuration
≥ 0	≥ 0	None needed
< 0	≥ 0	Common base stage
≥ 0	< 0	Common collector stage
< 0	< 0	Common emitter stage

1) Make an initial guess as to the transistor model structure (Hybrid π, Ebers Moll, Small signal low frequency, etc.) and the structure's associated element values.

2) Calculate the gradient and output error.

3) Adjust the element values using a gradient method such as steepest descent, conjugate gradient, etc.

4) Repeat from 2) until a suitable termination criterion is met.

Implementation of the previous design algorithm can be costly since computer looping between 2) and 4) is time consuming. Also, the negative gradient optimization technique seeks out only a local minimum solution, and generally many local minimum solutions exist to a problem. Hence, the local minimum solution converged upon depends entirely on how well the parameters are bounded as well as the initial guess made for the structures element values. The forthcoming small signal transistor model development with the preceding algorithm is indicative of the difficulties encountered with the bounding and initial guess problem. Then in section 5.2 a graphical analysis routine is developed to circumvent these difficulties by eliminating the optimization routine, as well as yielding an insensitive model at some desired center frequency point.

Consider this linear small signal model designed at some desired center frequency point. The gradient terms of equations (5.2), (5.3) and (5.4) must first be calculated to determine which transistor configuration should be grown.

Thus, if

$$\Delta\omega = \omega\Big|_{\Omega_1}^{\Omega_2} = \Omega_2 - \Omega_1$$

where the original network and adjoint network notations are indicated in Figure 5.1, then the gradient terms become

$$\frac{\partial E_{AC}}{\partial \mu} = -V_1\Phi_2\Delta\omega \tag{5.5}$$

and

$$\frac{\partial E_{AC}}{\partial \beta} = -I_1\Psi_2\Delta\omega \tag{5.6}$$

and

$$\frac{\partial E_{AC}}{\partial \mu\beta} = -V_1\Phi_2\Delta\omega - I_1\Psi_2\Delta\omega \ . \tag{5.7}$$

Now, assuming a network is being examined for possible transistor "growth" locations so as to enhance its gain (voltage in this case, but it could also be current), the gradient terms of the basic two port "zero transistor" block to be placed at this location will be developed. Hence, consider Figure 5.2. Thus,

$$V_o = I_1R_c = R_c\left(\frac{E_{in}}{R_b + R_c}\right)$$

$$I_1 = \frac{E_{in}}{R_b + R_c}$$

$$V_1 = V_2 = V_o = R_c\left(\frac{E_{in}}{R_b + R_c}\right)$$

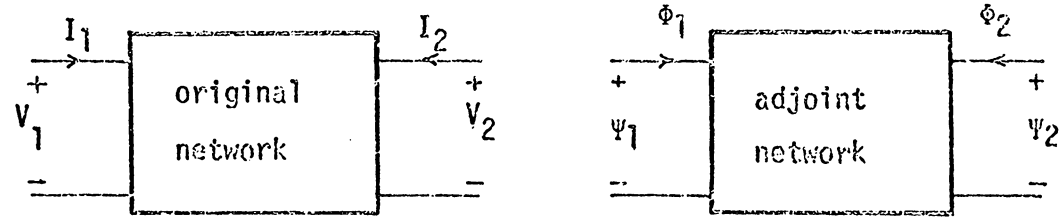

Figure 5.1. Typical two-port notation

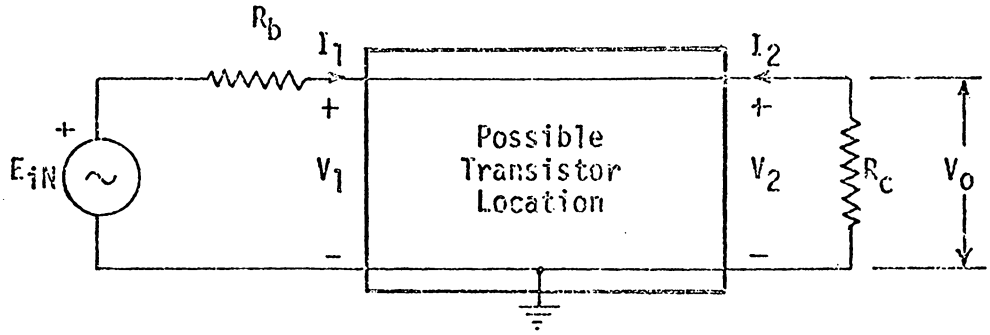

(a) Original network

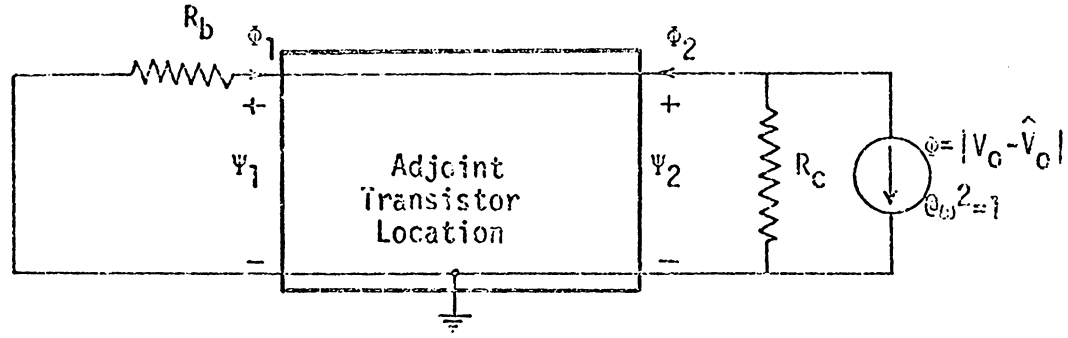

(b) Adjoint network

Figure 5.2. A possible transistor "growth" location in some network

$$\Psi_2 = -R_c\Phi\left(\frac{R_b}{R_b + R_c}\right) = -\frac{R_bR_c}{R_b + R_c}\left(\frac{E_{in}R_c}{R_b + R_c} - \hat{V}_o\right)$$

$$\Phi_2 = -\Phi_1 = -\left(\frac{R_c}{R_b + R_c}\right)\Phi$$

$$\Phi_2 = -\frac{R_c}{R_b + R_c}\left(\frac{E_{in}R_c}{R_b + R_c} - \hat{V}_o\right)$$

Therefore the gradient "growth" terms become:

$$\frac{\partial E_{AC}}{\Delta\omega\partial\mu} = -V_1\Phi_2 = \frac{E_{in}R_c^2}{(R_b + R_c)^2}\left(\frac{E_{in}R_c}{(R_b + R_c)} - \hat{V}_o\right) \tag{5.8}$$

$$\frac{\partial E_{AC}}{\Delta\omega\partial\beta} = -I_1\Psi_2 = \frac{E_{in}R_bR_c}{(R_b + R_c)^2}\left(\frac{E_{in}R_c}{(R_b + R_c)} - \hat{V}_o\right) \tag{5.9}$$

$$\frac{\partial E_{AC}}{\Delta\omega\partial\mu\beta} = \frac{\partial E_{AC}}{\Delta\omega\partial\mu} + \frac{\partial E_{AC}}{\Delta\omega\partial\beta} \tag{5.10}$$

Now, assuming that the gradient terms above indicate that a common emitter (CE) configuration should be grown (Condition #4 of Table 5.1) the gradient terms will be developed for the CE-small signal low frequency model of Figure 5.3.a.

$$I_1 = \frac{E_{in}}{(R_1 + R_b)}\ ;\quad V_1 = I_1R_1 = \frac{E_{in}R_1}{(R_1 + R_b)}$$

$$V_o = -I_2 R_c = V_2 = (I_2 - I_3)R_2$$

$$I_3 = \beta I_1$$

$$I_2 = -V_o/R_c$$

Therefore,

$$V_o = (-V_o/R_c - \beta I_1)R_2$$

$$V_o = -\frac{E_{in}\beta R_2 R_c}{(R_1 + R_b)(R_2 + R_c)}$$

and the adjoint model of Figure 5.3.b yields:

$$\Phi = -\frac{E_{in}R_2R_c\beta}{(R_1 + R_b)(R_2 + R_c)} + \hat{V}_o$$

$$\Phi_2 = \left(\frac{R_c}{R_2 + R_c}\right)\Phi = -\frac{R_c}{(R_2 + R_c)}\left(\frac{E_{in}R_2R_c\beta}{(R_1 + R_b)(R_2 + R_c)} - \hat{V}_o\right)$$

$$\Psi_2 = R_2\Phi_2$$

Therefore, the gradient terms become:

$$\frac{\partial E_{AC}}{\Delta\omega\partial\mu} = -V_1\Phi_2 = \frac{E_{in}R_1R_c}{(R_1 + R_b)(R_2 + R_c)}\left(\frac{E_{in}R_2R_c\beta}{(R_1 + R_b)(R_2 + R_c)} - \hat{V}_o\right) \quad (5.11)$$

$$\frac{\partial E_{AC}}{\Delta\omega\partial\mu\beta} = -I_1\Psi_2 = \frac{E_{in}R_2R_c}{(R_1 + R_b)(R_2 + R_c)}\left(\frac{E_{in}R_2R_c\beta}{(R_1 + R_b)(R_2 + R_c)} - \hat{V}_o\right) \quad (5.12)$$

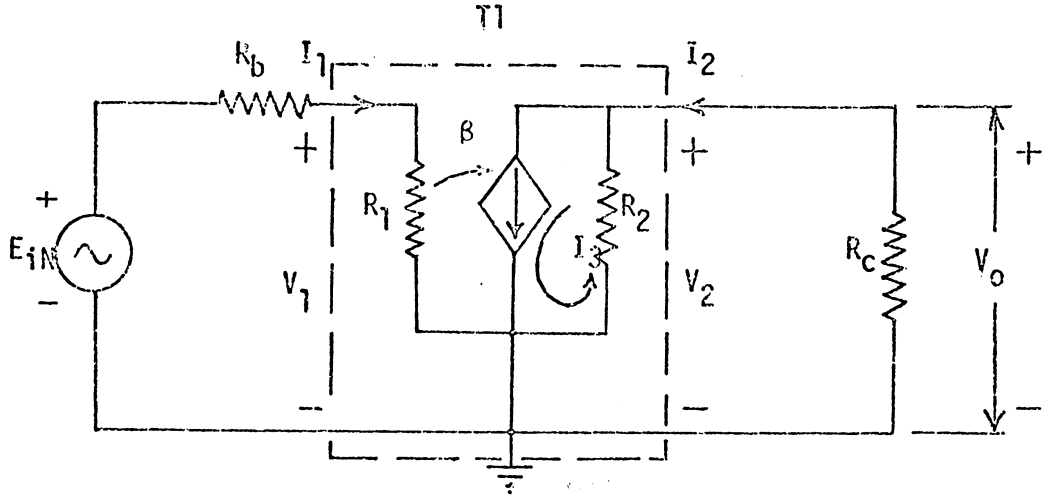

(a) Original network

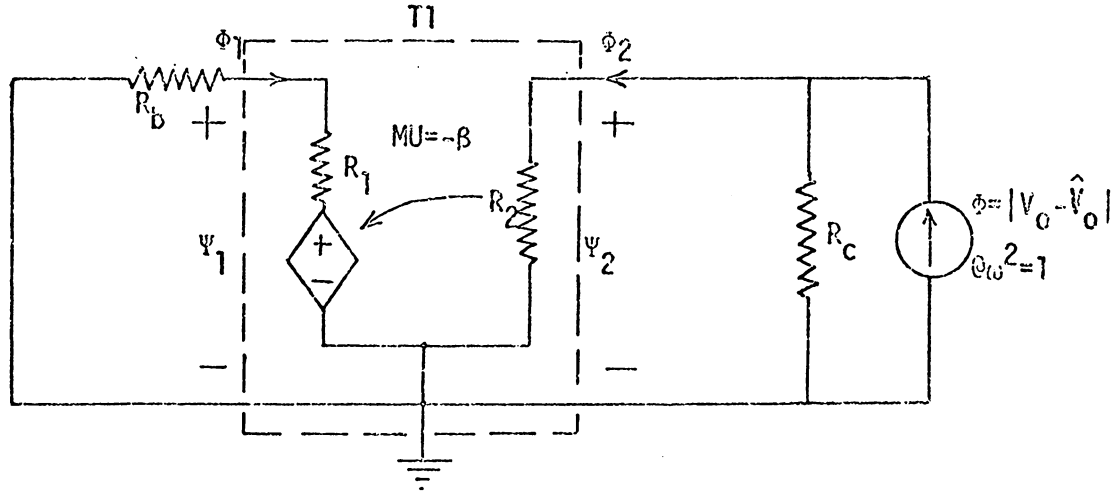

(b) Adjoint network

Figure 5.3. Small signal low frequency CE-model in possible transistor location of Figure 5.2

$$\frac{\partial E_{AC}}{\Delta\omega\partial\mu\beta} = -V_1\Phi_2 - I_1\Psi_2 = \frac{E_{in}R_c(R_1 + R_2)}{(R_1 + R_b)(R_2 + R_c)}\left(\frac{E_{in}R_2R_c}{(R_1 + R_b)(R_2 + R_c)} - \hat{V}_o\right) \tag{5.13}$$

$$\frac{\partial E_{AC}}{\Delta\omega\partial R_1} = -I_{R_1}\Phi_{R_1} = -\frac{E_{in}R_2R_c}{(R_1 + R_2)^2(R_2 + R_c)}\left(\frac{E_{in}R_2R_c\beta}{(R_1 + R_b)(R_2 + R_c)} - \hat{V}_o\right) \tag{5.14}$$

and

$$\frac{\partial E_{AC}}{\Delta\omega\partial R_2} = \frac{E_{in}R_c^2\beta}{(R_1 + R_b)(R_2 + R_c)^2}\left(\frac{E_{in}R_2R_c\beta}{(R_1 + R_b)(R_2 + R_c)} - \hat{V}_o\right) . \tag{5.15}$$

Now, the second-order partial derivatives will be calculated to form the Hessian matrix for use with the negative gradient technique in finding the optimal values of R_1, R_2 and β at different $\hat{V}_o$. By direct differentiation of the first-order partial derivatives:

$$\frac{\partial^2 E_{AC}}{\Delta\omega\partial R_1^2} = \frac{E_{in}R_2R_c\beta}{(R_2 + R_c)(R_1 + R_b)^3}\left\{\frac{3E_{in}R_2R_c\beta}{(R_2 + R_c)(R_1 + R_b)} - 2\hat{V}_o\right\} \tag{5.16}$$

$$\frac{\partial^2 E_{AC}}{\Delta\omega\partial R_1\partial R_2} = -\frac{E_{in}R_2R_c\beta}{(R_1 + R_b)^2(R_2 + R_c)^2}\left(\frac{2E_{in}R_2R_c\beta}{(R_1 + R_b)(R_2 + R_c)} - \hat{V}_o\right) \tag{5.17}$$

$$\frac{\partial^2 E_{AC}}{\Delta\omega\partial R_1\partial\beta} = -\frac{E_{in}R_2R_c}{(R_1 + R_b)^2(R_2 + R_c)}\left(\frac{2E_{in}R_2R_c\beta}{(R_1 + R_b)(R_2 + R_c)} - \hat{V}_o\right) \tag{5.18}$$

$$\frac{\partial^2 E_{AC}}{\Delta\omega\partial R_2^2} = -\frac{E_{in}R_c^2\beta}{(R_1 + R_b)(R_2 + R_c)^3}\left(\frac{E_{in}\beta(2R_2 - R_c)}{(R_1 + R_b)(R_2 + R_c)} - 2\hat{V}_o\right) \tag{5.19}$$

$$\frac{\partial^2 E_{AC}}{\Delta\omega\partial R_2\partial\beta} = \frac{E_{in}R_c^2}{(R_1 + R_b)(R_2 + R_c)^2}\left(\frac{2\beta R_2R_cE_{in}}{(R_1 + R_b)(R_2 + R_c)} - \hat{V}_o\right) \tag{5.20}$$

And now the "locally optimal" values of R_1, R_2 and β can be found for a given $\hat{V}_o$, E_{in}, R_b, R_c and $\Delta\omega$ using the negative gradient technique [25]. Hence, iterate the following expression:

$$\begin{bmatrix} R_1^{K+1} \\ R_2^{K+1} \\ \beta^{K+1} \end{bmatrix} = \begin{bmatrix} R_1^{K} \\ R_2^{K} \\ \beta^{K} \end{bmatrix} - \begin{bmatrix} \frac{\partial^2 E_{AC}^{K}}{\partial R_1^2} & \frac{\partial^2 E_{AC}^{K}}{\partial R_1 \partial R_2} & \frac{\partial^2 E_{AC}^{K}}{\partial R_1 \partial \beta} \\ \frac{\partial^2 E_{AC}^{K}}{\partial R_2 \partial R_1} & \frac{\partial^2 E_{AC}^{K}}{\partial R_2^2} & \frac{\partial^2 E_{AC}^{K}}{\partial R_2 \partial \beta} \\ \frac{\partial^2 E_{AC}^{K}}{\partial \beta \partial R_1} & \frac{\partial^2 E_{AC}^{K}}{\partial \beta \partial R_2} & \frac{\partial^2 E_{AC}^{K}}{\partial \beta^2} \end{bmatrix}^{-1} \begin{bmatrix} \frac{\partial E_{AC}^{K}}{\partial R_1} \\ \frac{\partial E_{AC}^{K}}{\partial R_2} \\ \frac{\partial E_{AC}^{K}}{\partial \beta} \end{bmatrix} \tag{5.21}$$

until the ac-error function is minimized (ideally, equal to zero). Consider the error function

$$E_{AC} = \frac{1}{2} \int_{\Omega} W^2 \left| \frac{E_{in} R_2 R_c \beta}{(R_1 + R_b)(R_2 + R_c)} - \hat{V}_o \right|^2 d\omega$$

and let $W^2 = 1$ so that

$$E_{AC} = \frac{1}{2} \int_{\Omega} \left(\frac{E_{in}^2 R_2^2 R_c^2 \beta^2}{(R_1 + R_b)^2 (R_2 + R_c)^2} - \frac{2\hat{V}_o E_{in} R_2 R_c \beta}{(R_1 + R_b)(R_2 + R_c)} + \hat{V}_o^2 \right) d\omega$$

Thus, it can be seen that this expression reduces to

$$E_{AC} = \frac{\Delta\omega}{2} \left(\frac{E_{in}^2 R_2^2 R_c^2 \beta^2}{(R_1 + R_b)^2 (R_2 + R_c)^2} - \frac{2\hat{V}_o E_{in} R_2 R_c \beta}{(R_1 + R_b)(R_2 + R_c)} + \hat{V}_o^2 \right) \tag{5.22}$$

Hence, digital computer iteration is required until

$$E_{AC}^{K+1} < \hat{E}_{AC} \quad \text{(ideally zero)}$$

where E_{AC}^{K+1} is the $(K+1)^{st}$ error and $\hat{E}_{AC}$ is the maximum acceptable error. Shown in Figure 5.4 is a computer flow chart for the calculation of the optimal values of R_1, R_2 and β using the negative gradient Hessian matrix technique [25]. The values converged upon by the negative gradient technique covered a wide range and convergence was largely dependent upon boundary restrictions placed on R_1, R_2, β and the initial values picked for R_1, R_2 and β. Some of these "locally optimal" values are listed below for $R_c = 3300\Omega$ and $R_b = 300\Omega$ in Table 5.2, and for $R_c = 10{,}000\Omega$ and $R_b = 1{,}000\Omega$ in Table 5.3.

The values listed in Tables 5.2 and 5.3 are "locally optimal" for R_1, R_2 and β. Electronic computer iteration began with the initial values R_{10}, R_{20} and β_o and searched by negative gradient techniques within the boundary restrictions under $R_1 \leq$, $R_2 \leq$ and $\beta \leq$. Also, to maintain a feasible circuit realization, the three search parameters were required to be positive definite throughout the iteration cycle. In each case the performance function converged to zero within 30 iterations, and in 80% of the cases converged within 10 iterations.

Any set of values listed in the preceding Tables 5.2 and 5.3 will yield the desired $\hat{V}_o$ indicated. In fact, there is an entire family of values for R_1, R_2 and β that yield the desired $\hat{V}_o$ provided E_{in}, R_c and R_b are specified by the network designer. And since $E_{in} = 1^V$ (or any reference, i.e., V, mV, μV, etc.) for standard sensitivity analysis [10], only R_b and R_c remain to be specified.

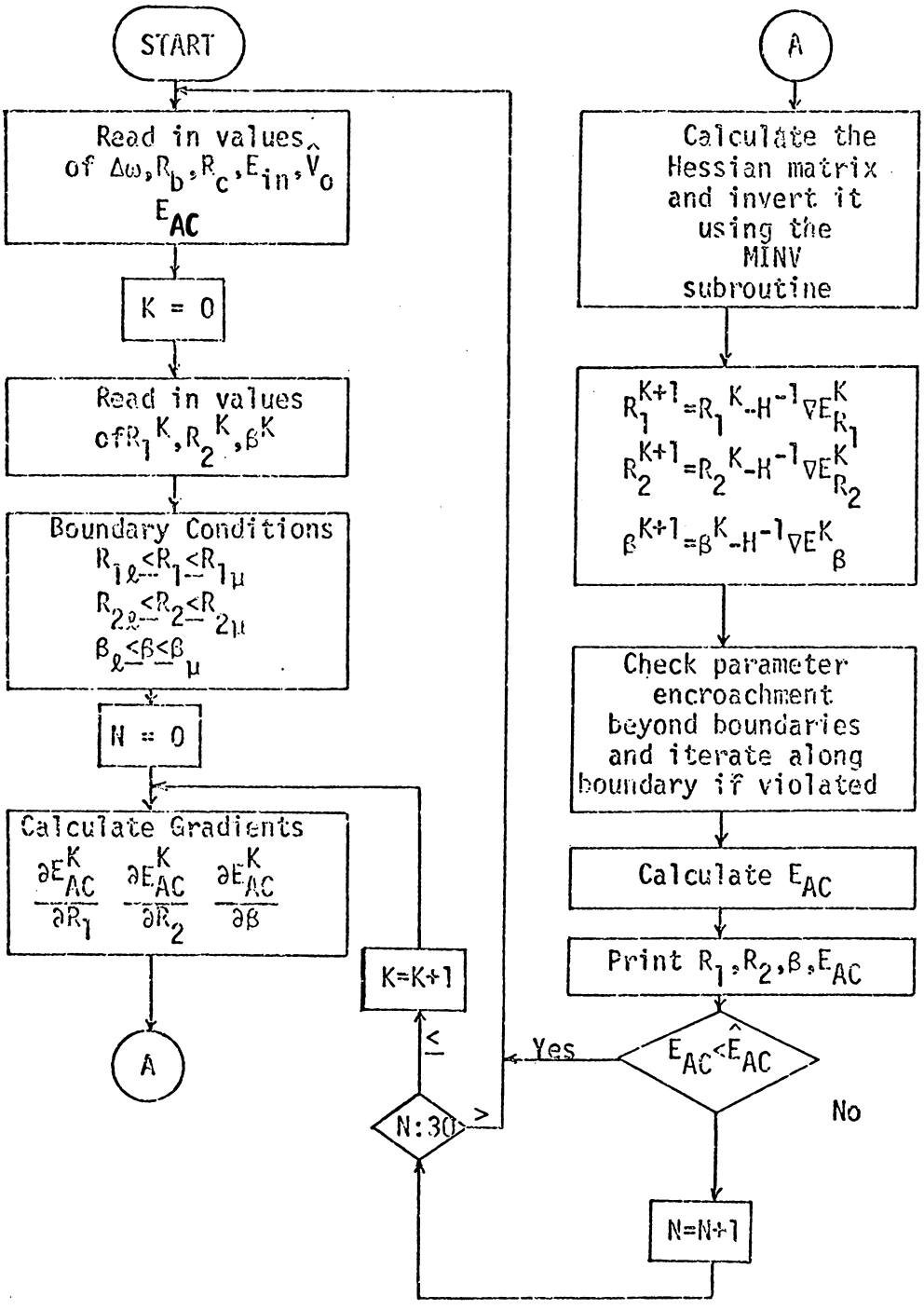

Figure 5.4. Computer flow chart for negative gradient-hessian matrix technique

Table 5.2

$\hat{V}_o$	R_1	R_2	β	$R_{1\leq}$	$R_{2\leq}$	$\beta_{\leq}$	R_{10}	R_{20}	β_o
300	56.93	1541.5	101.9	5,000.	50,000.	350	50	1000	100
250	77.37	1674.1	84.9	1,000.	10,000.	350	40	800	80
200	108.77	1732.2	71.9	500.	5,000.	350	32	640	54
150	435.7	1738.1	96.9	5,000.	50,000.	350	26	519	43
150	405.0	1588.1	98.6	1,000.	10,000.	350	50	1000	100
100	3132.8	2233.8	257.7	5,000.	50,000.	350	50	1000	100
100	330.8	1538.6	60.14	500.	5,000.	350	50	1000	100
100	525.9	1563.3	77.36	1,000.	10,000.	350	50	1000	100
100	2645.5	1496.9	286.0	5,000.	50,000.	350	20	405	34

Table 5.3

$\hat{V}_o$	R_1	R_2	β	$R_{1\leq}$	$R_{2\leq}$	$\beta_{\leq}$	R_{10}	R_{20}	β_o
300	460.6	4948.1	132.4	500	5,000.	350	50	1000	100
300	607.8	4724.9	150.3	1,000.	10,000.	350	100	2000	120
200	2141.7	4508.6	202.2	5,000.	50,000.	350	65	1250	80
150	202.4	4617.2	57.1	500.	5,000.	350	100	2000	120
100	2885.4	4849.9	119.1	5,000.	50,000.	350	50	1000	100
100	4984.9	5019.3	179.1	5,000.	50,000.	350	100	2000	120
100	981.1	5172.3	58.1	1,000.	10,000.	350	50	1000	100
50	5206.0	5075.0	92.2	5,000.	50,000.	350	34	540	36
10	1658.8	4081.0	9.2	5,000.	50,000.	350	25	400	20

5.2 A Graphical AC-Design Technique

Recognizing that all the gradient terms previously calculated have the same common factor, it is evident that they simultaneously can be made equivalent to zero. When the desired performance function of equation (5.1) has been achieved, the gradient terms of equations (5.11 - 5.15) will be equivalently zero; V_o having been made equal to $\hat{V}_o$. This implies that:

$$\hat{V}_o = \frac{E_{in} R_2 R_c \beta}{(R_1 + R_b)(R_2 + R_c)} . \qquad (5.23)$$

This equation involves the three unknown parameters R_1, R_2 and β along with the four specified parameters $\hat{V}_o$, E_{in}, R_b and R_c. Thus there is one equation of three unknown in which two unknowns may be arbitrarily chosen and the third unknown calculated. This lends itself to graphical interpretation rather handily since it is possible to make a two dimensional plot of R_1 vs. R_2 at the various feasible values of β. Consequently, Figures 5.9 - 5.20 illustrate some of the variations possible for different given parameters in this linear resistive model case, taken at a center frequency point. Figures 5.9 - 5.20 were constructed for typical values of transistor input resistance ($0 < R_1 \leq 6^{K}\Omega$), output resistance ($0 < R_2 \leq 100^{K}\Omega$), and current gain ($0 < \beta \leq 300$). Also, they realize a desired output voltage ($0 < \hat{V}_o \leq 300^{V}$) for the arbitrarily picked values of circuit-base resistance (R_b = 200Ω, 300Ω, 400Ω, 1000Ω) and the corresponding values of circuit-collector resistance (R_c = 4,300Ω, 3,300Ω, 2,300Ω,

10,000Ω). A point on any one of the curves satisfies

$$\frac{\partial E_{AC}}{\partial R_1} = \frac{\partial E_{AC}}{\partial R_2} = \frac{\partial E_{AC}}{\partial \beta} = 0 \tag{5.24}$$

and stresses the "local optimality" of the solutions. However, a degree of uniqueness may be given these solutions by considering the minimization of the Figure 5.3.a circuit voltage transfer ratio to parameter sensitivity. Blostein advanced the multiparameter sensitivity approach [21] that the summation of the various voltage transfer ratio to parameter sensitivities should equal zero [21]. Consequently,

$$\sum_{i=1}^{N_R} S_{R_i}^{T_V} + \sum_{i=1}^{N_L} S_{L_i}^{T_V} - \sum_{i=1}^{N_c} S_{C_i}^{T_V} + \sum_{i=1}^{N_r} S_{r_i}^{T_V} - \sum_{i=1}^{N_g} S_{g_i}^{T_V} = 0 \tag{5.25}$$

where $S_{K_i}^{T_V}$ is the normalized voltage transfer function to parameter K sensitivity. Each $S_{K_i}^{T_V}$ sensitivity is summed over i = 1 to i = N_K (where N_K is the number of K-elements in the network). Also, R_i, L_i and C_i denote individual passive elements, and r_i and g_i denote transfer constraints on the current-to-voltage and voltage-to-current transduction, respectively.

Consider the voltage transfer ratio of the circuit in Figure 5.3.a

$$T_V = \frac{V_{out}}{V_{in}} = \frac{-\dfrac{E_{in} R_2 R_c \beta}{(R_1 + R_b)(R_2 + R_c)}}{E_{in}} = -\frac{R_2 R_c \beta}{(R_1 + R_b)(R_2 + R_c)} \tag{5.26}$$

expressed in bilinear form [21], i.e.

$$T_V = \frac{N(K)}{D(K)} = \frac{N_1 + KN_2}{D_1 + KD_2} \tag{5.27}$$

where K is the factored parameter (subscript of $S_K^{T_V}$). Hence, using expression 5-54 from Mitra [21]

$$S_K^{T_V} = \frac{D_1}{D} - \frac{N_1}{N}$$

yields

$$S_\beta^{T_V} = \frac{(R_1 + R_b)(R_2 + R_c)}{(R_1 + R_b)(R_2 + R_c)} = 1$$

and

$$S_{R_1}^{T_V} = \frac{R_b(R_2 + R_c)}{(R_1 + R_b)(R_2 + R_c)} - \frac{\beta R_2 R_c}{\beta R_2 R_c}$$

$$S_{R_1}^{T_V} = \frac{R_b}{R_1 + R_b} - 1 \; . \tag{5.28}$$

Also,

$$S_{R_2}^{T_V} = \frac{R_c(R_1 + R_b)}{(R_1 + R_b)(R_2 + R_c)} = \frac{R_c}{R_2 + R_c} \tag{5.29}$$

and

$$S_{R_b}^{T_V} = \frac{R_1(R_2 + R_c)}{(R_1 + R_b)(R_2 + R_c)} - \frac{R_2 R_c \beta}{R_2 R_c \beta}$$

$$S_{R_b}^{T_V} = \frac{R_1}{R_1 + R_b} - 1 \tag{5.30}$$

and

$$S_{R_c}^{T_V} = \frac{R_2(R_1 + R_b)}{(R_1 + R_b)(R_2 + R_c)}$$

$$S_{R_c}^{T_V} = \frac{R_2}{(R_2 + R_c)} . \qquad (5.31)$$

Hence, applying Blostein's equation (5.25) for a totally resistive network yields

$$\sum_{i=1}^{N_R} S_{R_i}^{T_V} = 0 . \qquad (5.32)$$

And substituting equations (5.28 - 5.31) into equation (5.32)

$$\frac{R_b}{(R_1 + R_b)} - 1 + \frac{R_2}{(R_2 + R_c)} + \frac{R_1}{(R_1 + R_b)} - 1 + \frac{R_2}{(R_2 + R_c)} = 0$$

$$0 \equiv 0$$

reduces it to an identity and satisfies Blostein's requirement.

However, since R_1 and R_2 are internal transistor values h_{ie} and h_{oe} respectively, a more stringent requirement on sensitivity would be to require

$$S_{R_1}^{T_V} + S_{R_2}^{T_V} = 0 . \qquad (5.33)$$

Thus, it is seen that

$$\frac{R_b}{(R_1 + R_b)} - 1 + \frac{R_c}{(R_2 + R_c)} = 0$$

and

$$\frac{R_b(R_2 + R_c) + R_c(R_1 + R_b)}{(R_1 + R_b)(R_2 + R_c)} = 1$$

and

$$R_b R_c = R_1 R_2 \tag{5.34}$$

is required for the circuit "T_V" to be insensitive to the transistor h_{ie} and h_{oe} parameters.

Expression (5.34) combined with expression (5.23) yields a unique point for each β-value at which the model supplies the desired $\hat{V}_o$ together with a total voltage transfer function to resistance sensitivity of zero. Hence, the resulting contours resemble those depicted in Figure 5.5. The typical curves of Figure 5.5 are drawn for given values of R_b, R_c, E_{in} and $\hat{V}_o$ at various values of β.

Considering the previous development, an ac-design algorithm emerges which eliminates electronic computer search techniques to find an optimal solution. The design algorithm can now be enunciated as follows:

I) Given: A network structure whose overall voltage or current gain requires enhancement within some frequency range.

II) Basic AC-design algorithm:

1) Select the possible transistor "growth" location (points A-B-0 in Figure 5.6).

2) Assign the required values to V_{A0} and V_{B0} to yield the desired V'_{out}/V'_{in} ratio.

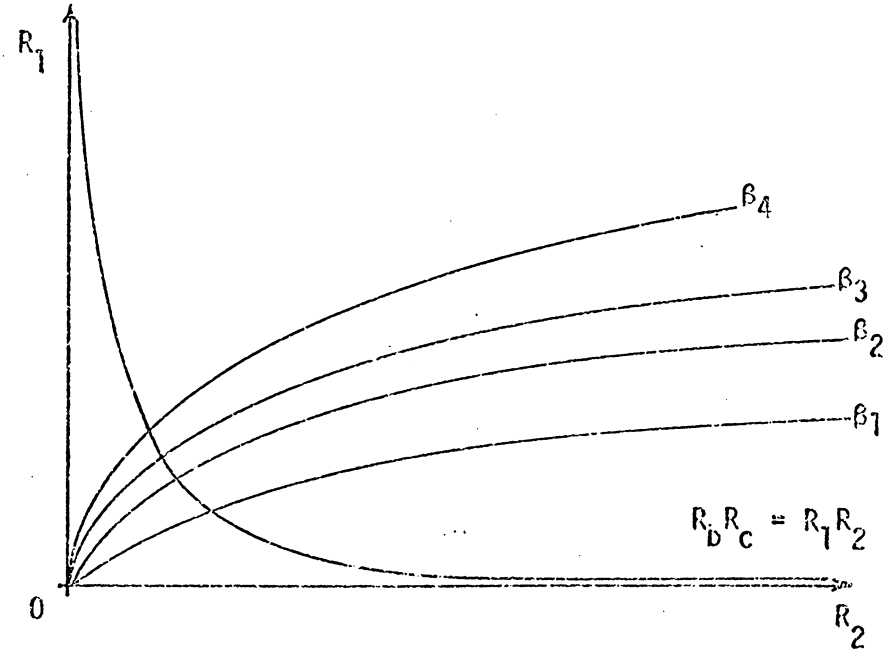

Figure 5.5. Typical contours

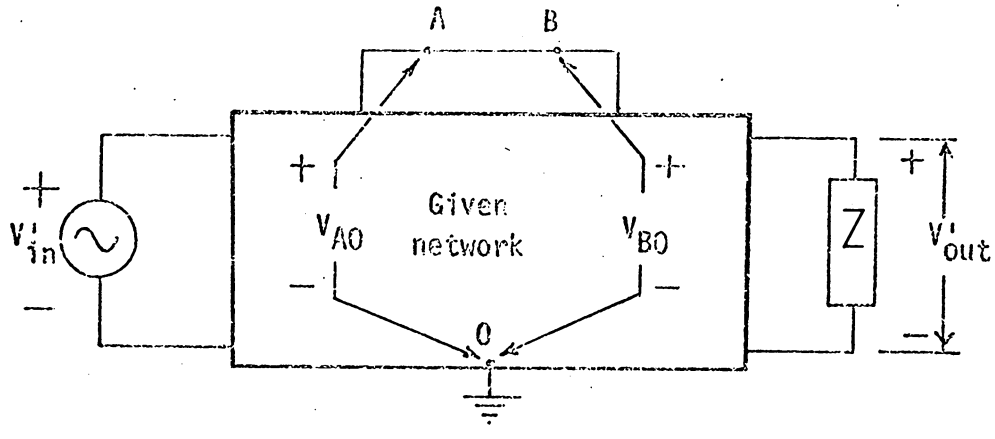

Figure 5.6. Given network

3) Analyze the original and adjoint network using Director and Rohrer's technique [35] to determine the transistor "growth" indicator gradients.

4) If the "growth" gradients show that a common emitter small signal transistor configuration is required, then equations (5.34) and (5.23) are applied to determine a set of curves similar to Figure 5.5.

5) Select from the curves the best combination of R_1, R_2 and β to yield a minimally sensitive model for the required V_{BO}/V_{AO} ratio.

5.2.1 Differential amplifier design example

Consider the low frequency AC-design of a simple differential amplifier. The given network appears in Figure 5.7.a including biasing circuitry.

The desired excitation-response requirement is the following. If

$$|V_S(j\omega)| = 1.0^V$$

then

$$|V_{out}(j\omega)| = 100.0^V$$

for

$$0 \leq \omega \leq 1 \text{ MHz}.$$

Now, since the common-mode amplifier operation has a zero valued driving source, consider design for the differential mode of operation only. In the differential mode of operation the given network can be reduced to the following for AC-design [10].

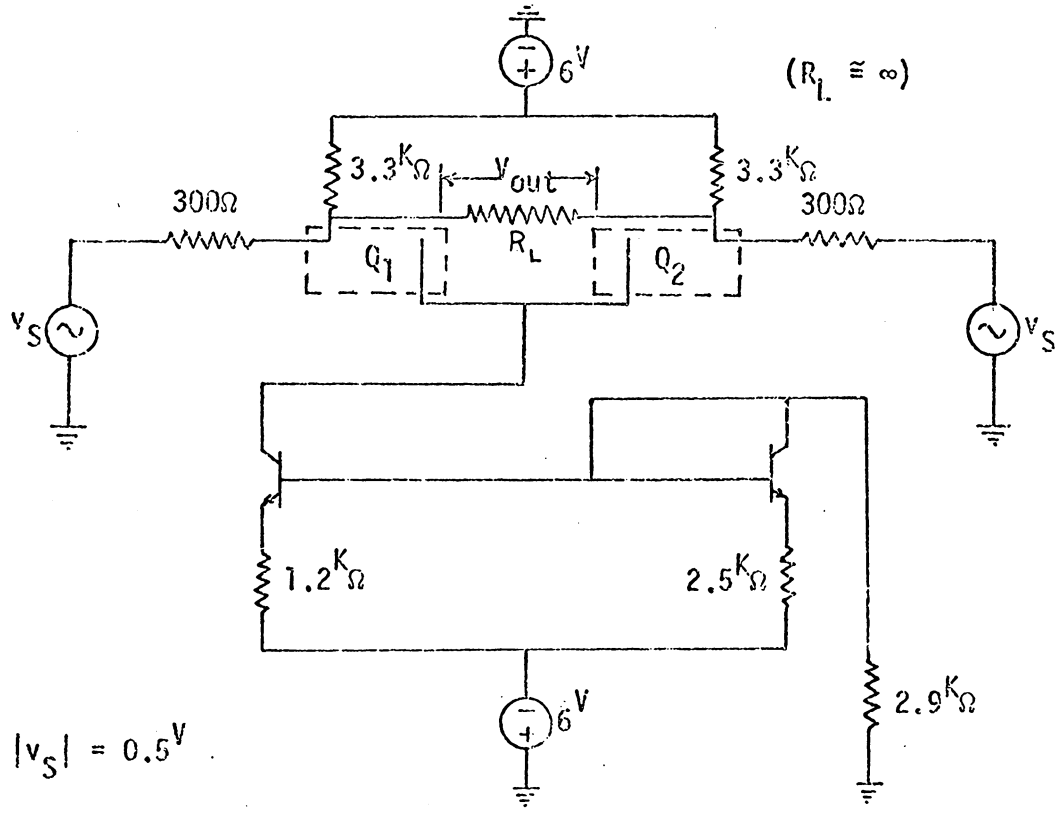

Figure 5.7.a. Differential amplifier

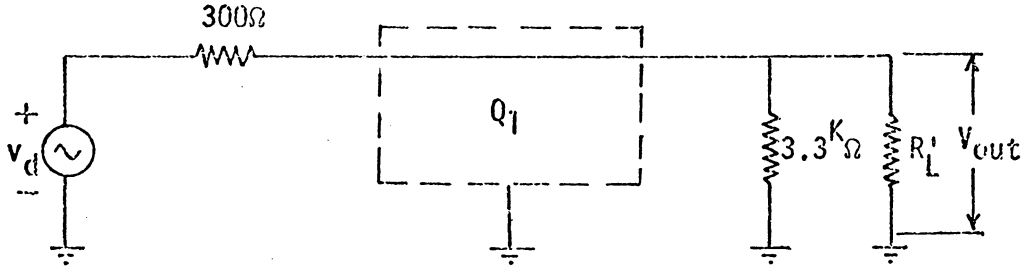

$$|V_S(j\omega)| = |v_d| = 2|v_S| = 1.0^V$$

Figure 5.7.b. Reduced differential amplifier

Now, considering the preceding network and analyzing it for the "growth" indicator gradients of a "zero valued" transistor at location Q_1, it is seen that:

$$\frac{\partial E_{AC}}{\partial \beta} = -\Delta\omega I_1 \Psi_2 = -24.184 \cdot 10^6$$

$$\frac{\partial E_{AC}}{\partial \mu} = -\Delta\omega V_1 \Phi_2 = -266.014 \cdot 10^6$$

$$\frac{\partial E_{AC}}{\partial \mu\beta} = -\Delta\omega [I_1 \Psi_2 + V_1 \Phi_2] = -290.198 \cdot 10^6$$

Thus the "growth" gradients indicate that a common-emitter configuration can be placed at location Q_1 as well as its symmetrical location Q_2 (i.e. condition #4 of Table 5.1). Also, if the 300Ω resistor and the $3.3^K\Omega$ resistor is included in the developed model as R_b and R_c, respectively, then $V_{AO} = E_{in} = v_d$ and $V_{BO} = V_{out}$. Equations (5.34) and (5.23) can now be utilized to determine a set of curves for the given R_b=300Ω, $R_c = 3.3^K\Omega$, $E_{in} = 1^V$ and $V_{out} = 100.0^V$. These curves are depicted in Figure 5.10. Consequently, for a transistor whose β = 100, Figure 5.10 indicates that R_1 (h_{ie} of the transistor) = 700Ω and R_2 (h_{oe} of the transistor) = 1414.3Ω are also required for a minimum voltage transfer function to resistance sensitivity of zero.

The preceding values were determined from the intersection of the $R_1R_2 = R_bR_c$ curve with the β = 100 curve. In the second case, letting R_b = 400Ω and R_c = 2300Ω at β = 100, R_1 and R_2 were found from Figure 5.10 to be 500Ω and 1,840Ω, respectively. Similarly, letting R_b = 200Ω and R_c = 4,300Ω, R_1 and R_2 were determined to equal 740Ω and 1162.1Ω.

The three previous examples are indicative of the variations in

R_1 and R_2 as R_b and R_c are varied. Considering the values $R_b = 300\Omega$ and $R_c = 3.3^{K}\Omega$, the final realization of Figure 5.7.a is shown in Figure 5.8.

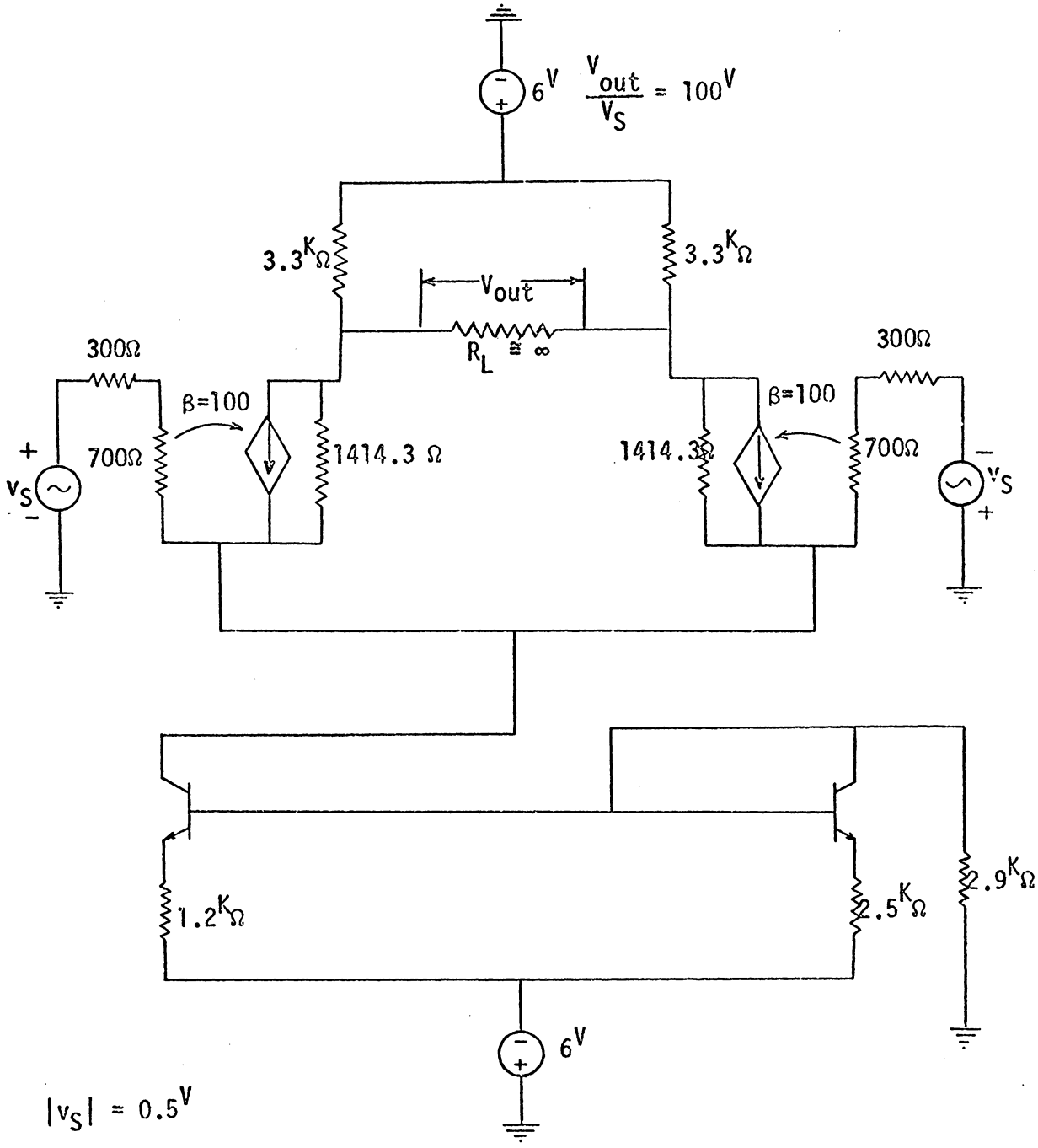

Figure 5.8. The final differential amplifier realization

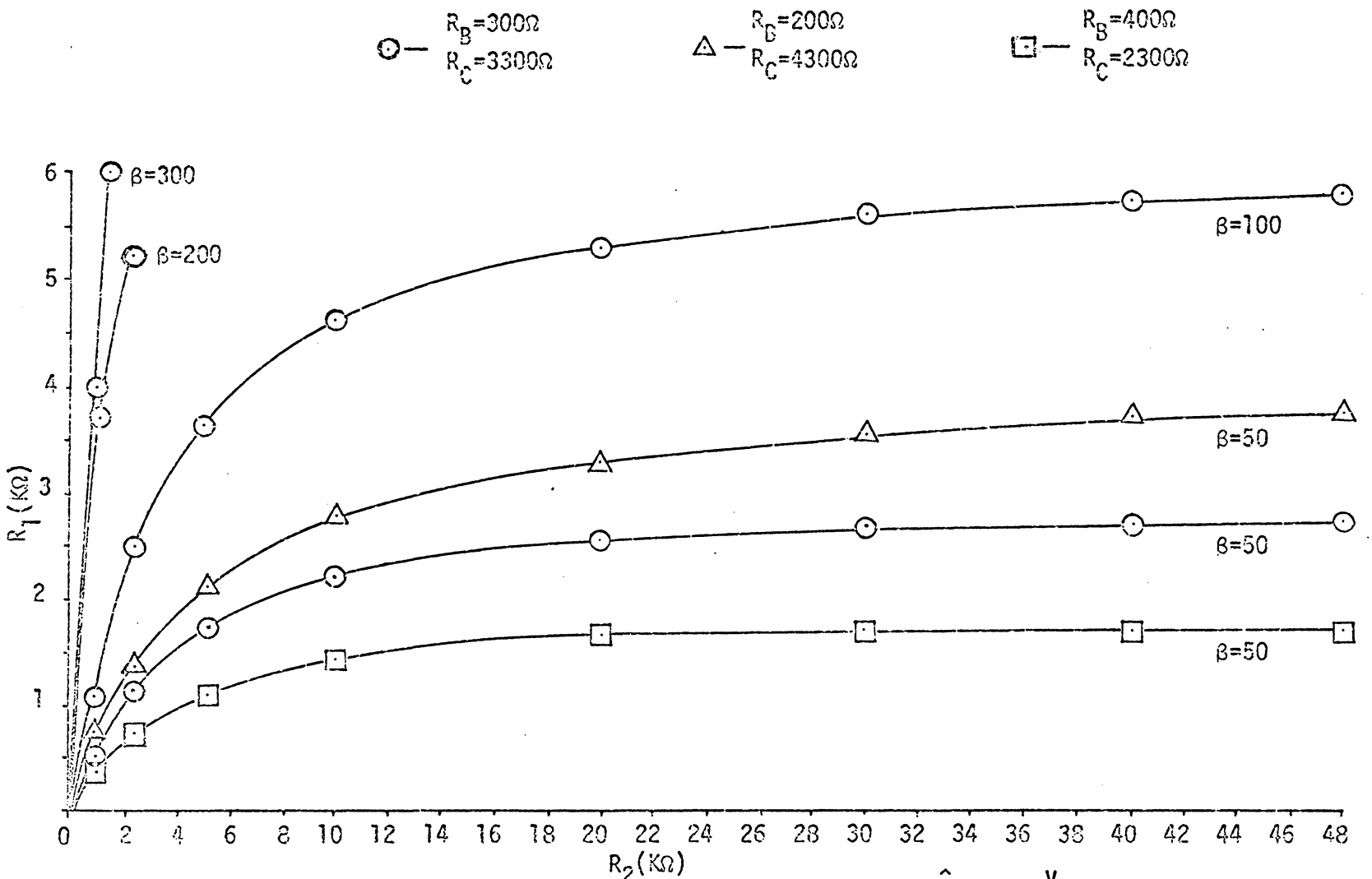

Figure 5.9. Small signal model characteristics at $\hat{V}_o = 50^V$

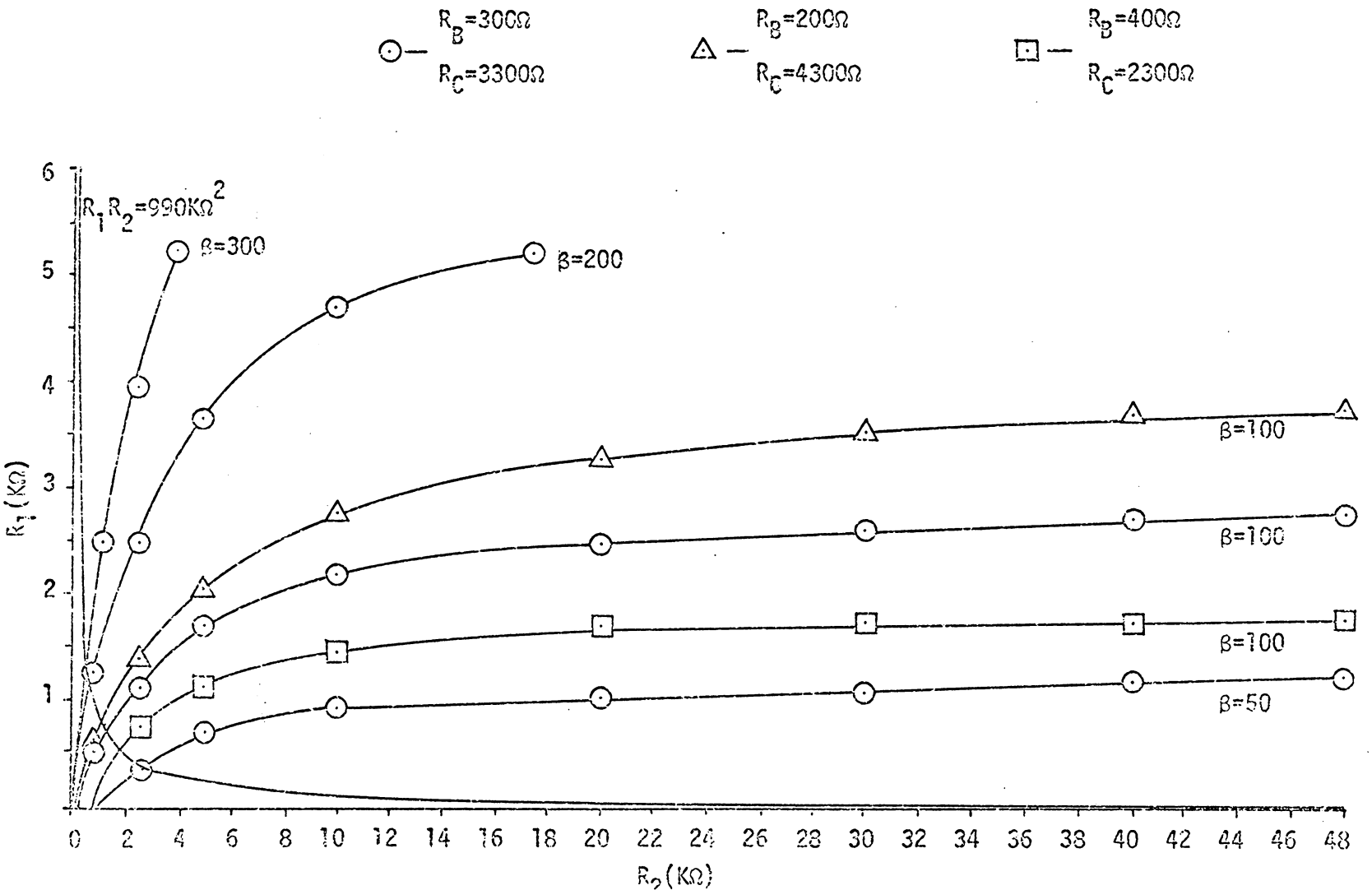

Figure 5.10. Small signal model characteristics at $\hat{V}_o = 100^V$

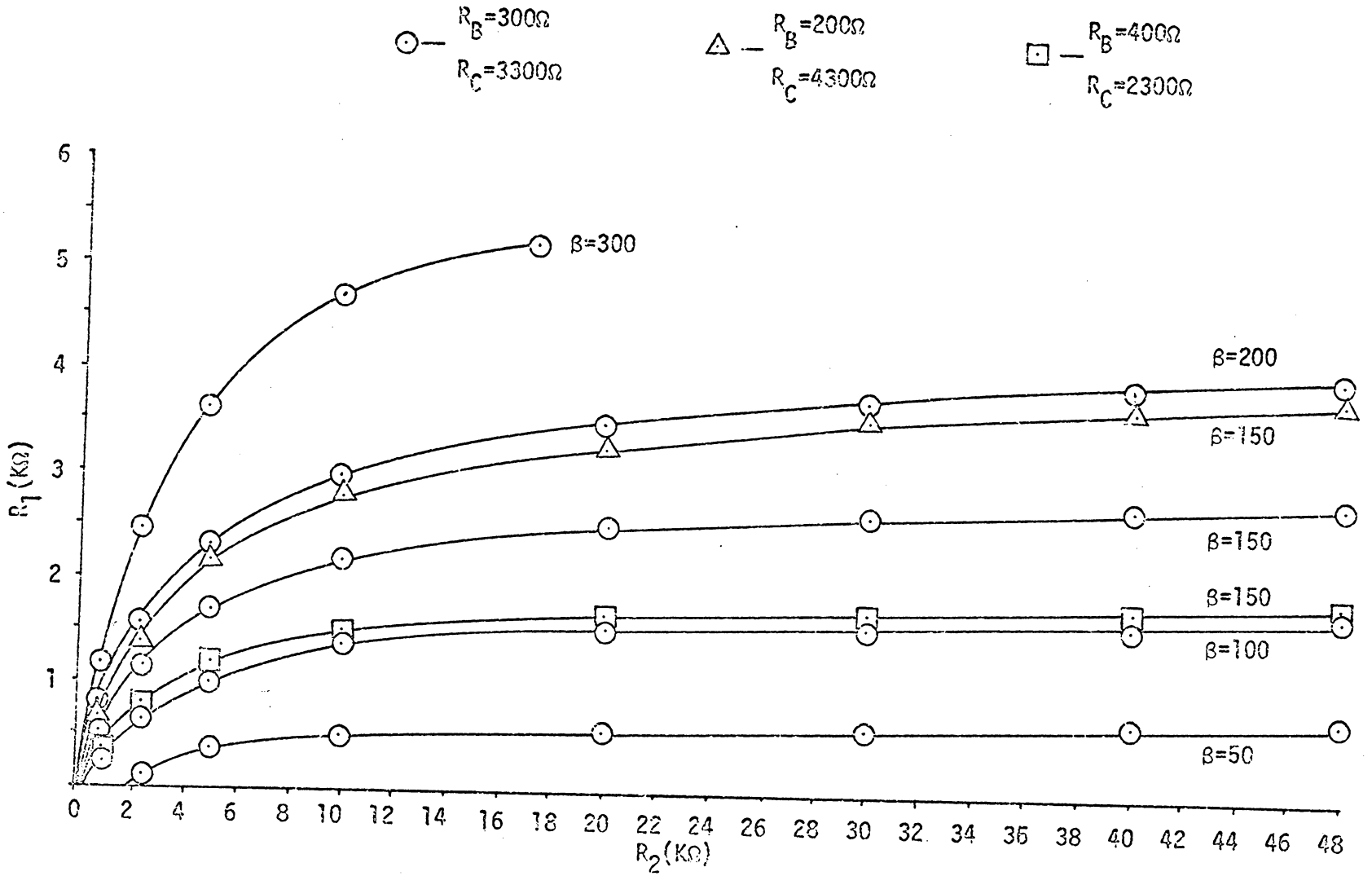

Figure 5.11. Small signal model characteristics at $\hat{V}_o$=150^V

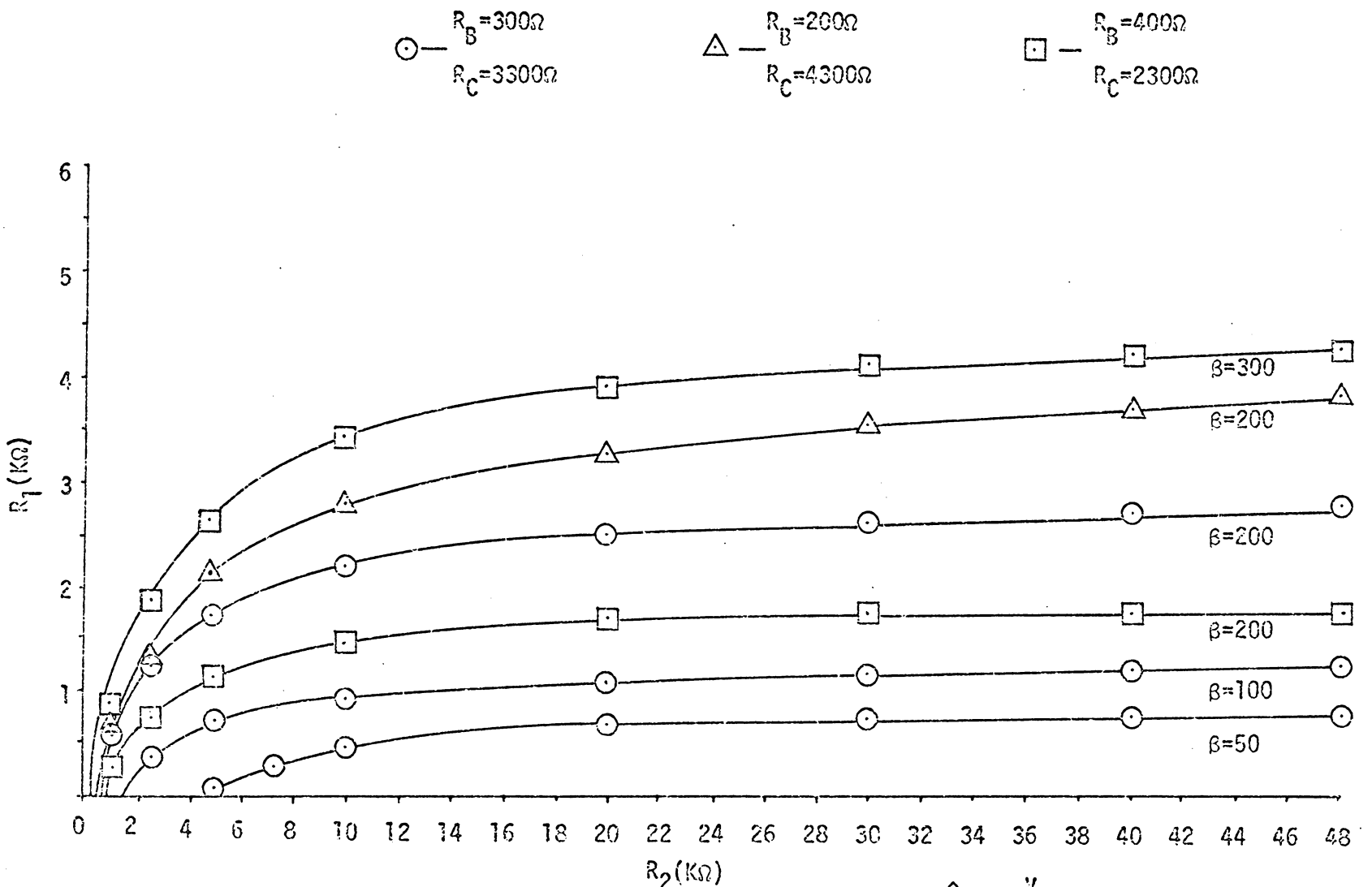

Figure 5.12. Small signal model characteristics at $\hat{V}_c$=200^V

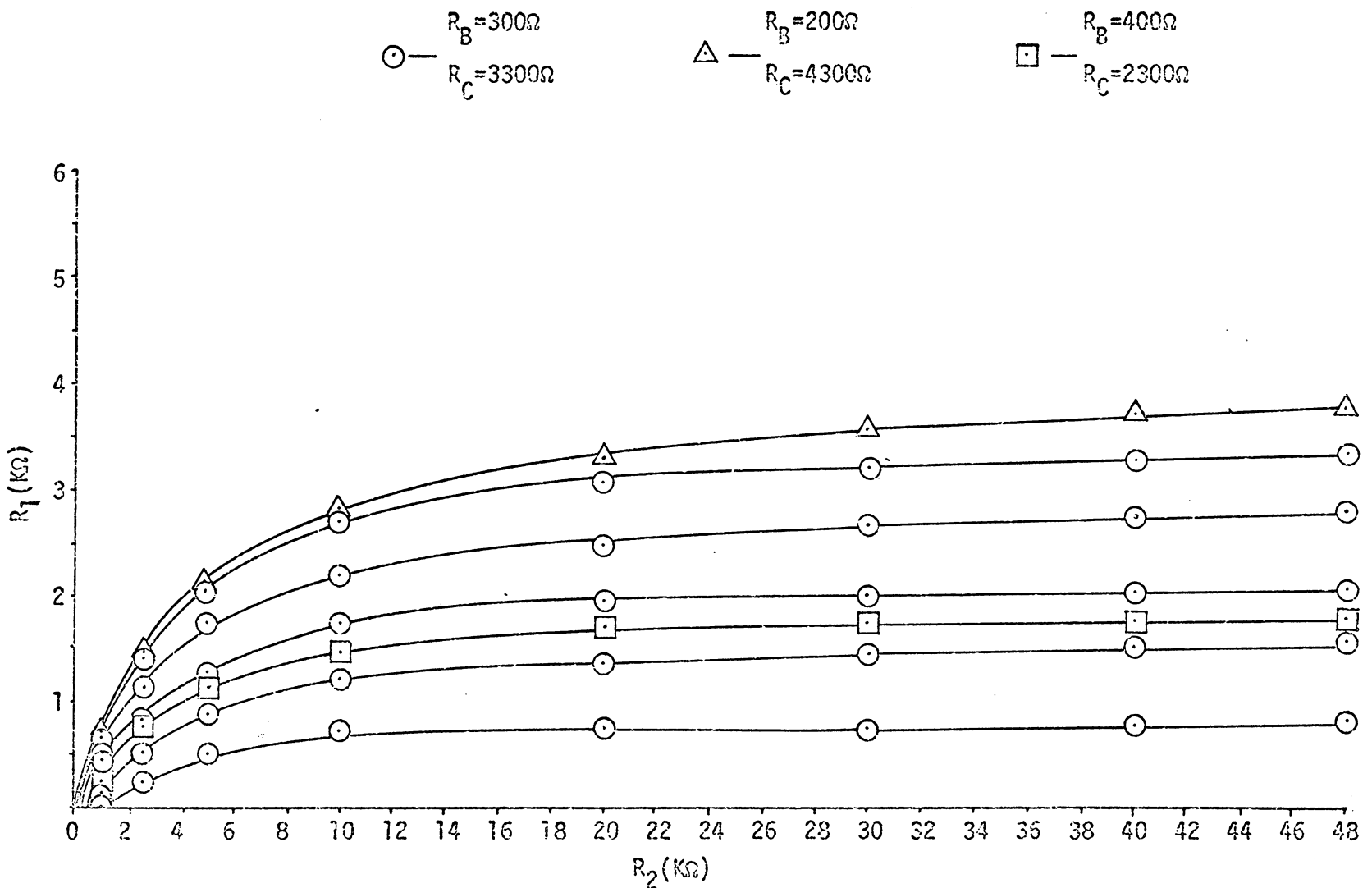

Figure 5.13. Small signal model characteristics at $\hat{V}_o$=250^V

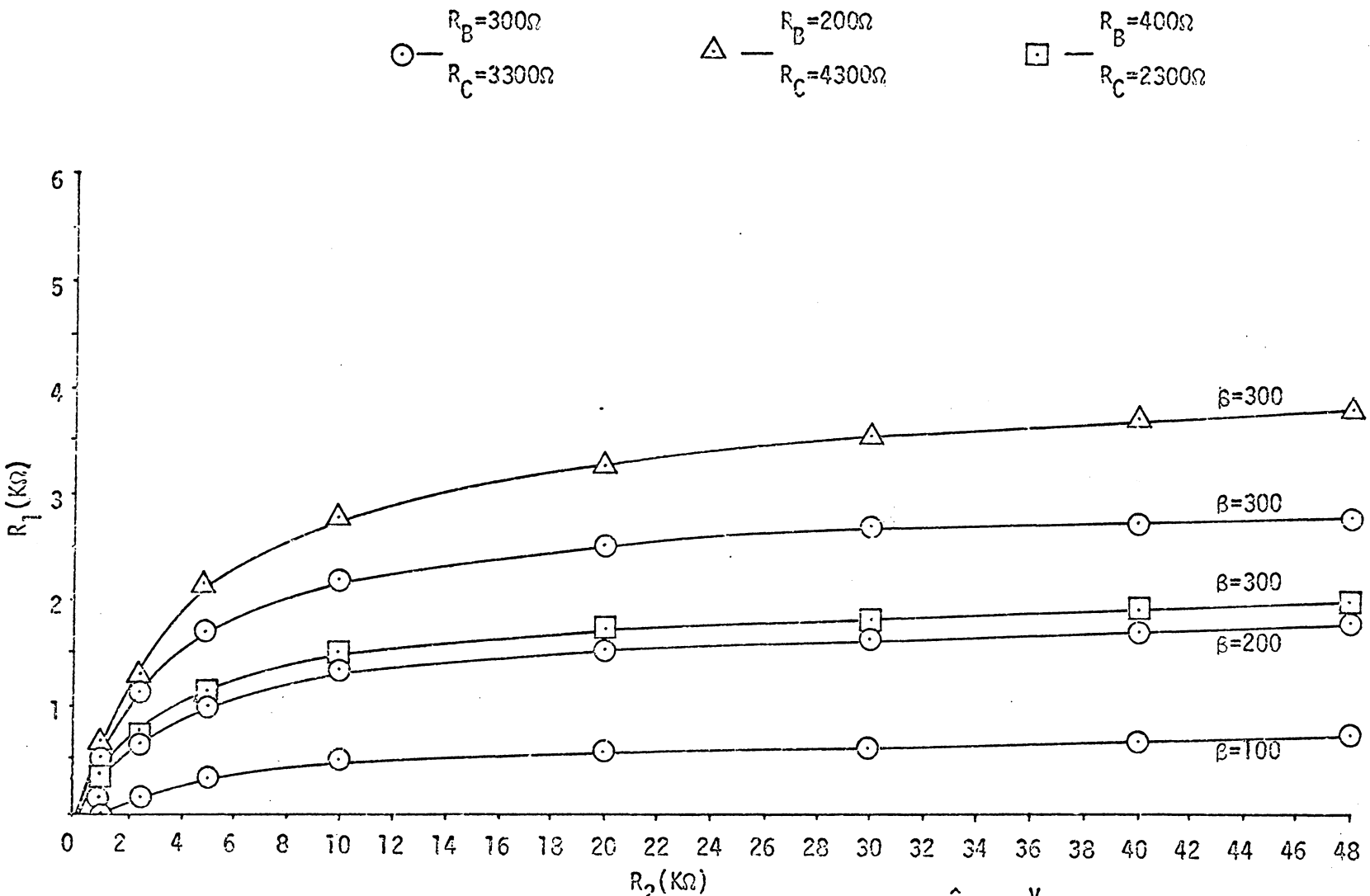

Figure 5.14. Small signal model characteristics at $\hat{V}_o$=300^V

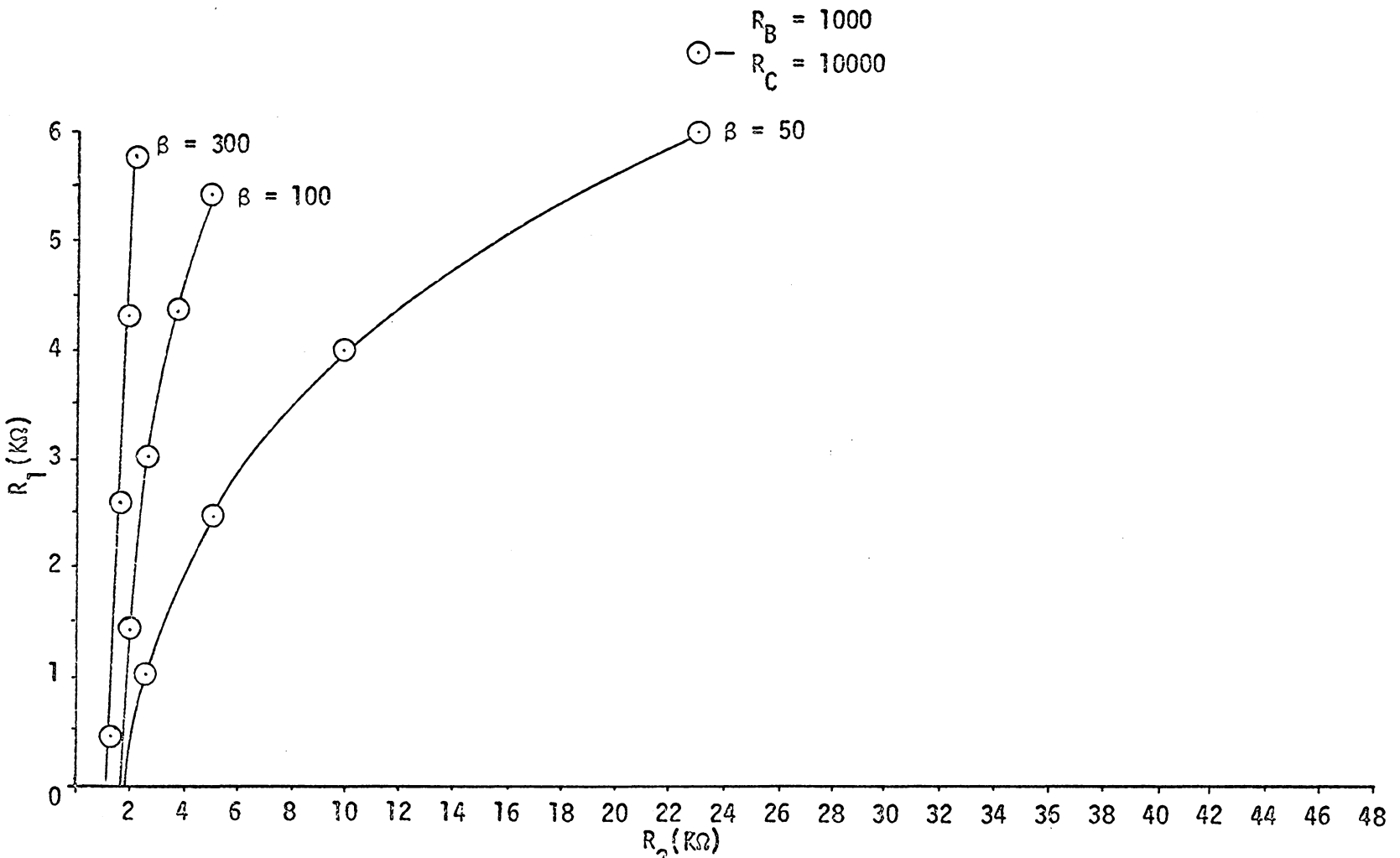

Figure 5.15. Small signal model characteristics at $\hat{V}_o = 50^V$

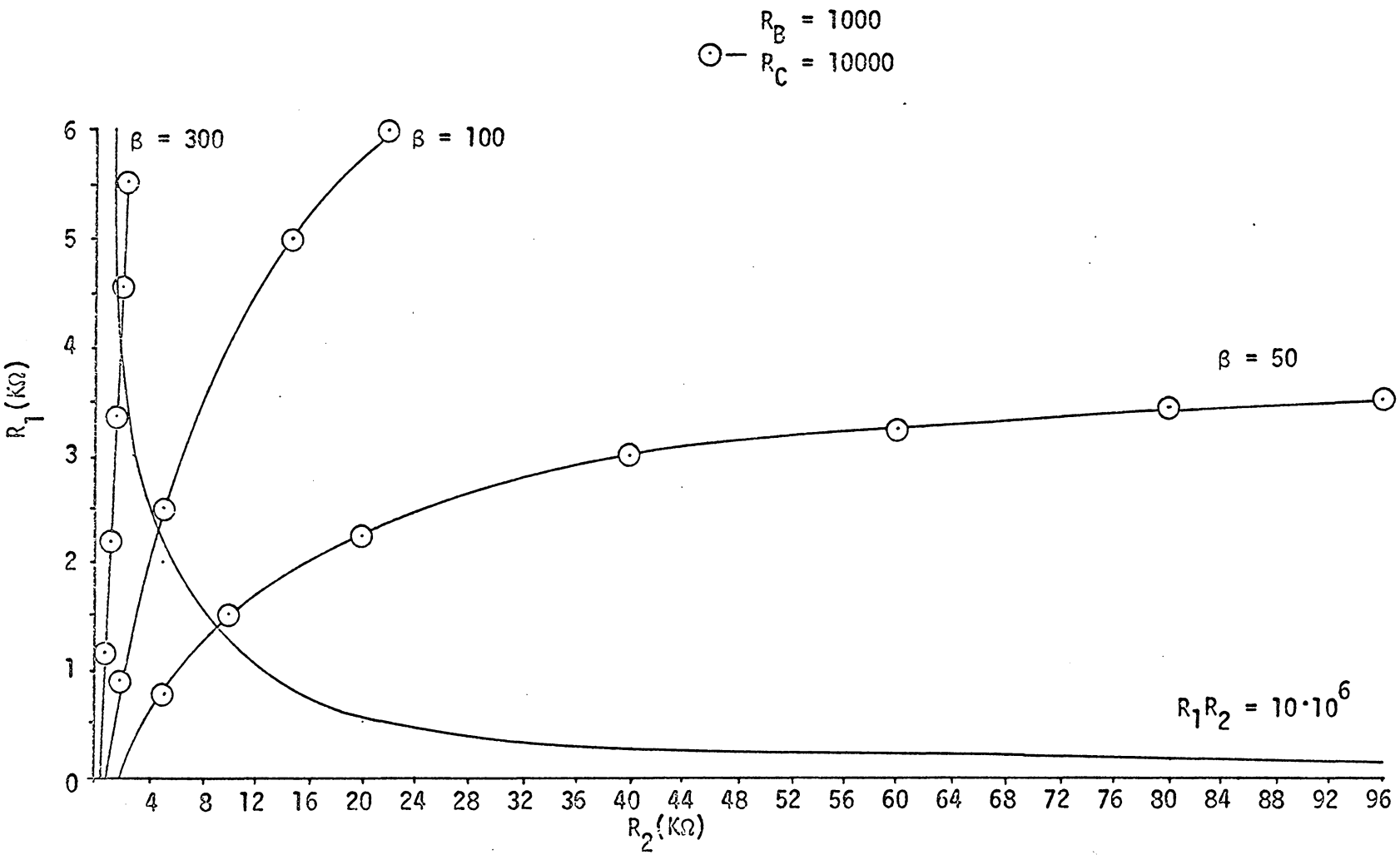

Figure 5.16. Small signal model characteristics at $\hat{V}_o = 100^V$

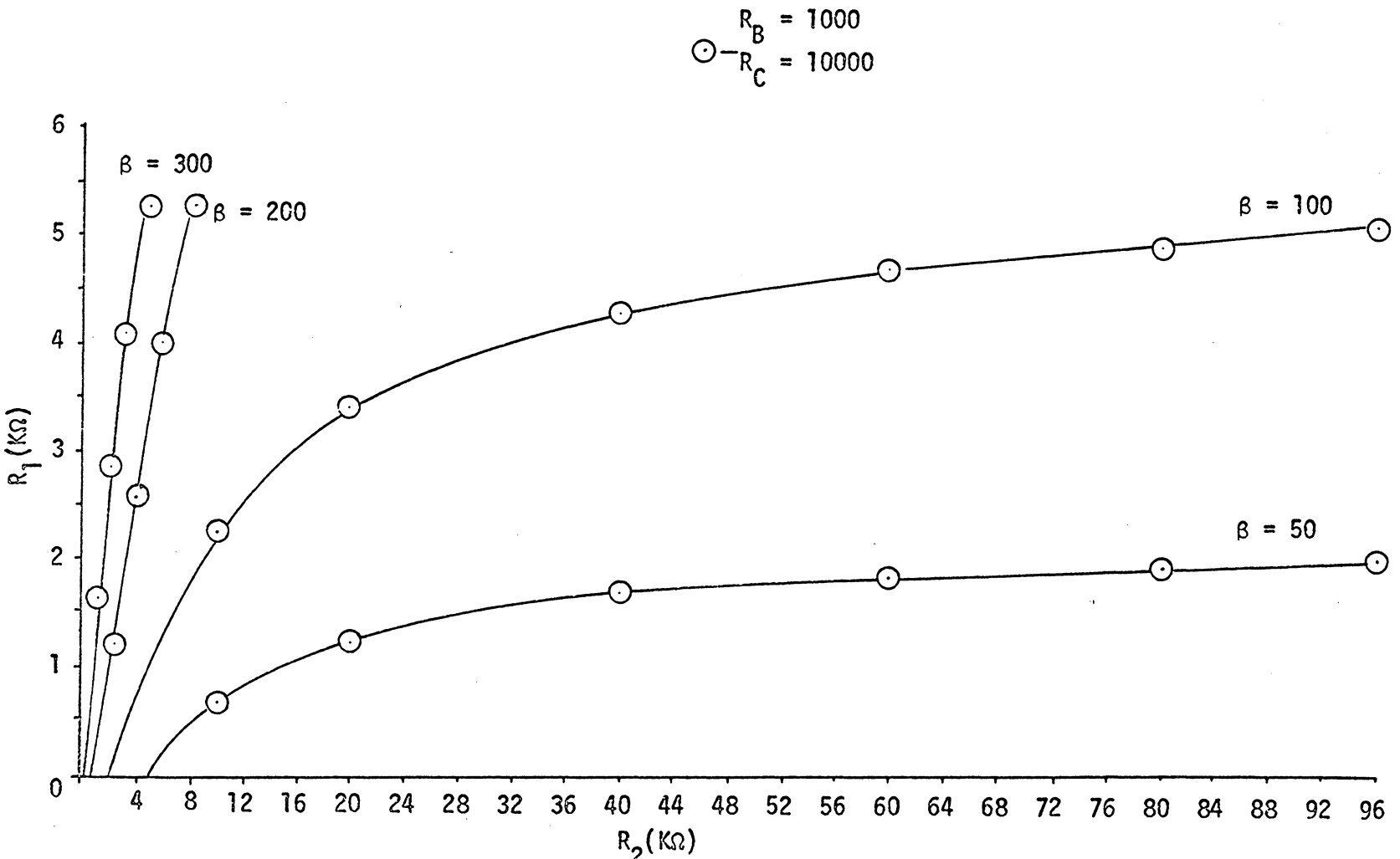

Figure 5.17. Small signal characteristics at $\hat{V}_o = 150^V$

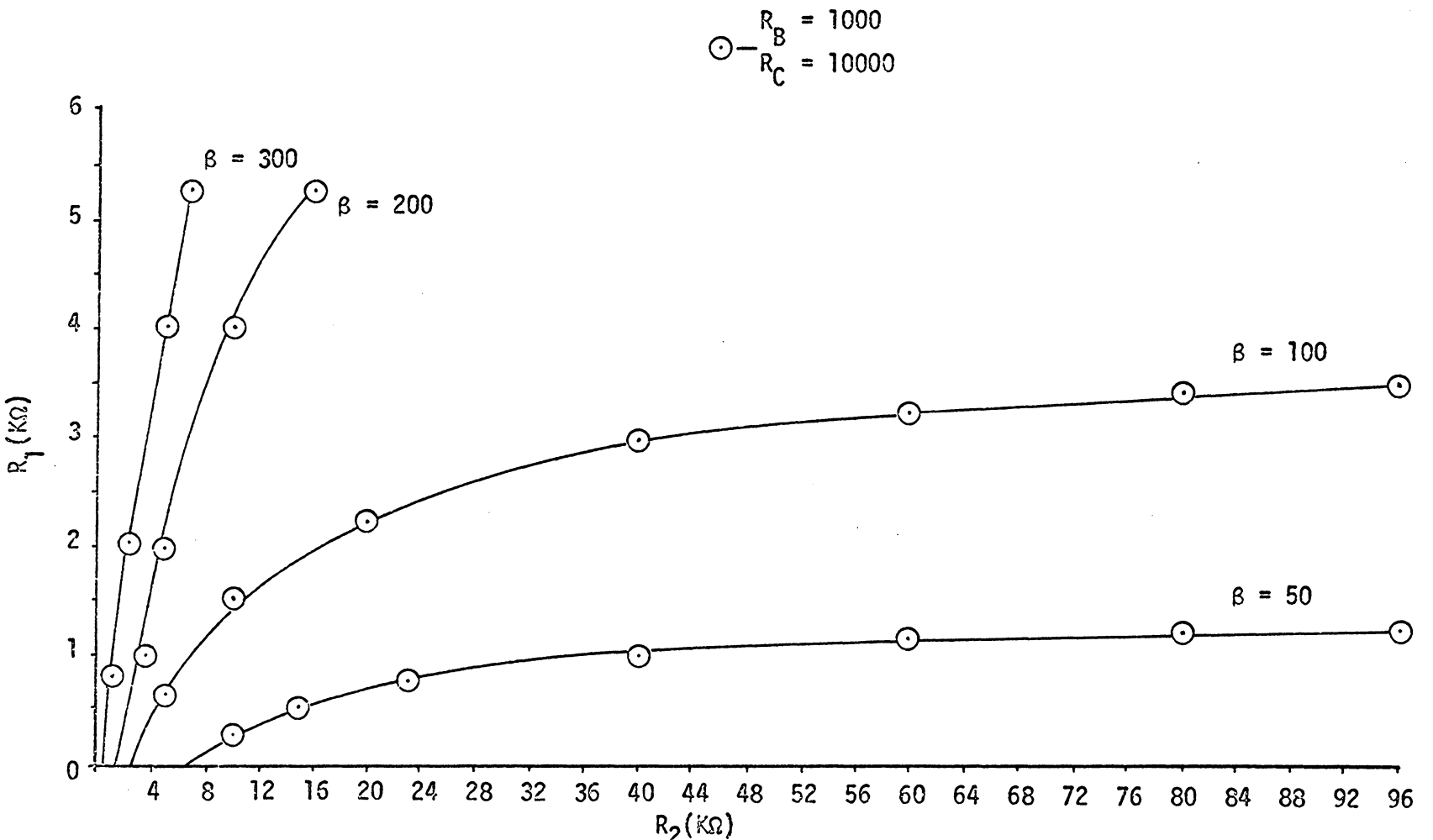

Figure 5.18. Small signal characteristics at $\hat{V}_o = 200^V$

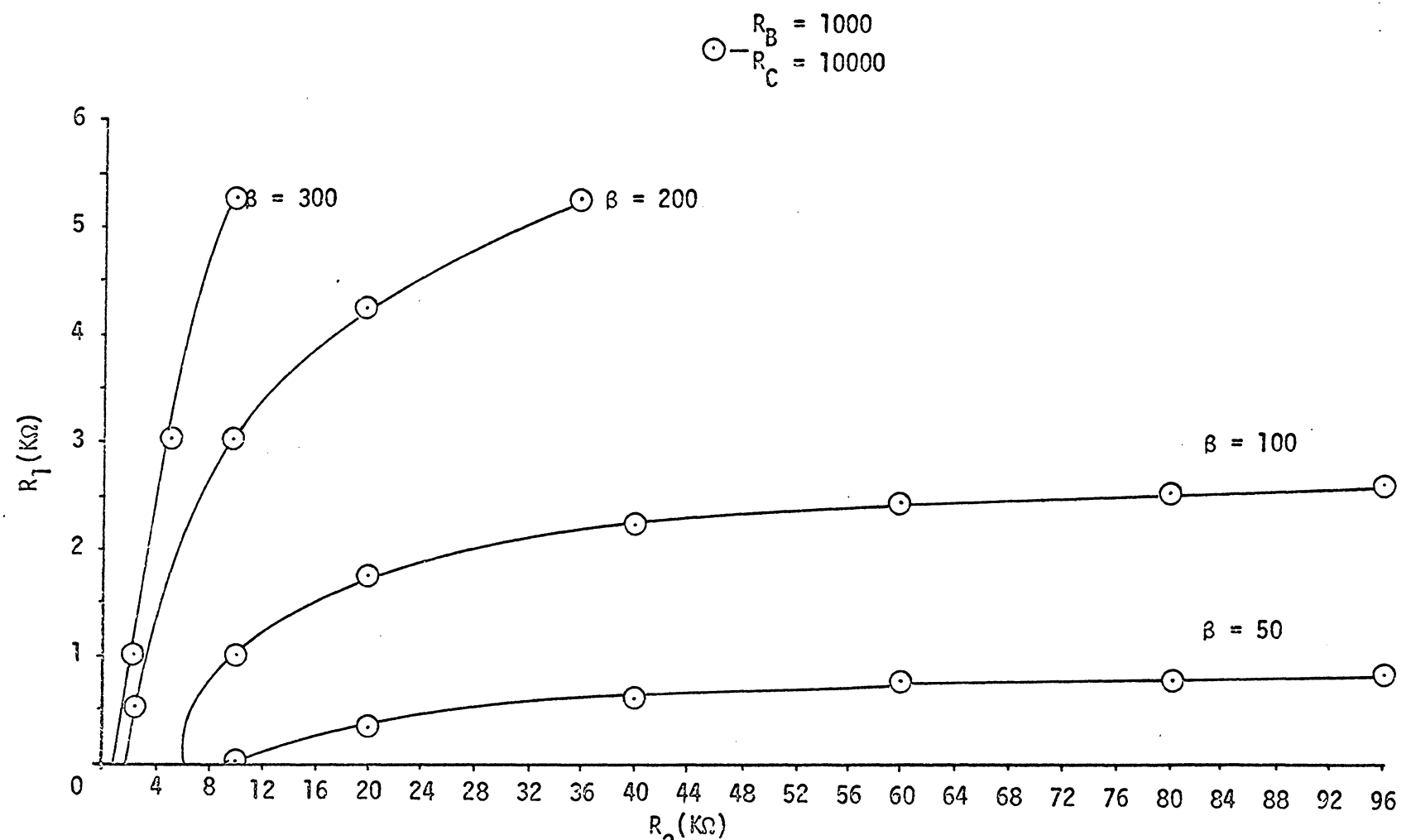

Figure 5.19. Small signal characteristics at $\hat{V}_o = 250^V$

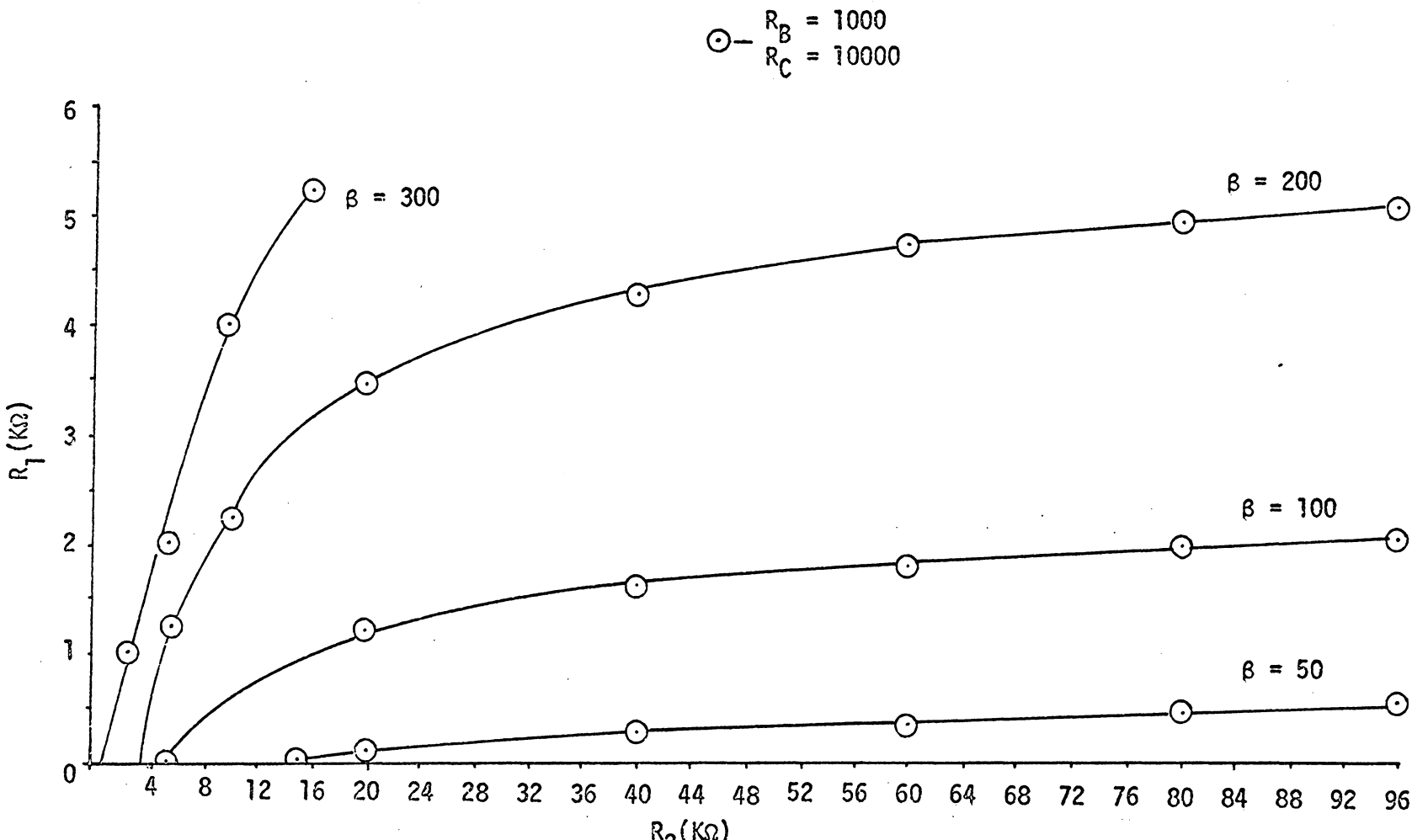

Figure 5.20. Small signal characteristics at $\hat{V}_o = 300^V$

VI. TRANSIENT MODEL "GROWTH" ALGORITHM

Device modeling using the basic variable structure design technique presented in section 4.2.2 is advanced in this chapter. Also, it is shown mathematically that only three initial "growth"-indicator gradients are required to calculate those of the six elements in the basic building block structure needed to emulate a desired transient response. Furthermore, these gradients are developed into $v_v(t)$ and $\hat{v}_i(t)$ explicit form, hence making their calculation less tedious. Lastly, the basic design algorithm is enunciated and example problems are employed.

6.1 Basic Variable Structure Technique

The simple fixed structure, linear, time-invariant network of Figure 3.1 provides the basic building block for device transient models. Previous automated design modeling techniques [30] have been ones in which the basic fixed structure was appended with elements in the appropriate gradient indicated locations.

These techniques require a change in network topology with each new element added to the model. Consequently, the model circuit solution program for subsequent gradient computations requires updating to allow for the addition of branch and/or node points. One way to circumvent any change in structure topology, and hence updating the circuit solution program [required in step 2 of the section 4.1.2 algorithm], is to develop the model only in the basic fixed structure form given in Figure 3.1. Then a number of these structures can be cascaded with dependent source coupling (Figure 6.1); using the response of each previous

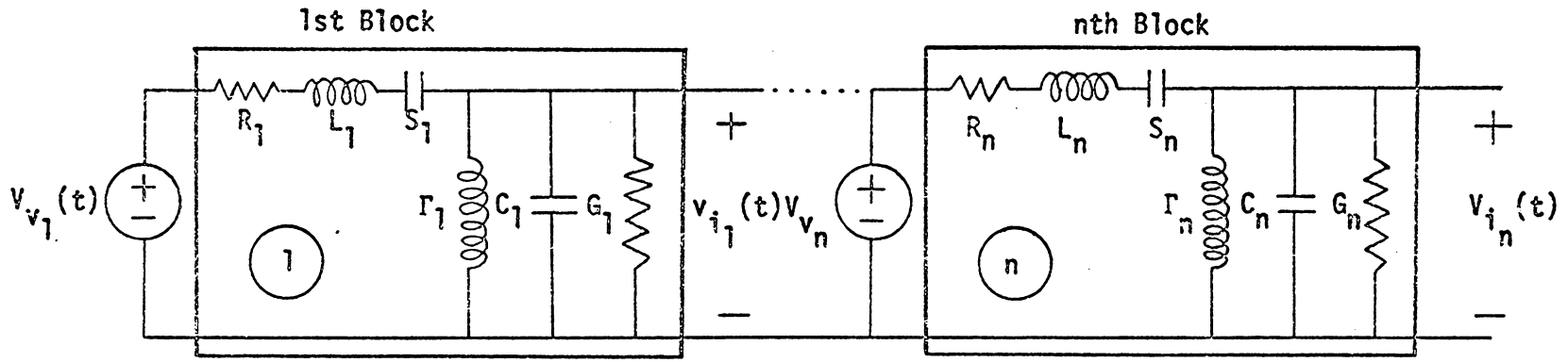

$$T_v = \frac{V_{i_n}}{V_{v_1}} = \prod_{m=1}^{n} \frac{\mu_m s^2 / L_m C_m}{s^4 + s^3\left(\frac{R_m}{L_m} + \frac{G_m}{C_m}\right) + s^2\left(\frac{\Gamma_m}{C_m} + \frac{S_m}{L_m} + \frac{R_m G_m}{L_m C_m} + \frac{1}{L_m C_m}\right) + s\left(\frac{\Gamma_m R_m}{L_m C_m} + \frac{S_m G_m}{L_m C_m}\right) + \frac{S_m \Gamma_m}{L_m C_m}}$$

Figure 6.1. Basic block cascading configuration and overall voltage transfer function in Laplace transform

block as the forcing function of the next block. Unit valued coupling (i.e. $\mu = 1$, $\beta = 1$) provides isolation so as to keep each newly cascaded block from loading or changing the previous blocks output response. Dependent source coupling of the voltage-voltage transducer (VVT) variety can be implemented when the model is designed to emulate a desired voltage response, and a current-current transducer (CCT) when a current response is desired. Also, greater than unity valued coupling (i.e. $\mu > 1$, $\beta > 1$) can be used to "boost" a blocks response and hence reduce any steady-state error. Coupling building blocks in this manner allows device transient responses to be more closely "fitted". For example, a cascade configuration involving three building blocks would generally "fit" a 12th order $v_i(t)$ response to the optimal $\hat{v}_i(t)$ response. In general if n is the number of cascaded building blocks the order z of the "fitted" response would become:

$$z = 4n \tag{6.1}$$

And, once the device model has been realized in the fixed structure form shown in Figure 6.1, the unnecessary elements existing in the fixed structure can be omitted via short and open circuits. These element values are usually down by three orders of magnitude or more from the next element value [35]. However, the initial "growth"-indicator gradients provide a concise means for discerning those of the elements that make negligible contribution toward achieving the desired response function. Consequently, these indicated elements can be included in the fixed structure design at very small values in the series element

cases (R, L, S) and very small values in the parallel element cases (T, C, G). This "protects" the fixed structure topology required by the circuit analysis program for the section 4.1.2 algorithm and after the model has been realized allows these elements to be eliminated by short or open circuits, hence making this a variable structure technique.

6.1.1 Initial "growth" gradients

Once a block has been inserted into the basic model shown in Figure 6.1 only three initial "growth"-indicator gradients need be calculated to determine which elements should be omitted from the final model realization.

Consider the initial circuit structure of Figure 6.2.a in which

$$v_i(t) = -i_v(t)$$

and

$$i_v(t) = -v_v(t)/2$$

and

$$v_i(t) = v_v(t)/2 \; . \qquad t\varepsilon(-\infty, \infty)$$

Also,

$$v_i(t) = -i_v(t)$$

and in backward time ($t = t_o + t_f - \xi$)

$$v_i(t_o + t_f - \xi) = -i_v(t_o + t_f - \xi) \tag{6.2}$$

Similarly, for the adjoint network of Figure 6.2.b, it is seen that

$$\phi_i(\xi) = -\frac{1}{2}]v_v(t_o + t_f - \xi) - 2\hat{v}_i(t_o + t_f - \xi)]$$

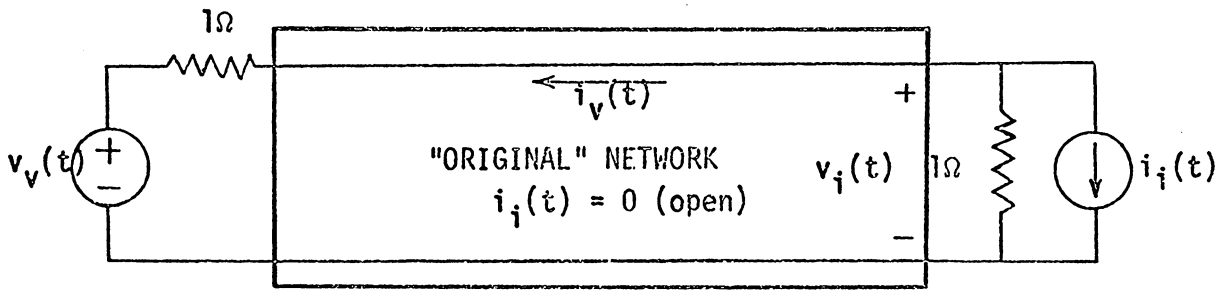

Figure 6.2.a "Original" network used for calculating initial "growth"-indicator gradients

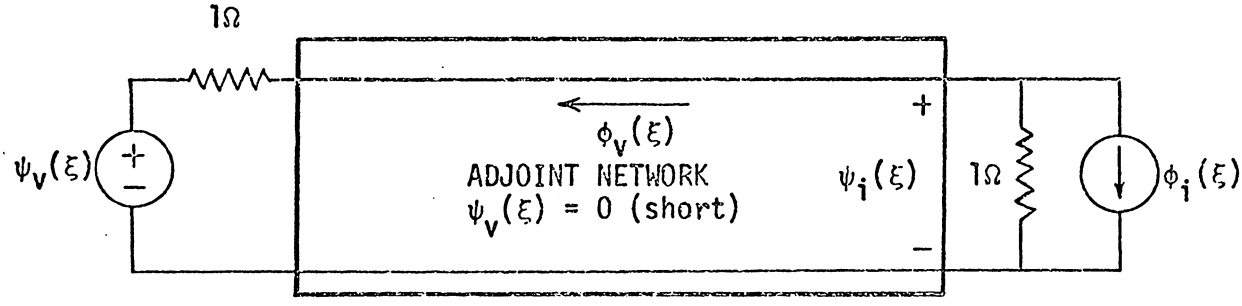

Figure 6.2.b Adjoint network used for calculating initial "growth"-indicator gradients

and

$$\phi_v(\xi) = -\frac{1}{2}\phi_i(\xi)$$

requiring

$$\psi_i(\xi) = -\frac{1}{2}\phi_i(\xi)$$

and hence

$$\psi_i(\xi) = \phi_v(\xi) \ . \tag{6.3}$$

Now, consider the unnormalized resistor initial "growth"-indicator gradient (section 4.2.2)

$$\frac{\partial \hat{E}}{\partial R} = \int_{t_o}^{t_f} -i_v(t_o + t_f - \xi)\phi_v(\xi)d\xi \tag{6.4}$$

and substitute equations (6.2) and (6.3) into (6.4) to yield

$$\frac{\partial \hat{E}}{\partial R} = \int_{t_o}^{t_f} v_i(t_o + t_f - \xi)\psi_i(\xi)d\xi \ . \tag{6.5}$$

Hence, it becomes apparent that the resistance and conductance initial "growth"-indicator gradients of section 4.2.2 are equal and require one integration for both gradients since

$$\frac{\partial \hat{E}}{\partial R} = \frac{\partial \hat{E}}{\partial G} = \int_{t_o}^{t_f} v_i(t_o + t_f - \xi)\psi_i(\xi)d\xi \tag{6.6}$$

In a similar manner it can be shown that

$$\frac{\partial \hat{E}}{\partial L} = \frac{\partial \hat{E}}{\partial C} = \int_{t_o}^{t_f} \dot{i}_v(t_o + t_f - \xi)\phi_v(\xi)d\xi \qquad (6.7)$$

and

$$\frac{\partial \hat{E}}{\partial \Gamma} = \frac{\partial \hat{E}}{\partial S} = \int_{t_o}^{t_f} v_i(t_o + t_f - \xi) \int_{t_o}^{\xi} \psi_i(\eta)d\eta d\xi \ , \qquad (6.8)$$

Consequently, only three gradient calculations are required to determine those elements to be omitted from each block in the final realization. However, the equalities presented in (6.6), (6.7) and (6.8) are applicable only in the initial sense of Figure 6.2 and should not be confused with the six independent gradients of section 4.2.2 that are used in the "growing" process.

6.1.2 Initial "growth"-indicator gradients expressed explicitly in terms of $v_v(t)$ and $v_i(t)$

The initial "growth"-indicator gradients required for the final structure realization can be expressed explicitly in terms of the model defining "known" or "given" quantities $v_v(t)$ and $\hat{v}_i(t)$. Doing so creates a simplistic technique by which the final block by block realization indicated in Figure 6.1 can be reduced to the minimal number of elements capable of producing the desired model transient response. Beginning with the first building block, $v_{v_1}(t)$ is the input or forcing function and $\hat{v}_{i_1}(t)$ is the desired (optimal) block response. The second block would require the $v_{v_2}(t)$ function to be $\mu_2 v_{i_1}(t)$ of the first block and etc.; with the desired $\hat{v}_{i_n}(t)$ the same for each subsequent nth block. Thus, by knowing the $v_{v_n}(t) = \mu_n v_{i_{n-1}}(t)$ for the nth building block and the specified $\hat{v}_{i_n}(t)$, it becomes an easy matter to calculate these gradient

terms; once the gradient expressions of (6.6), (6.7) and (6.8) have been put into $v_{v_n}(t)$ and $\hat{v}_{i_n}(t)$ explicit form.

Recall from Figure 6.2 that

$$-i_{v_n}(t_o + t_f - \xi) = v_{i_n}(t_o + t_f - \xi) = v_{v_n}(t_o + t_f - \xi)/2 \qquad (6.9)$$

and

$$\phi_{v_n}(\xi) = \psi_{i_n}(\xi) = \frac{1}{4}[v_{v_n}(t_o + t_f - \xi) - 2\hat{v}_{i_n}(t_o + t_f - \xi)] \qquad (6.10)$$

and

$$-\dot{i}_{v_n}(t_o + t_f - \xi) = \dot{v}_{i_n}(t_o + t_f - \xi) = \dot{v}_{v_n}(t_o + t_f - \xi)/2 \; . \qquad (6.11)$$

Hence, substituting equations (6.9) and (6.10) into (6.6) yields

$$\frac{\partial \hat{E}}{\partial R} = \frac{\partial \hat{E}}{\partial G} = \frac{1}{8} \int_{t_o}^{t_f} \{v^2_{v_n}(t_o + t_f - \xi) - 2\hat{v}_{v_n}(t_o + t_f - \xi)\hat{v}_{i_n}(t_o + t_f - \xi)\}d\xi \qquad (6.12)$$

and equations (6.10) and (6.11) into (6.7) yields

$$\frac{\partial \hat{E}}{\partial L} = \frac{\partial \hat{E}}{\partial C} = \frac{1}{8} \int_{t_o}^{t_f} \{v_{v_n}(t_o + t_f - \xi) - 2\hat{v}_{i_n}(t_o + t_f - \xi)\}dv_{v_n}(t_o + t_f - \xi) \qquad (6.13)$$

and equations (6.9) and (6.10) into (6.8) yields

$$\frac{\partial \hat{E}}{\partial \Gamma} = \frac{\partial \hat{E}}{\partial S} = \frac{1}{8} \int_{t_o}^{t_f} v_{v_n}(t_o + t_f - \xi) \int_{t_o}^{\xi} [v_{v_n}(\eta) - 2\hat{v}_{i_n}(\eta)]d\eta d\xi. \qquad (6.14)$$

Consequently, the initial "growth"-indicator gradients are now in the proper explicit form and can be calculated by direct differentiation if $\dot{v}_{v_n}(t)$ and $\hat{v}_{i_n}(t)$ are in continuous function form. If $v_{v_n}(t)$

and $\hat{v}_{i_n}(t)$ are in discrete data form, then trapezoidal rule or Simpson's rule integration can be easily implemented on the digital computer.

As an example problem to demonstrate the ease of using the initial "growth"-indicator gradients of expressions (6.12), (6.13) and (6.14), consider the input and desired output functions

$$v_v(t) = 1(t)$$

and

$$\hat{v}_i(t) = 1/2\ 1(t - 1) \quad . \qquad t\xi(-\infty, \infty)$$

Calculation of the resistance and conductance gradient follows:

$$\frac{\partial \hat{E}}{\partial R} = \frac{\partial \hat{E}}{\partial G} = \frac{1}{8}\int_{-\infty}^{\infty}\{[1(-\xi)]^2 - 2\cdot 1(-\xi)\cdot \frac{1}{2}\,1(-\xi - 1)\}d\xi$$

$$\frac{\partial \hat{E}}{\partial R} = \frac{\partial \hat{E}}{\partial G} = \frac{1}{8}\int_{-\infty}^{\infty}\{[1 - 1(\xi)]^2 - [1 - 1(\xi)][1 - 1(\xi + 1)]\}d\xi$$

$$\frac{\partial \hat{E}}{\partial R} = \frac{\partial \hat{E}}{\partial G} = -\frac{1}{8}$$

Also, calculation of the inductance and capacitance gradient yields:

$$\frac{\partial \hat{E}}{\partial L} = \frac{\partial \hat{E}}{\partial C} = \frac{1}{8}\int_{-\infty}^{\infty}\{[1 - 1(\xi)] - [1 - 1(\xi + 1)]\}\delta(\xi)d\xi$$

$$\frac{\partial \hat{E}}{\partial L} = \frac{\partial \hat{E}}{\partial C} = -\frac{1}{16}$$

And, calculation of the elastance and inverse inductance gradient yields:

$$\frac{\partial \hat{E}}{\partial \Gamma} = \frac{\partial \hat{E}}{\partial S} = \frac{1}{8} \int_{-\infty}^{\infty} [1 - 1(\xi)] \int_{-\infty}^{\infty} \{1(\eta) - 1(\eta - 1)\} d\eta d\xi$$

$$\frac{\partial \hat{E}}{\partial \Gamma} = \frac{\partial \hat{E}}{\partial S} = \frac{1}{8} \int_{-\infty}^{\infty} d\xi = \infty$$

Hence, the initial "growth"-indicator gradients imply that a series resistance and inductance and shunt capacitance and conductance should be grown. The elastance and inverse inductance are not required due to the positive nature of the "growth"-indicator gradient. However, to preserve the basic structure topology, they can be included in the model at small values (three orders of magnitude or more) and eliminated from the model with short and open circuits after the model has been parametrically developed using the section 4.1.2 algorithm.

6.2 Basic Variable Structure Block Cascading Algorithm

The following iterative design scheme emerges from the developments in the three previous sections:

I) Define the problem with a "given" $v_{v_1}(t)$, $\hat{v}_{i_1}(t)$ and maximum allowable block error $\hat{E}'$ as well as maximum allowable cascaded configuration error $\hat{E}''$.

II) Calculate the initial "growth"-indicator gradients using equations (6.12), (6.13) and (6.14) and assign very small values to those elements having positive gradients in the Figure 3.1 block structure.

III) Develop the remaining elements in the Figure 3.1 structure using the algorithm presented in section 4.1.2 until the block error E has satisfied $E < \hat{E}'$ in step 6). Iterate one or more times beyond the iterate satisfying $\hat{E}'$ to inspect for $\hat{E}''$ satisfaction (i.e. $E < \hat{E}''$). Store the final $v_{i_n}(t)$. *The advantage of this technique is encountered in this step since the circuit solution program required in step 2) of the section 4.1.2 algorithm is the same for all subsequent blocks of the cascaded configuration.

IV) If $\hat{E}'' \leq E \leq \hat{E}'$, then cascade another block into the Figure 6.1 structure picking μ_n or β_n by either a) or b) below. Then assign this new block an input function $v_{v_n}(t) = \mu_n v_{i_{n-1}}(t)$ and a desired output function $\hat{v}_{i_n}(t) \equiv \hat{v}_{i_{n-1}}(t)$. Return to step II) with the new input and desired output functions, and continue the process until an acceptably small error E is obtained ($E < \hat{E}''$).

a) For each subsequent block input $v_{v_n}(t)$ equal to the output $v_{i_{n-1}}(t)$ of the previous block, pick $\mu_n = 1$ or $\beta_n = 1$.

b) If the previous blocks output $v_{i_{n-1}}(t)$ has a steady state error with respect to the desired $\hat{v}_{i_{n-1}}(t)$ output, then pick

$$\mu_n = \lim_{t \to \infty} \left[\frac{\hat{v}_{i_{n-1}}(t)}{v_{i_{n-1}}(t)} \right] \tag{6.15}$$

or, for a desired current response function $\hat{i}_{v_n}(t)$, pick

$$\beta_n = \lim_{t\to\infty} \left[\frac{\hat{i}_{v_{n-1}}(t)}{i_{v_{n-1}}(t)} \right]. \qquad (6.16)$$

V) Once $E < \hat{E}"$, omit the positive value gradient-indicated elements (step II) from the cascaded block structure by shorting them out if they are an R, L,or S and open circuiting them if they are an Γ, C, or G. This completes the final device model realization.

Figure 6.3 offers a general variable-structure block-cascading flow chart by which a maximum "J"-number of blocks can be cascaded to "fit", in general, a "4n"th order transient response curve. The index "I" fixes the number of iterations by which the section 4.1.2 algorithm searches beyond $E < \hat{E}'$ satisfaction so as to attempt to satisfy $E < \hat{E}"$. This technique will generally "fit" a 4nth order curve with a 4nth order curve to within some specified $\hat{E}"$ maximum allowable error, or a 4nth order curve to a higher order curve satisfying $\hat{E}'$ but not necessarily $\hat{E}"$.

6.2.1 One block (fourth order) design example

Consider the problem of realizing a one block (fourth order) response $v_i(t)$ to emulate the desired $\hat{v}_i(t)$ response shown in Figure 6.4.b. Take the $v_v(t)$ block input to be the following:

$$v_v(t) = 125(1 - e^{-3.449t})$$

Hence, using the prescribed $v_v(t)$ and $\hat{v}_i(t)$ functions, trapezoidal rule integration was performed on the initial "growth"-indicator gradients

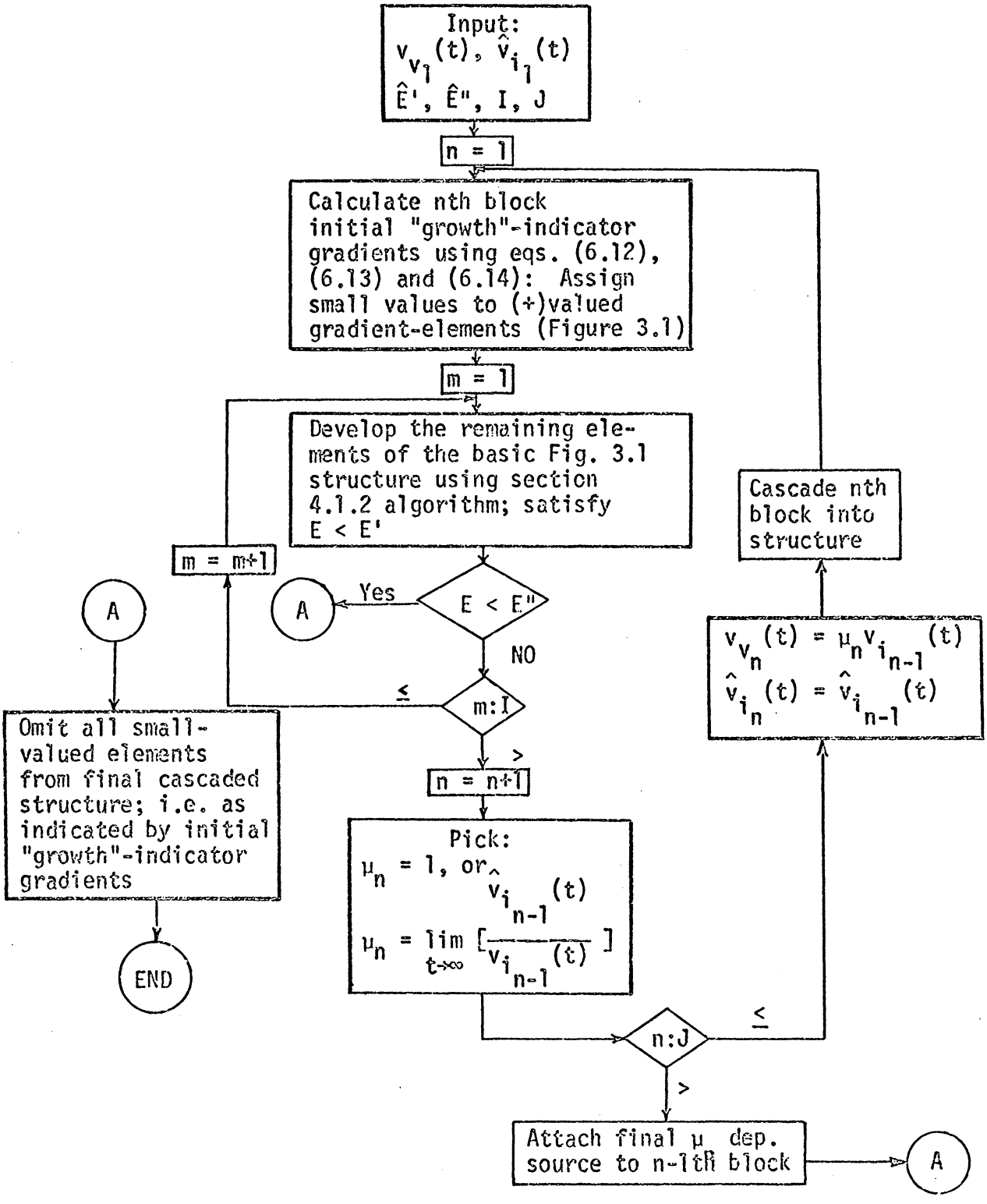

Figure 6.3. Variable-structure block-cascading flow chart

described by equations (6.12), (6.13) and (6.14). These gradients indicated by their negative values that an R, G, S and Γ can be "grown" to meet the $\hat{v}_{i_1}(t)$ response; while the L and C elements of the basic structure (Figure 3.1) have positive valued gradients and are therefore assigned small values (i.e. 1E-8). Four iteration cycles were undertaken using the negative gradient technique to reduce the block error to $E^4 = 0.00327$. Each of the four cycles is shown in Figure 6.4.a, with the individual iterative-cycle responses depicted in Figure 6.4.b.

6.2.2 Two block (eighth order) design realization of a DC motor transient torque model

As a second example problem for implementation of the section 6.2 algorithm consider the realization of $\hat{v}_{i_2}(t)$ shown in Figure 6.5.b for the following truncated romp input $v_{v_1}(t)$ function:

$$v_{v_1}(t) = 50t \qquad 0 \leq t \leq .1$$

$$v_{v_1}(t) = 5.00 \qquad .1 \leq t \leq 10.0$$

The input function $v_{v_1}(t)$ and output function $\hat{v}_{i_2}(t)$ are typical forcing and transient response functions for a DC motor loaded by a DC generator. The $\hat{v}_{i_2}(t)$ function is a brush recorder voltage response produced by a torque transducing helical torsion spring dynamometer [32]. And $v_{v_1}(t)$ represents the mechanical load imposed upon the DC motor by the DC generator when the generator armature is loaded with a truncated ramp function. For the 1st block design a maximum allowable error was specified at $E_1^1 = 0.700$. The initial "growth"-indicator gradients showed that R_1, L_1, C_1, and G_1 could be grown. In four iterations $E_1^4 = 0.197$ with the

parameter values given in Figure 6.5.a and the response $v_{i_1}(t)$ function shown in Figure 6.5.b. Obviously this $v_{i_1}(t)$ response curve does not adequately fit the desired $\hat{v}_{i_2}(t)$ curve, thus a second block was cascaded into the configuration and a maximum allowable two block error was taken at $\hat{E}''_{12} = 0.0200$. The initial "growth"-indicator gradients showed that an L_2 and C_2 could be developed. Subsequently five iterations reduced the error to $E^5_{12} = 0.00189$ and yielded the final realizations depicted in Figures 6.5.a and 6.5.b.

6.2.3 Two block (eighth order) design example

Now consider the realization of a transient model which fits the desired response curve $\hat{v}_{i_2}(t)$ shown in Figure 6.6.b. Once again take the input forcing function to be the following:

$$v_{v_1}(t) = 125(1 - e^{-3.449t})$$

Calculation of the initial "growth" indicator gradients using $v_{v_1}(t)$ and $\hat{v}_{i_2}(t)$ show that R_1, S_1, T_1 and G_1 may be grown while C_1 and L_1 need not be grown. A maximum allowable 1st block error $\hat{E}'_1$ was specified at 0.0500 and four iterations reduced the error to $E^4_1 = 0.0452$. However, this error did not give a satisfactory $v_{i_1}(t)$ [$v_{i_1}(t)$ coincides with 1st iteration - Fig. 6.6.b] curve-fit to the desired $\hat{v}_{i_2}(t)$. Additional iterations failed to improve on the error E^4_1 and hence a second block was cascaded onto the first, with a maximum allowable error $\hat{E}''_{12}$ specification of 0.0099 to insure a closer fit. Once again the initial "growth" indicator gradients were calculated and they indicated that the development of an S_2 and Γ_2 would grow the first blocks response curve $v_{i_1}(t)$ toward

fitting $\hat{v}_{i_2}(t)$ within $\hat{E}''_{12}$. Also, since there was no steady-state error between $v_{i_1}(t)$ and $\hat{v}_{i_2}(t)$ the VVT multiplier μ was taken to be 1. After four iterations were performed upon block two the error function E^4_{12} was well within the prescribed error $\hat{E}''_{12}$, yielding the results depicted in Figure 6.6.b. The first and second block 4th iterate realizations can be evidenced in Figure 6.6.a.

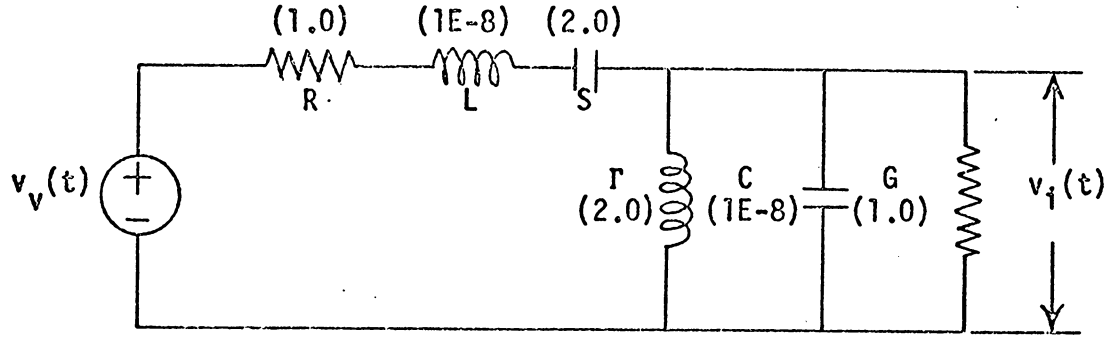

(i) initial circuit

iteration	1	2	3	4
R	1.0	.321	.195	.100
S	2.0	40.0	19.12	21.00
Γ	2.0	3.205	4.566	8.403
G	1.0	0.386	0.337	0.320

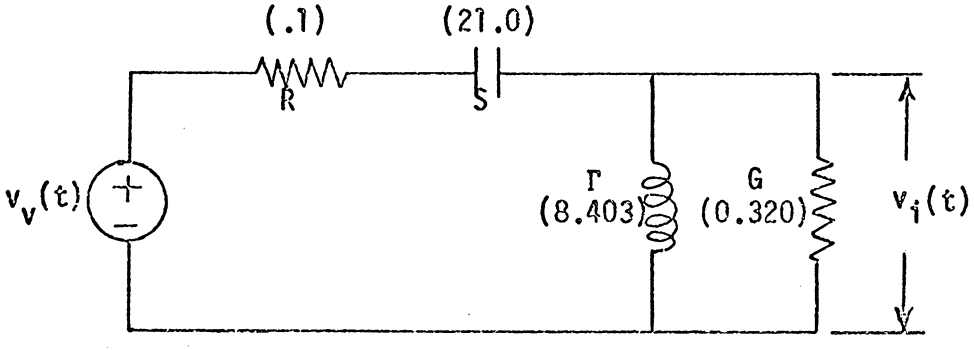

(ii) final circuit

Figure 6.4.a. A one block realization example

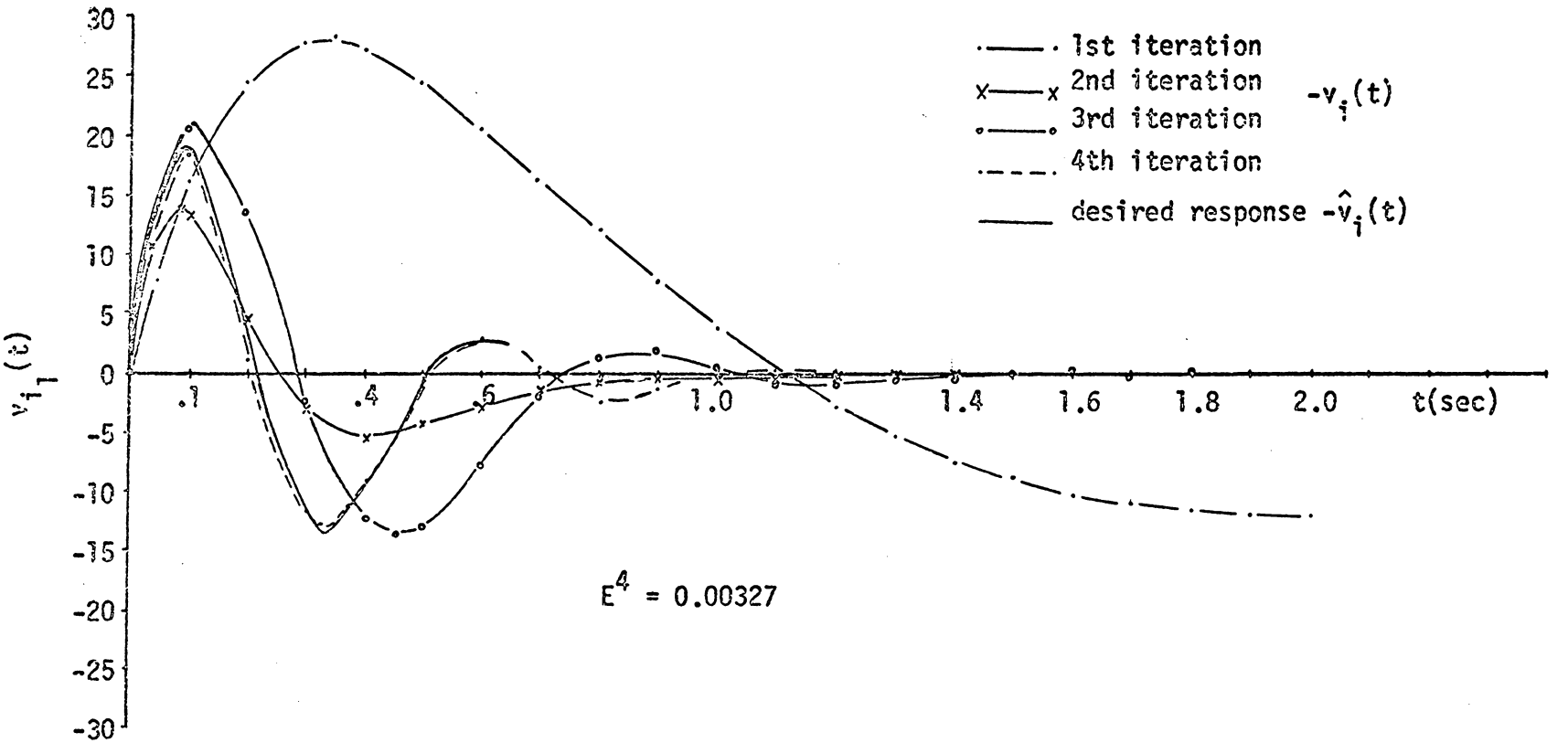

Figure 6.4.b. The block response $v_i(t)$ and desired response $\hat{v}_i(t)$

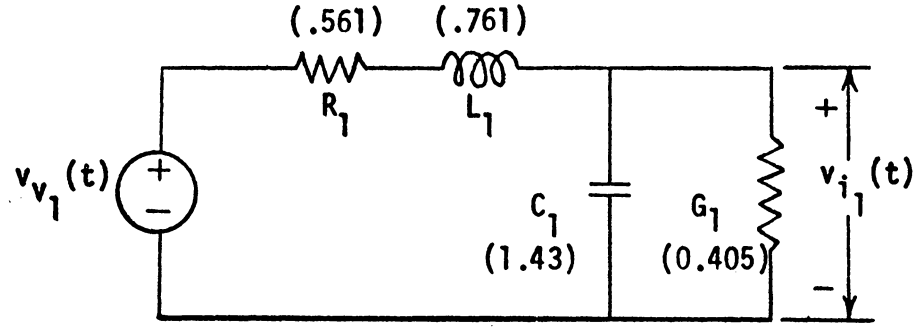

(i) 1st block final realization

iteration	1	2	3	4
R_1	1.00	0.263	0.512	0.561
L_1	2.00	1.542	0.839	0.761
C_1	2.00	1.762	1.495	1.430
G_1	1.00	0.821	0.400	0.405

$E_1^4 = 0.197$

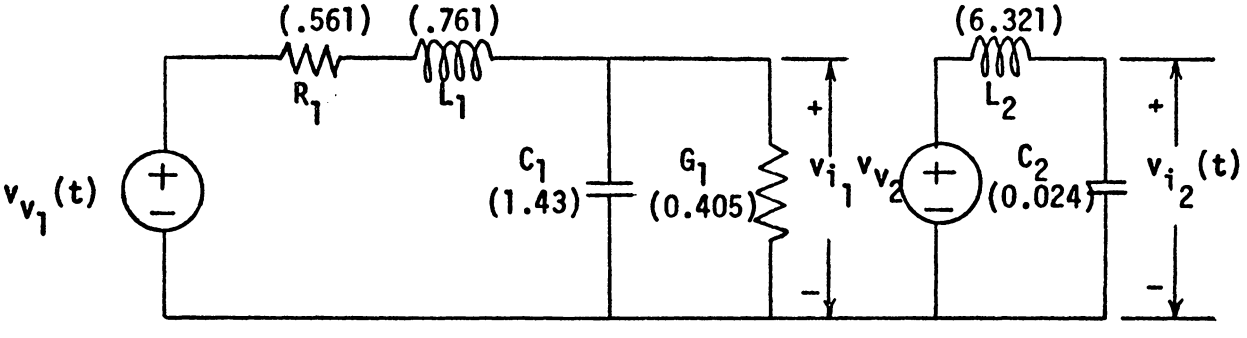

(ii) 1st and 2nd block final realizations

iteration	1	2	3	4	5
L_2	6.725	8.611	7.553	6.538	6.321
C_2	0.876	0.197	0.090	0.044	0.024

Figure 6.5.a. A two block realization for a DC motor transient model

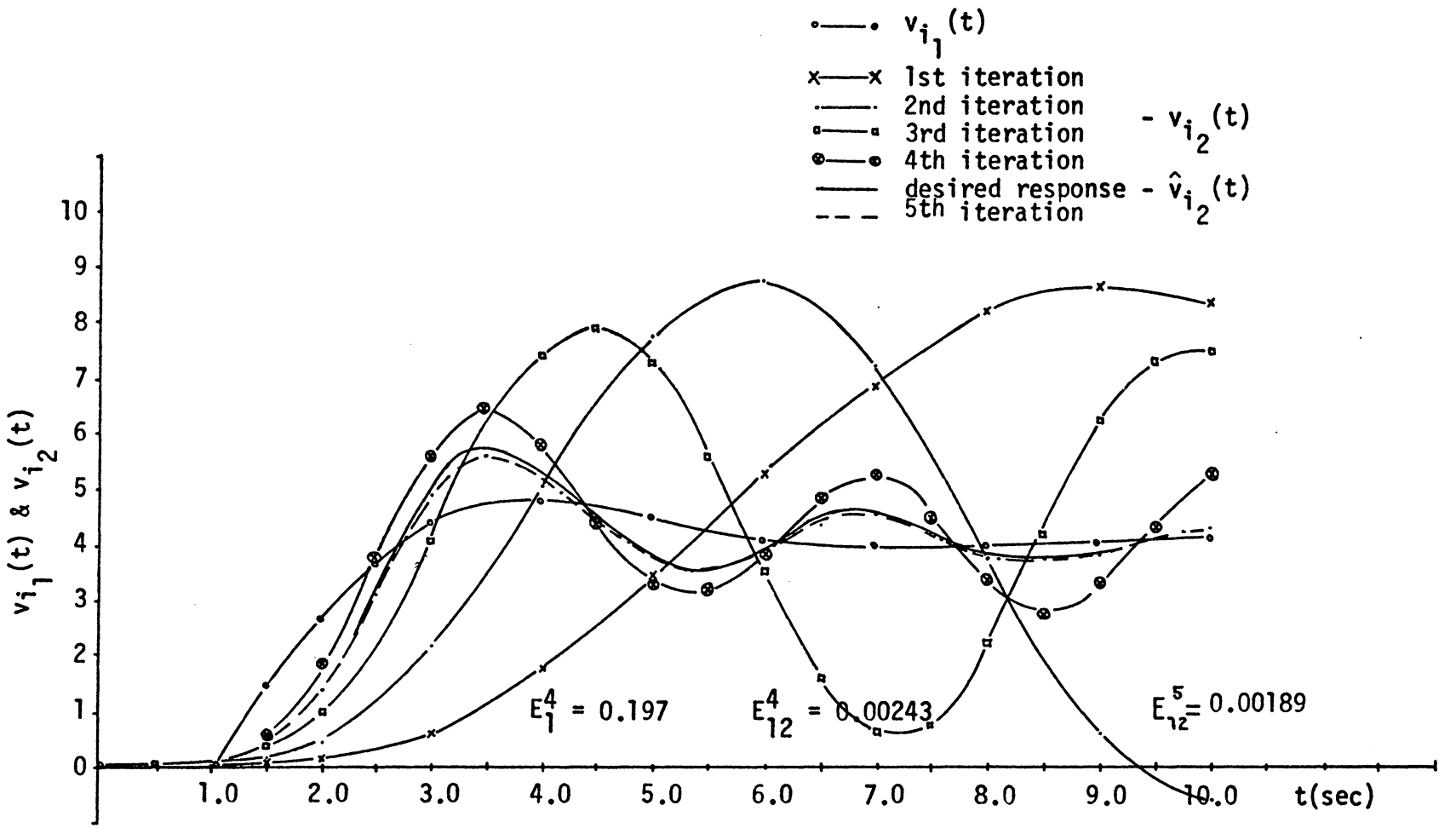

Figure 6.5.b. DC Motor Transient Model Block Responses $v_{i_1}(t)$, $v_{i_2}(t)$ and the desired response $\hat{v}_{i_2}(t)$

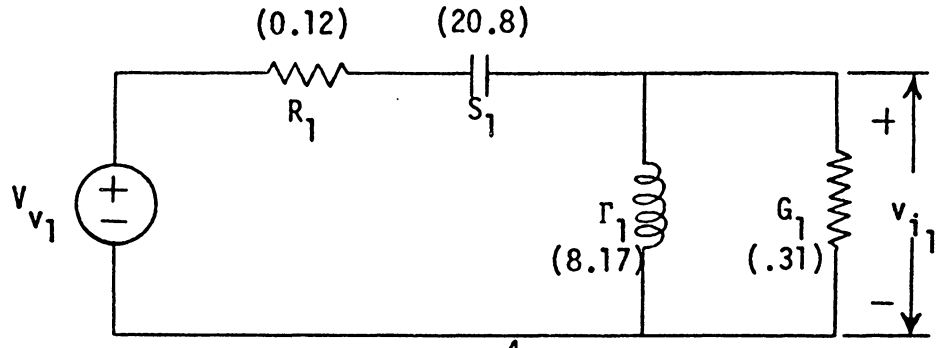

(i) first block, $E_1^4 = 0.0452$

iteration	1	2	3	4
R_1	1.0	0.334	.157	0.12
S_1	2.0	35.69	24.91	20.80
Γ_1	2.0	4.596	6.592	8.17
G_1	1.0	0.768	0.456	0.31

$V_{v_2} = \mu V_{i_1}$

$\mu = 1$

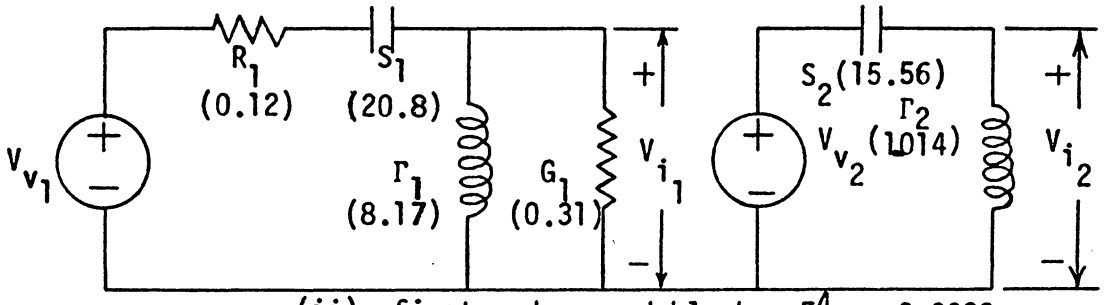

(ii) first and second blocks, $E_{12}^4 = 0.0028$

iteration	1	2	3	4
S_2	5.0	8.326	16.04	15.560
Γ_2	0.1	0.189	0.355	1.014

Figure 6.6.a. A two block realization example

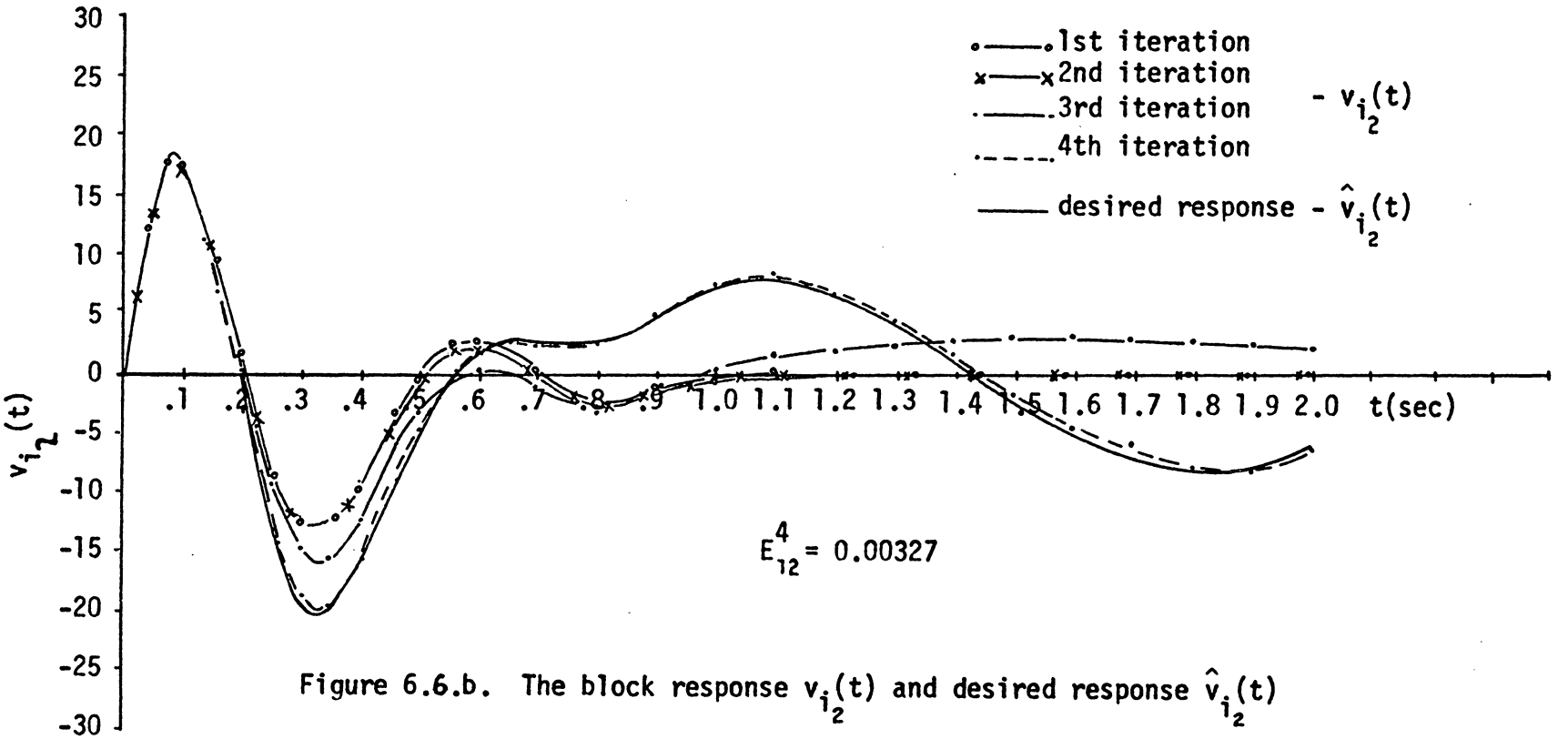

Figure 6.6.b. The block response $v_{i_2}(t)$ and desired response $\hat{v}_{i_2}(t)$

VII. CONCLUSIONS

New concepts in both frequency and time domain device modeling techniques were introduced in Chapters V and VI. These concepts involved approaching the device modeling problem from an error gradient minimization viewpoint so as to obtain the minimal index of performance function. In Chapter V the AC error gradients for small signal transistor models were characterized to provide the advantages listed below:

(i) Simplicity. This technique requires no optimization scheme and completely eliminates computer computation costs. Also, it guarantees an exact solution to the small signal model since no search in an unknown parameter space is involved.

(ii) Insensitive model. Following the procedure listed in Chapter V the small signal model not only can be realized to meet certain subnetwork performance requirements, but can also be designed to be voltage and/or current transfer function insensitive; with respect to drifts in h_{ie} and h_{oe} transistor parameters.

(iii) Basic building block. This small signal model design technique offers a basic building block upon which higher frequency model realization techniques, the hybrid pi model for example, can be implemented. A hybrid pi model constructed from the small signal model simply involves placing capacitors into the small signal model at the required locations and then "growing" them to meet an index of performance [35].

In Chapter VI the time domain cascaded building block modeling technique provides among its main features:

(i) Simplicity. Although an optimization procedure is required in this technique the circuit analysis program incorporated in the section 4.1.2 algorithm is fixed in terms of the topological structure it must analyse. That is, it need not be updated to calculate new gradient terms for a topologically changing structure as is required by previous variable structure modeling techniques [31].

(ii) Capable of fitting high order responses within a relaxed block by block error margin. Optimization processes are notorious for their ability to become stuck in a local valley or flat portion of the index of performance surface. And many times a block in the cascaded structure can encounter this problem, hence making it more difficult to realize strict error margins by the index of performance. However, each subsequent block offers the ability to begin with the previous blocks best "fit" to $\hat{v}_i(t)$ and the prospect of not being stuck in an IP flat portion or valley. Thus, no individual block in the structure may be required to achieve a certain strict error margin, while the structure in its entirity may achieve the strict margin.

(iii) Direct approach. This device modeling technique offers a concise approach to the modeling problem. The design engineer need only know a device characteristic response in order to approach the problem.

Recommendations for further research in this area are the following:

(i) In the frequency domain, characterization of error gradients for other well known models such as the hybrid pi model may also lead to a graphic model development technique which circumvents any optimization process requirement.

(ii) In the time domain, perhaps a block by block building structure approach for the series, parallel, series-parallel, or parallel-series type of connections [21] would prove even more beneficial than the cascaded block approach presented in Chapter VI.

BIBLIOGRAPHY

[1] "1620 Electronic Circuit Analysis Program (ECAP), User's Manual, IBM Corporation, Data Processing Div., White Plains, N. Y., Application Program 1620-EE-02X, pp. 6, 160-164.

[2] D. L. Hester, "Matrix Algebra Proof of the Derived Network Approach to Frequency Domain Sensitivity Calculation", Bell Telephone Laboratories Technical Memorandum MM 70-6324-7, May 6, 1970.

[3] J. V. Leeds, Jr., "Transient and Steady-State Sensitivity Analysis", IEEE Trans. C. T., Vol. CT-13, No. 2, pp. 288-289, Sept., 1966.

[4] J. V. Leeds, Jr. and G. I. Ugron, "Simplified Multiple Parameter Sensitivity Calculations and Continuously Equivalent Networks", IEEE Trans. C. T., Vol. CT-14, No. 2, pp. 188-191, June, 1967.

[5] S. W. Director and R. A. Rohrer, "A Generalized Adjoint Network and Network Sensitivities", IEEE Trans., Vol. C. T.-16, August, 1969, pp. 330-336.

[6] D. D. H. Tellegen, "A Generalized Network Theorem, with Applications", Phillips Res. Rpt., no. 7, 1952, pp. 259-269.

[7] G. D. Hachtel and R. A. Rohrer, "Design and Synthesis of Switching Circuits", Proc. IEEE, Vol. 55, no. 11, Nov., 1967, pp. 1864-1876.

[8] Peter V. Kokotovic, and James E. Heller, "Direct and Adjoint Sensitivity Equations for Parameter Optimization", IEEE Trans. Automatic Control, October, 1967, pp. 609-610.

[9] H. V. Sahasrabuddhe, H. K. Kesavan, W. J. Vetter, "Sensitivity Models for Computer-Aided Design", 12th Midwest Ckt. Symposium, University of Texas, Austin, Texas.

[10] S. W. Director and R. A. Rohrer, "On the Efficient Computation of First-Order Network Sensitivities (for frequency domain studies of lumped, linear, time-invariant networks), Second IFAC Symposium on System Sensitivity and Adaptivity, Dubrounil, Yugoslavia, August 26-31, 1968.

[11] H. F. VanLandingham and C. F. Smith, "A Computer-Oriented Approach to Parameter Sensitivity", 1st Annual Houston Conference on Ckts. and Systems, Houston, Texas, 1969.

[12] H. F. VanLandingham, C. F. Smith, S. Godbole, "Network Optimization Via Second Order Sensitivity Functions", IEEE International Symposium on Circuit Theory, Dec., 1970.

[13] Huelsman, L. P., "Theory and Design of Active R.C. Circuits", New York, N.Y., McGraw-Hill Book Co., 1968, Chapter 2.

[14] S. W. Director, "Increased Efficiency of Network Sensitivity Computation by Means of LU Factorization", Proc. 12th Midwest Circuit Symposium, pp. III 3.1-III 3.7, 1969.

[15] G. S. Moschytz, "Active Filters Using Operational Amplifiers", Bell Telephone Laboratories Technical Paper No. E-7351B, July, 1967.

[16] J. D. Schoeffler, "The Synthesis of Minimum Sensitivity Networks", IEEE Trans. on Ckt. Theory, CT-11, 270-276, June, 1964.

[17] D. A. Calahan, "Computer Generation of Equivalent Networks", IEEE International Conv. Rec., 17 (Part 1) 330-337, 1964.

[18] F. F. Kuo and A. J. Goldstein, "Multi-parameter Sensitivity", IEEE Trans. on Circuit Theory, CT-8, 177-178, June 1961.

[19] J. G. Truxal, Automatic Feedback Control System Synthesis, McGraw-Hill, 1963.

[20] R. Tomovic, Sensitivity Analysis of Dynamic Systems, McGraw-Hill, 1963.

[21] S. K. Mitra, Analysis and Synthesis of Linear Active Networks, John Wiley, 1969.

[22] D. L. Hester, "A.C. Sensitivity Calculations Using PCAP", Bell Telephone Laboratories Technical Memorandum, Case 39843-53, May 6, 1970.

[23] Sydney R. Parker, "Sensitivity Analysis and Models of Non-linear Circuits", IEEE Trans. C.T., Vol. CT-16, No. 4, November, 1969.

[24] S. W. Director, "Increased Efficiency of Network Sensitivity Computations by Means of LU Factorization", Proc. 12th Midwest Circuit Symposium, pp. III 3.1-III 3.7, 1969.

[25] D. A. Calahan, "The Adjoint Network and Its Application to Circuit Optimization", Computer-Aided Circuit Design Seminar, Univ. of South Florida, Tampa, Florida, Feb. 16-19, 1970.

[26] H. H. Skilling, Electrical Engineering Circuits, John Wiley, 1957.

[27] S. J. Mason, Feedback Theory-Some Properties of Signal Flow Graphs, Proc. IRE, Vol. 41, No. 9, pp. 1144-1156, September, 1953.

[28] H. W. Bode, "Network Analysis and Feedback Amplifier Design", p. 68, D. VanNostrand Co., Inc., New York 1945.

[29] M. L. Blostein, "Some bounds on sensitivity in RLC networks", Proc. 1st Allerton Conf. on Circuit and System Theory, Univ. of Illinois, pp. 488-501, 1963.

[30] S. W. Director and R. A. Rohrer, "Automated Network Design - The Frequency-Domain Case", IEEE Trans. on CT, Vol. CT-16, No. 3, August 1969.

[31] R. A. Rohrer, "Fully Automated Network Design by Digital Computer: Preliminary Considerations", IEEE Trans. on CT, Vol. CT-55, No. 11, November 1967.

[32] E. E. Saunders, "Design and Application of a Helical Torsion Spring Dynamometer", Master's Thesis, Virginia Polytechnic Institute and State University, Blacksburg, Virginia, 1968.

[33] D. A. Calahan, Computer-Aided Network Design, McGraw-Hill Book Co., 1967.

[34] S. W. Director, "Survey of Circuit-Oriented Optimization Techniques," IEEE Trans. on CT, Vol. CT-18, No. 1, January 1971.

[35] A. J. Brodersen, S. W. Director, W. A. Bristol, "Simultaneous Automated AC and DC Design of Linear Integrated Circuit Amplifiers", IEEE Trans. on CT, Vol. CT-18, No. 1, January 1971.

APPENDIX A

FIBONACCI SEARCH TECHNIQUE

There are two types of one dimensional search techniques: those that iterate along the search direction until the limits that bound a minimal point of the performance function (interval of uncertainty) have been reduced to within some interval tolerance, and those that assume a particular shape of the performance function and set α equal to the explicitly calculated minimum [34].

Interpolation polynomial techniques such as Davidson's [25] are representative of the second of the two types mentioned. Search by golden section [34] and Fibonacci search [33] are representative of the first type.

Search by the Fibonacci technique is about 17 percent more efficient than golden section with regard to interval reduction of the interval of uncertainty at each step. The Fibonacci search is initiated after the interval of uncertainty has been bounded, assuming the performance measure to be unimodal [33]. Then the bounded interval of uncertainty is divided according to the Fibonacci sequence 1 1 2 3 5 8 1 3 . . . . ., as shown in Figure A.1. The major disadvantage of the Fibonacci technique is that the total number of iterations must be specified a priori. Hence, the search procedure begins by choosing a value for N, a number which can be determined by the total interval reduction desired.

The efficient scheme can be evolved by assuming, on the final iteration, the interval is divided into thirds. Proceeding backward

to the (N - 1)st iteration under the assumption that

(1) inequalities of the form of Equation A.1 were applied at the (N - 1)st iteration (where E_a, E_b, E_c and E_d are performance function values evaluated at interval points a, b, c and d; and either E_b or E_d will be common to any two successive iterations),

(2) the Nth and (N - 1)st iterations share a common interior point,

(3) b and d are symmetric about the center of the interval [a, c],

then, the intervals between the abcissas at the (N - 1)st iteration are [2Δ, Δ, 2Δ] respectively. By comparing E_b and E_d we can shrink the bound on $\hat{\alpha}^i$ since

$$\begin{array}{lll} b > d & \text{and } E_b > E_d & a \leq \hat{\alpha}^i \leq b \\ & \text{and } E_d > E_b & d \leq \hat{\alpha}^i \leq c \\ d > b & \text{and } E_b > E_d & b \leq \hat{\alpha}^i \leq c \\ & \text{and } E_d > E_b & a \leq \hat{\alpha}^i \leq d \end{array} \qquad \text{(A.1)}$$

and $\hat{\alpha}^i$ is the optimal (minimal) value for α calculated at each respective iterate.

Consequently, after an N value has been chosen, the interval reduction factor [33] quickly asymptotes to 0.618, so the total reduction for N iterations becomes $(0.618)^N$. For example, ten iterations, requiring eleven evaluations of E, reduces the bound on $\hat{\alpha}^i$ by a factor of 100.

Calahan [33] has written a Fortran IV computer program which is easily implemented as a subroutine program. It is listed on page 292

of the preceding reference and requires six input variables for each $\hat{\alpha}$ calculation. The subroutine form is:

SUBROUTINE FIBMIN(X1,X2,XMIN,ITER,KEY1,F,F1,F2) where the input data is:

X1 Lefthand α bounding value

F1 Performance Function calculated at X1

X2 Righthand α bounding value

F2 Performance Function Calculated at X2

ITER the number of iterations N

KEY1 Set equal to 2 initially

and the resultant output data becomes:

XMIN the minimal $\hat{\alpha}$ value

F the performance function calculated at $\hat{\alpha}$

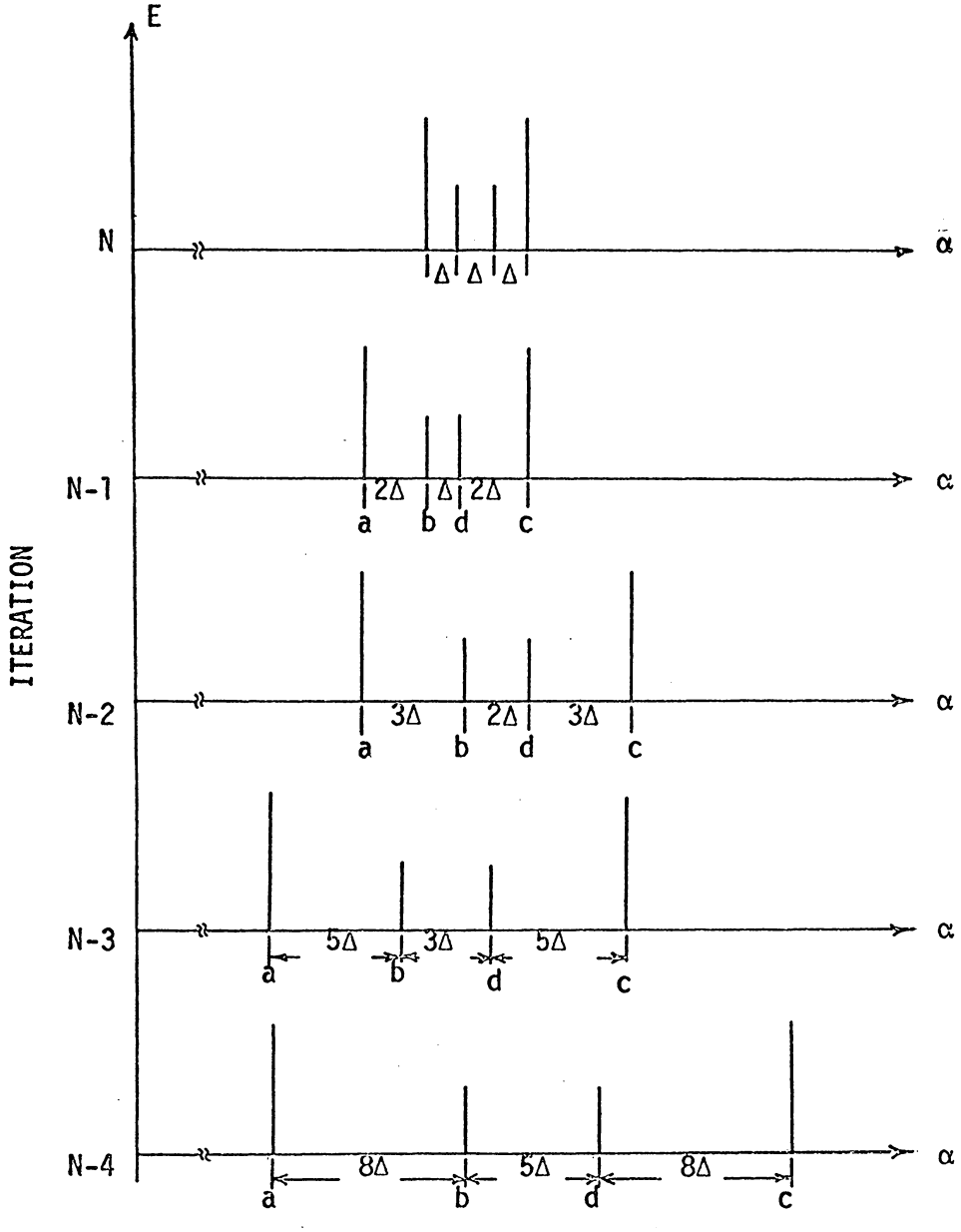

Figure A.1. Interval Reduction Using Fibonacci Search

The vita has been removed from the scanned document

MODEL REALIZATION USING SENSITIVITY FUNCTIONS

by

Ernest Edward Saunders, Jr.

(ABSTRACT)

New concepts in linear, time invariant model realization using sensitivity functions are presented. These concepts involve approaching the device modeling problem from an error gradient minimization viewpoint. This leads to the attainment of a minimal index of performance function (IP) and, consequently, emulates a desired device model response either in the frequency or time domain.

In the frequency domain the problem of characterizing the AC error gradients for a small signal transistor model is considered. The integral of the weighted squared-error is the IP functional incorporated. It is found that the error gradients all contain a similar expression whose values, when chosen properly, create zero valued gradients and a zero valued (globally minimal) IP functional. Hence a graphical analysis routine based on the similarity expression is developed to provide the advantages listed below:

(i) Simplicity. This technique requires no optimization scheme and completely eliminates computer computation costs.

(ii) Insensitive model. A design scheme is affixed to the graphical analysis scheme so as to yield insensitive voltage and/or current transfer functions; with respect to drifts in h_{ie} and h_{oe} transistor parameters.

(iii) Basic building block. The small signal model design technique offers a basic building block upon which high frequency model realization techniques, the hybrid pi model for example, can be implemented.

In the time domain a variable structure cascaded building block technique was designed and provides among its main features:

(i) Simplicity. Although an optimization procedure is required in this technique the circuit analysis program incorporated in the negative gradient algorithm is fixed in terms of the topological structure it must analyse. That is, it need not be updated to calculate new gradient terms for a topologically changing structure as is required by previous variable structure modeling techniques.

(ii) Capable of fitting high order responses within a relaxed block by block IP functional. No individual block in the structure may be required to achieve a certain strict IP functional, while the structure in its entirity may achieve the strict functional.

(iii) Direct approach. This device modeling technique offers a concise approach to the modeling problem. The design engineer need only know a device characteristic response in order to approach the problem.

Further research possibilities include characterization of the AC error gradients for the hybrid pi transistor model and possibly

a series, parallel, series-parallel, or parallel-series connection would prove even more beneficial than the cascaded block time domain approach.